

**Thermal-neutron capture by  $^{58}\text{Ni}$ ,  $^{59}\text{Ni}$ , and  $^{60}\text{Ni}$** S. Raman,\* Xiaoping Ouyang,<sup>†</sup> and M. A. Islam<sup>‡</sup>*Physics Division, Oak Ridge National Laboratory, Oak Ridge, Tennessee 37831, USA*

J. W. Starner, E. T. Jurney,\* and J. E. Lynn

*Los Alamos National Laboratory, Los Alamos, New Mexico 87545, USA*

G. Martínez-Pinedo

*ICREA and Institut d'Estudis Espacials de Catalunya, Universitat Autònoma de Barcelona, E-08193 Bellaterra, Spain*

(Received 5 March 2003; published 29 October 2004)

We have studied the primary and secondary  $\gamma$  rays (414 in  $^{59}\text{Ni}$ , 390 in  $^{60}\text{Ni}$ , and 240 in  $^{61}\text{Ni}$ ) following thermal-neutron capture by the stable  $^{58}\text{Ni}$ , radioactive  $^{59}\text{Ni}$ , and stable  $^{60}\text{Ni}$  isotopes. Most of these  $\gamma$  rays have been incorporated into the corresponding level schemes consisting of 65 levels in  $^{59}\text{Ni}$ , 88 levels in  $^{60}\text{Ni}$ , and 40 levels in  $^{61}\text{Ni}$ . The measured neutron separation energies ( $S_n$  in keV) for  $^{59}\text{Ni}$ ,  $^{60}\text{Ni}$ , and  $^{61}\text{Ni}$  are, respectively,  $8999.28 \pm 0.05$ ,  $11\,387.73 \pm 0.05$ , and  $7820.11 \pm 0.05$ . The measured thermal-neutron capture cross sections (in barns) for  $^{58}\text{Ni}$ ,  $^{59}\text{Ni}$ , and  $^{60}\text{Ni}$  are, respectively,  $4.13 \pm 0.05$ ,  $73.7 \pm 1.8$ , and  $2.34 \pm 0.05$ . In all three cases, primary electric-dipole ( $E1$ ) transitions account for the bulk of the total capture cross section. We have calculated these  $E1$  partial cross sections (in  $^{59}\text{Ni}$  and  $^{61}\text{Ni}$ ) using direct-capture theory and models of compound-nuclear capture. The agreement between theory and experiment is good. The experimental level schemes have been compared with the results from a large-basis shell-model calculation. The agreement was also found to be quite good.

DOI: 10.1103/PhysRevC.70.044318

PACS number(s): 25.40.Lw, 21.60.Cs, 27.50.+e

**I. INTRODUCTION**

In a series of papers [1–16] we have examined off-resonance slow-neutron capture by light nuclides ( $A \leq 50$ ) and have shown that the direct-capture mechanism as originally formulated by Lane and Lynn [17,18] and further developed in Refs. [1–3] provides a sound description of the partial cross sections of the electric-dipole ( $E1$ ) primary transitions in these nuclides. In this paper, we study the primary and secondary  $\gamma$  rays following thermal-neutron capture by  $^{58}\text{Ni}$ ,  $^{59}\text{Ni}$ , and  $^{60}\text{Ni}$ . In all three cases,  $E1$  primary transitions account for the bulk of the total capture cross section. We calculate the  $E1$  partial cross sections using direct-capture theory employing the same methods as developed in the earlier papers. In particular, we use a global optical model plus a valence correction. We find again that direct capture accounts for a major fraction of the cross sections of primary  $E1$  transitions and that the differences between theory and experiment can be explained by admixtures of compound-nuclear amplitudes into the direct-capture amplitudes. The resulting average compound-nuclear cross sections are reasonably consistent with theoretical expectations.

From a variety of studies [19–83] discussed in greater detail in later sections,  $\sim 200$  bound levels are known below 7.6 MeV in  $^{59}\text{Ni}$ ,  $\sim 150$  levels below 10.0 MeV in  $^{60}\text{Ni}$ , and

$\sim 170$  levels below 5.5 MeV in  $^{61}\text{Ni}$ . In each nucleus, about a third of all known levels are populated significantly in the current (thermal  $n, \gamma$ ) study. For each final nucleus, we have provided a conspectus of bound levels and their spin and parity ( $J^\pi$ ) assignments. We have also compared the experimentally known levels in  $^{59}\text{Ni}$ ,  $^{60}\text{Ni}$ , and  $^{61}\text{Ni}$  with those calculated with a large-basis shell-model interaction.

**II. EXPERIMENTAL PROCEDURES**

The ( $n, \gamma$ ) measurements were carried out with enriched targets obtained from the research materials collection maintained by the Oak Ridge National Laboratory. Measurements were also made with natural nickel. Each target was studied in the thermal column of the internal target facility at the Los Alamos Omega West Reactor. The target was placed in a graphite holder, which was inside an evacuated bismuth channel. The target position was 1.5 m from the edge of the reactor core. At this position, the thermal-neutron flux was  $\sim 6 \times 10^{11} \text{ n cm}^{-2} \text{ s}^{-1}$ . The Los Alamos facility and the data analysis procedures have been described in detail in Ref. [1]. Gamma-ray spectra were obtained with a 30-cm<sup>3</sup> coaxial intrinsic Ge detector positioned inside a 20-cm-diameter by 30-cm-long NaI(Tl) annulus. This Ge detector was located 6.3 m from the target and was operated either in the Compton-suppressed mode (0.454 keV/channel) or in the pair-spectrometer mode (0.629 keV/channel). The latter mode utilizes the lengthwise optical division of the annulus so that only double-escape peaks appear in the pulse-height spectrum. At lower energies the two annulus halves are connected together electrically to operate in the conventional

\*Deceased.

<sup>†</sup>Permanent address: Institute of Modern Physics, Fudan University, Shanghai, People's Republic of China.<sup>‡</sup>Permanent address: Rajshahi University, Rajshahi, Bangladesh.

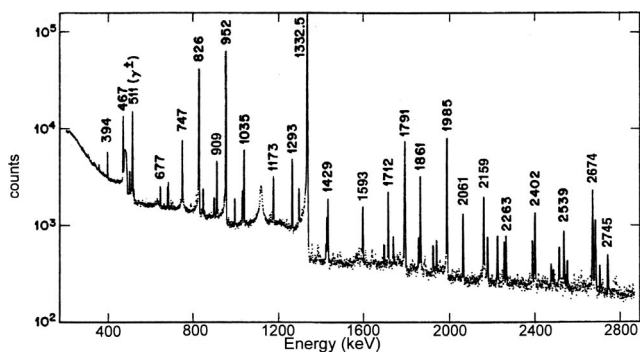


FIG. 1. Gamma-ray spectra from thermal-neutron capture by  $^{59}\text{Ni}$ . The Ge detector was operated in the Compton-suppression mode. All energies are in keV.

Compton-suppressed mode. The pulse-height analyzer had 16 384 channels. In the Compton-suppressed mode, the full width at half maximum (FWHM) values for our system were 1.5, 1.8, 2.3, and 2.9 keV, respectively, for  $\gamma$ -ray energies of 0.5, 1.0, 2.0, and 3.0 MeV. Figure 1 shows a sample spectrum obtained with the  $^{59}\text{Ni}$  target in this mode. In the pair-spectrometer mode, the FWHM values were 2.5, 3.3, 4.0, and 4.7 keV, respectively, for  $\gamma$ -ray energies of 3, 5, 7, and

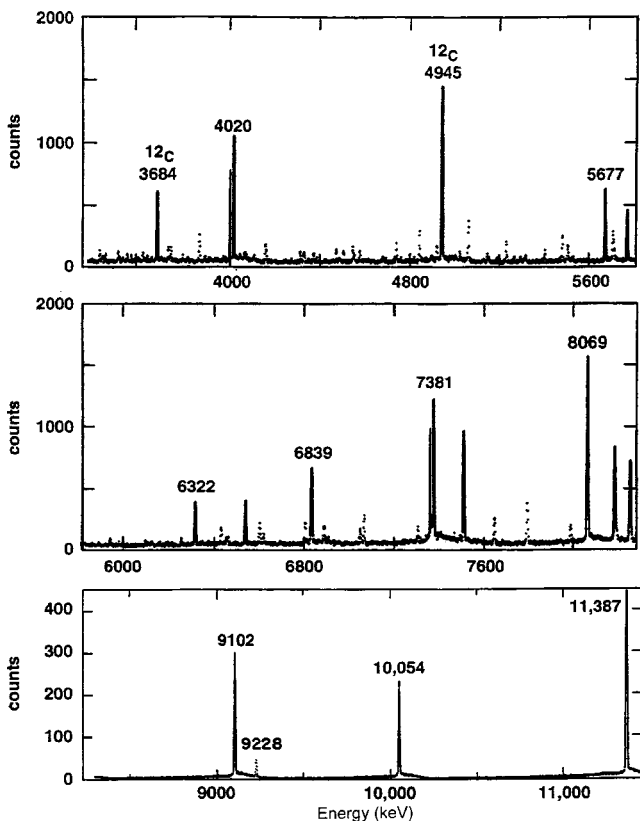


FIG. 2. Gamma-ray spectra from thermal-neutron capture by  $^{59}\text{Ni}$ . The Ge detector was operated in the pair-spectrometer mode. All energies are in keV.

9 MeV. Figure 2 shows a sample spectrum obtained with the  $^{59}\text{Ni}$  target in the latter mode.

Energy calibrations in the pair-spectrometer mode were performed with the prompt  $\gamma$ -ray spectrum from neutron capture in melamine ( $\text{C}_3\text{H}_6\text{N}_6$ ). In the Compton-suppressed mode, the prompt  $\gamma$  ray from the  $^1\text{H}(n, \gamma)$  reaction plus the annihilation radiation were employed for this purpose. In both modes, nonlinearity corrections to the measured energies were made (see Fig. 2 of Ref. [15]), using precisely known  $\gamma$  rays appropriate to the range of energies of interest. The primary calibration energies were those recommended by Wapstra and his co-worker [84,85]:  $510.999 \pm 0.001$  keV for the annihilation radiation,  $2223.255 \pm 0.003$  keV for the  $\gamma$  ray from the  $^1\text{H}(n, \gamma)$  reaction, and  $4945.302 \pm 0.003$  keV for the ground-state transition in the  $^{12}\text{C}(n, \gamma)$  reaction. Secondary calibration energies were provided by the  $\gamma$  rays in the  $^{14}\text{N}(n, \gamma)$  reaction [15].

Intensity calibrations (see Fig. 3 of Ref. [15]) were determined in the Compton-suppressed mode with a set of standard radioisotopic sources with precalibrated  $\gamma$ -ray intensities. The efficiency curve in the pair-spectrometer mode was derived from the relative intensities of  $\gamma$  rays from the  $^{14}\text{N}(n, \gamma)$  reaction [15,86]. The effect of possible variations in neutron flux was taken into account by normalizing the data to the neutron fluence for each run measured with a small fission counter located near the target position in the thermal column. The capture cross sections reported in the current work for  $^{58}\text{Ni}$  and  $^{60}\text{Ni}$  are based on measurements in which each target was studied together with a 100.0-mg  $\text{CH}_2$  standard. The cross sections are normalized to the recommended value of  $\sigma_\gamma(2200 \text{ m/s}) = 332.6 \pm 0.7$  mb [87] for  $^1\text{H}$  present in the standard. The  $^{59}\text{Ni}$  capture cross section is based on the  $^{58}\text{Ni}$  and  $^{60}\text{Ni}$  capture cross sections and the isotopic composition of the sample. The thermal-neutron flux at the target position approximates a Maxwellian distribution corresponding to a temperature of 350 K, for which the most probable neutron velocity is 2400 m/s. To determine the cross sections at 2200 m/s, we have assumed a  $1/v$  dependence of the capture cross section for  $^1\text{H}$  and for all target isotopes.

### III. PRESENTATION OF RESULTS

This paper contains a large body of data on three nickel isotopes. There are common threads among the tables presented in this paper. We discuss our overall philosophy and methods of presentation in this section.

#### A. Previous measurements

Because almost all the reactions that are likely to give useful information on the energy levels in  $^{59}\text{Ni}$ ,  $^{60}\text{Ni}$ , and  $^{61}\text{Ni}$  have already been studied—some several times—and because of the lessened activity in conventional nuclear spectroscopy expected in future years, significant new information on these levels will likely appear with greatly reduced frequency. Thus we feel a review of the currently available information is timely. We start with a list of references to previous measurements. When several references are avail-

TABLE I. Partial list of references to previous measurements on  $^{59}\text{Ni}$  levels. See Ref. [89] for additional references.

Measurement	Author(s)	Year	Facility <sup>a</sup>	Reference
$^{50}\text{Cr}(^{12}\text{C}, 2pn\gamma)$ reaction	Pichevar <i>et al.</i>	1976	Saclay	[19]
$^{56}\text{Fe}(\alpha, n\gamma)$ reaction	Hutton <i>et al.</i>	1973	TUNL	[20]
	Monseu, Forssten, and Sawa	1974	Stockholm	[21]
	Pichevar <i>et al.</i>	1976	Saclay	[19]
$^{58}\text{Ni}(\alpha, ^3\text{He})$ reaction	Roussel <i>et al.</i>	1970	Saclay	[22]
$^{58}\text{Ni}(^3\text{He}, 2p\gamma)$ reaction	Juutinen <i>et al.</i>	1989	U. Jyväskylä	[23]
$^{59}\text{Co}(p, n)$ reaction	Stelson	1967	Oak Ridge	[24]
$^{59}\text{Co}(p, n\gamma)$ reaction	Stelson, Dickens, and Perey	1967	Oak Ridge	[25]
	Mittal, Avasthi, and Govil	1983	Panjab U.	[26]
$^{58}\text{Ni}(\text{thermal } n, \gamma)$ reaction	Hofmeyr	1975	Pelindaba	[27]
	Ishaq <i>et al.</i>	1977	McMaster U.	[28]
	Harder	1992	Grenoble	[29]
	Harder <i>et al.</i>	1993	Grenoble	[30]
$^{58}\text{Ni}(\text{polarized } n, \gamma)$ reaction	Stecher-Rasmussen <i>et al.</i>	1972	Petten	[31]
$^{58}\text{Ni}(d, p)$ reaction	Fulmer <i>et al.</i>	1964	Aldermaston	[32]
	Cosman <i>et al.</i>	1966	MIT	[33]
	Litvin <i>et al.</i>	1972	Leningrad	[34]
	Chowdhury and Sen Gupta	1973	Aldermaston	[35]
$^{58}\text{Ni}(\text{polarized } d, p)$ reaction	Aymar <i>et al.</i>	1973	U. Notre Dame	[36]
	Taylor and Cameron	1980	McMaster U.	[37]
$^{59}\text{Cu}(\beta^+ + \varepsilon)$ decay	Van Patter, Rauch, and Stein	1973	U. Frankfurt	[38]
	Sen, Sen, and Basu	1977	SUNY	[39]
$^{60}\text{Ni}(p, d)$ reaction	Sherr <i>et al.</i>	1965	U. Colorado	[40]
$^{60}\text{Ni}(\text{polarized } p, d)$ reaction	Nann <i>et al.</i>	1983	Indiana U.	[41]
$^{60}\text{Ni}(^3\text{He}, \alpha)$ reaction	Zimmerman <i>et al.</i>	1978	U. Colorado	[42]
	Sen Gupta <i>et al.</i>	1990	U. Birmingham	[43]

<sup>a</sup>Facility where the actual measurements were done. The symbol U stands for a university.

able for a given reaction, we list only those that we feel give definitive results.

### B. Known energy levels

From the list of references to previous measurements, we select those that give information leading to a skeleton level scheme. We specifically exclude previous  $(n, \gamma)$  studies. The construction of this skeleton level scheme is nontrivial because it is necessary to establish a one-to-one correspondence between the levels reported in different experiments. In this paper, we have provided critically evaluated lists of the bound states in  $^{59}\text{Ni}$ ,  $^{60}\text{Ni}$ , and  $^{61}\text{Ni}$  and their spin and parity ( $J^\pi$ ) assignments. Our summaries are independent of similar summaries appearing in Refs. [88–96].

### C. Observed $\gamma$ rays

The energies and intensities of  $\gamma$  rays observed in this work from the respective  $(n, \gamma)$  reactions are given in separate tables. Unplaced and multiply placed  $\gamma$  rays are noted and, for each placed  $\gamma$  ray, the preferred placement is indicated in the table. Alternate placements are given at the end of the table.

### D. Level schemes

The construction of a level scheme based on  $(n, \gamma)$  data is somewhat akin to solving a jigsaw puzzle. The problem is rendered easier to the extent to which the energy levels and their branching ratios are known from other experiments. Each and every known level that could reasonably be expected to receive population in the  $(n, \gamma)$  reaction was checked against the  $\gamma$ -ray data. In this paper, the level schemes of  $^{59}\text{Ni}$ ,  $^{60}\text{Ni}$ , and  $^{61}\text{Ni}$  based on our  $(n, \gamma)$  studies are presented in tabular form. The level energies listed in these tables were obtained through an overall least-squares fit involving all placed transitions except those noted as multiply placed. In deducing these level energies, nuclear recoil was taken into account. Also presented in these tables are the summed cross section for populating each level, the summed cross section for deexciting each level, and the intensity imbalance. The level scheme based on our  $(n, \gamma)$  work is then carried over to an earlier table for comparison with the previous best  $(n, \gamma)$  level scheme and with all previously known levels.

Multiple placements of  $\gamma$  rays are inevitable in a complex level scheme. In this work, we initially placed  $\gamma$  rays in all

TABLE II. Known energy levels in  $^{59}\text{Ni}$ .

Known $E(\text{level})^a$ (keV)	$J^\pi$	Previous	This work	Known $E(\text{level})^a$ (keV)	$J^\pi$	Previous	This work
		$(n, \gamma)$ $E(\text{level})^a$ (keV)	$(n, \gamma)$ $E(\text{level})^a$ (keV)			$(n, \gamma)$ $E(\text{level})^a$ (keV)	$(n, \gamma)$ $E(\text{level})^a$ (keV)
0.0	$0^+$	0.0	0.0	3187.5			
339.36	$7^-$	339.419 22	339.399 16	3297.1			
464.97	$7^-$	464.971 22	464.935 16	3308.1			
878.04	$8^-$	877.941 21	877.961 15	3315			
1189.08	$9^-$	1188.783 24	1188.789 16	3340.0			
1301.48	$7^-$	1301.40 3	1301.437 17	3347.5			3343.22 6
1337.86	$8^-$		1337.89 3	3354.5			
1679.75	$8^-$	1679.69 3	1679.700 24	3363.5			
1734.74	$7^-$	1734.72 3	1734.687 17	3377.00	$(\frac{11}{2}^-)$		
1739.19	$22^-$			3377.5		3377.41 9	3377.22 6
1746.1	$7^-$			3380.7			
1767.42	$9^-$			3408.5			
1948.02	$11^-$		1948.32 17	3415.5	$\frac{1}{2}^+$		3413.55 15
2349.22	$14^-$			3452.5	$\frac{3}{2}^-$	3452.41 11	3452.34 10
2414.84	$18^-$	2414.97 3	2414.892 17	3505.5			
2422.5			2421.95 6	3521.5			
2526.5				3534.5	$(\frac{5}{2}^+)$		
2530.47	$15^-$			3538.60	$(\frac{9}{2}^-)$		
2533.0	$21^-$					3540.05 12	3540.05 7
2535.46	$23^-$			3545.9			
2553.4	$21^-$			3559.54	$(\frac{11}{2}^-)$		
2627.28	$17^-$		2627.05 8	3563.5	$\frac{1}{2}^-, \frac{3}{2}^-$	3563.10 9	3562.98 3
2681.1	$7^-$		2679.57 14	3590.5			
2685.5				3638.5			
2698.5				3686.5	$\frac{3}{2}^+, \frac{5}{2}^+$	3686.20 10	3686.109 22
2705.29	$14^-$			3718.5			
2713.1	$21^-$		2715.03 11	3730	$\frac{7}{2}^-$		
2893.5	$5^-$	2893.61 4	2893.521 20	3735.5		3730.38 10	3730.24 5
3027.5	$(\frac{1}{2}^-, \frac{3}{2}^-)$	3025.82 8	3025.769 25	3781.5			
3038.0	$21^-$			3796.5			
3054.52	$14^-$			3802.5			
3125.53	$18^-$			3856.5	$\frac{3}{2}^-$	3853.71 11	3853.63 6
3126.8	$12^-$		3126.10 17			3858.26 12	
3177.5	$5^-$	3181.63 8	3181.564 18	3887.5		3889.74 12	3889.70 7

possible positions in the level scheme warranted by the spin change and agreement—within twice the energy uncertainty—between the level energy difference and the  $\gamma$ -ray energy. We then either removed or retained multiple placements, depending on the intensity balance considerations for each level. Multiply placed  $\gamma$  rays were excluded in the overall least-squares routine used to determine the best level energies and their uncertainties.

If a level scheme is complete and internal conversion can be neglected, the quantities  $\Sigma I_\gamma$  (primary),  $\Sigma E_\gamma I_\gamma / S_n$ , and  $\Sigma I_\gamma$  (to ground state) should all be the same within their stated uncertainties. We have listed these quantities for all three isotopes.

### E. Previous $(n, \gamma)$ measurements

For all three nickel isotopes, the current spectroscopic data are more extensive and definitive than previous  $(n, \gamma)$  studies. The detection limit (for a  $\gamma$  ray in the 0.1–10.0 MeV region), enrichment of the sample, and sample purity were all better than in previous measurements. This improvement, in turn, has resulted in a significant increase in the number of  $\gamma$  rays identified in this work as belonging to a particular isotope. This increasing complexity is quantified in respective tables for the three nickel isotopes. A limiting factor in the current measurements was the presence of trace impurities in the enriched targets. In separate experiments, we have

TABLE II. (Continued.)

Known $E(\text{level})^a$ (keV)	$J^\pi$	Previous ( $n, \gamma$ ) $E(\text{level})^a$ (keV)	This work ( $n, \gamma$ ) $E(\text{level})^a$ (keV)	Known $E(\text{level})^a$ (keV)	$J^\pi$	Previous ( $n, \gamma$ ) $E(\text{level})^a$ (keV)	This work ( $n, \gamma$ ) $E(\text{level})^a$ (keV)
3899 5				4668 5			
3933 5				4682 7			
3994 5				4690 20	$\frac{7}{2}^-$		
4004 5				4697 5			
4025 5	$\frac{1}{2}^-, \frac{3}{2}^-$	4021.90 11	4021.87 5	4709 10			
4076 5				4716 5	$\frac{1}{2}^-, \frac{3}{2}^-$	4715.33 13	4715.34 4
4103.11 16	$(\frac{11}{2}^+)$			4756 7			
4109 5				4787 5	$\frac{3}{2}^+, \frac{5}{2}^+$		4782.91 17
4122 5				4810 5			
4141.13 16	$(\frac{13}{2}^-)$			4844 5			
4143 5	$\frac{1}{2}^-, \frac{3}{2}^-$	4140.31 11	4140.242 25	4857 5			
4160 20	$\frac{7}{2}^-$			4875 5			
4166 5				4908 5			
4202 5				4927 5			
4230 20	$\frac{7}{2}^-$			4947.20 22	$(\frac{15}{2}^-)$		
4253 5	$(\frac{1}{2}^-, \frac{3}{2}^-)$	4253.01 11	4252.74 6	4948 5	$(\frac{1}{2}^-, \frac{3}{2}^-)$		4949.17 5
4282 5				4968 5	$\frac{1}{2}^-, \frac{3}{2}^-$	4968.87 13	4968.89 4
4317 5				5015 7			
4345 5				5024 5			
		4352.45 12	4352.46 8	5049 7			
4384 5				5068 5	$\frac{1}{2}^-, \frac{3}{2}^-$	5068.98 13	5069.10 5
4396 5				5098.27 23	$(\frac{13}{2}^-)$		
4408 5				5106 7			
4418.84 24	$(\frac{13}{2}^-)$			5137 5	$\frac{1}{2}^+$		5131.94 18
4455.28 17	$(\frac{13}{2}^+)$			5201 5	$\frac{3}{2}^+, \frac{5}{2}^+$		
4458 5				5246 5			
4494 5	$\frac{5}{2}^+$		4494.18 12	5251.3 3	$(\frac{17}{2}^+)$		
4531 5			4532.8 3	5256 7			
4545 5				5280 5			
4560 20	$\frac{7}{2}^-$			5293.04 25	$(\frac{15}{2}^-)$		
4613 10				5360 5			
4615.95 24	$(\frac{9}{2}^+)$			5381.38 29	$(\frac{15}{2}^+)$		
4634 5				5383 5	$\frac{3}{2}^+, \frac{5}{2}^+$	5384.69 14	5384.76 7
4651 7				5417 5	$(\frac{7}{2}^+, \frac{9}{2}^+)$		

obtained spectra under similar conditions from several commonly occurring elements to aid in the identification of peaks resulting from impurities and to correct for them in case of interference. We have also made use of existing compilations of  $\gamma$  rays from neutron capture by natural elements [97,98].

#### F. Comparison of capture data with calculations

In most, if not all, light nuclei, the direct-capture mechanism accounts for the major part of the thermal-neutron capture cross section in which the primary transition is electric dipole. In simple terms, direct capture can be described as

the transition from the orbit of a neutron being scattered by a smooth potential field representing the target nucleus to the single-particle component of the bound final state. Because the major part of the integrand in the radial matrix element lies beyond the nuclear potential radius (this part is “channel capture” [17,18]), the direct-capture cross section to a given final state can be calculated quite accurately if the  $s$ -wave neutron scattering length and the  $p$ -wave single-neutron spectroscopic factor of the final state are known. It has been shown [1,2] that the direct-capture cross section can be constructed from a potential-capture amplitude calculated from

TABLE II. (*Continued.*)

Known $E(\text{level})^a$ (keV)	$J^\pi$	Previous ( $n, \gamma$ ) $E(\text{level})^a$ (keV)	This work ( $n, \gamma$ ) $E(\text{level})^a$ (keV)	Known $E(\text{level})^a$ (keV)	$J^\pi$	Previous ( $n, \gamma$ ) $E(\text{level})^a$ (keV)	This work ( $n, \gamma$ ) $E(\text{level})^a$ (keV)
5446 5	$\frac{3}{2}^+, \frac{5}{2}^+$		5443.87 13	6236 5			
5496 5			5494.23 11	6260 5			
5516 5				6275 5			6279.86 7
5558 5	$\frac{1}{2}^+$			6296 5	$\frac{3}{2}^+, \frac{5}{2}^+$		
5597 5				6330 5			
5618 5	$\frac{1}{2}^-, \frac{3}{2}^-$	5617.20 15	5617.33 6	6345 5			
5637 5		5632.06 15	5632.17 6	6371 5	$\frac{1}{2}^+$		
5681 5	$\frac{1}{2}^+$		5676.87 18	6425 5			6431.34 9
		5702.34 16	5702.11 18	6446 5	$(\frac{3}{2}^+, \frac{5}{2}^+)$		
5736 5				6473 5			
5746 7				6499 5			6498.21 17
5751 5	$\frac{1}{2}^-, \frac{3}{2}^-$	5754.54 16	5754.67 9	6502.43 25	$(\frac{19}{2}^-)$		
5772 5				6513 5			
5794 5				6527 5			
5810 5			5808.80 8	6559 5			6562.16 6
5833 5	$(\frac{3}{2}^+, \frac{5}{2}^+)$			6575 5			
5861 5				6597 5		6598.19 18	6598.48 5
5883 5	$(\frac{3}{2}^+, \frac{5}{2}^+)$			6641 5	$\frac{3}{2}^+, \frac{5}{2}^+$		
5913 5				6672 5			
5936 5				6683 5			
5957 5		5957.25 16	5957.56 7	6702 5	$\frac{3}{2}^+, \frac{5}{2}^+$		
5978 5	$(\frac{1}{2}^-, \frac{3}{2}^-)$			6719 5	$\frac{3}{2}^+, \frac{5}{2}^+$		
5989.2 3				6742 5	$\frac{3}{2}^+, \frac{5}{2}^+$		
		5994.17 15		6764 5			
6003 5				6781 5			
6024 5	$(\frac{1}{2}^-, \frac{3}{2}^-)$	6030.54 16	6030.59 14	6800 5			
6061 5				6828 5	$\frac{3}{2}^+, \frac{5}{2}^+$		
6076.13 22	$(\frac{15}{2}^-, \frac{17}{2}^-)$			6853 5			
		6101.39 16	6101.73 9	6874 5			6873.64 7
6104 5			6106.73 12	6913 5	$\frac{1}{2}^+$		
6139 5	$\frac{1}{2}^-, \frac{3}{2}^-$	6141.52 16	6141.79 9	6950 5	$\frac{1}{2}^+$		6948.41 15
6179 5			6183.68 14	6969 5			
6196 5	$\frac{3}{2}^+, \frac{5}{2}^+$			6989 5			
6216 5	$(\frac{3}{2}^+, \frac{5}{2}^+)$			7018 5			

the real part of the scattering wave function in a global optical potential model and a valence amplitude resulting from the neutron width amplitude of one or more local resonance levels that account for the difference between the global potential scattering length and the actual thermal-neutron scattering length. The direct-capture cross sections of the  $E1$  transitions observed in the  $^{58}\text{Ni}$  and  $^{60}\text{Ni}$  neutron capture reactions have been calculated in this way; the results are given in this paper. The direct-capture cross sections of transitions in the  $^{59}\text{Ni}$  capture reaction cannot be estimated because there are no spectroscopic factors available from the ( $d, p$ ) reaction.

The differences between the calculated direct-capture cross sections  $\sigma_{\text{dir}, \gamma}$  and the experimental values  $\sigma_{\text{expt}, \gamma}$  are attributed to the admixture of a true compound-nuclear component  $\sigma_{\text{CN}, \gamma}$  whose value is found from the formula

$$\sigma_{\text{expt}, \gamma}^{1/2} = \sigma_{\text{CN}, \gamma}^{1/2} + \sigma_{\text{dir}, \gamma}^{1/2}. \quad (1)$$

The signs of  $\sigma_{\text{expt}, \gamma}^{1/2}$  and  $\sigma_{\text{dir}, \gamma}^{1/2}$  are unknown, of course. This uncertainty implies that there are two possible values of the compound-nuclear capture cross section for each transition. In many of our previous studies of capture by light nuclei [4, 11, 16], the values of the measured cross section and

TABLE II. (Continued.)

Known		Previous	This work	Known		Previous	This work
$E(\text{level})^a$	$J^\pi$	$(n, \gamma)$	$(n, \gamma)$	$E(\text{level})^a$	$J^\pi$	$(n, \gamma)$	$(n, \gamma)$
(keV)		$E(\text{level})^a$	$E(\text{level})^a$	$E(\text{level})^a$		$E(\text{level})^a$	$E(\text{level})^a$
		(keV)	(keV)	(keV)		(keV)	(keV)
7037	5			7279	5		
7068	5			7301	5		
7088	5			7322	5		
7107	5			7351	5		
7120	5			7382	5		
7137	5			7406	5		
7156	5			7432	5		
7163.9	3	$\left(\frac{19}{2}^-, \frac{21}{2}^-\right)$		7454	5		
7183	5		7187.22	7477	5		14
7200	5			7490	5		
7234	5	$\frac{3}{2}^+, \frac{5}{2}^+$		7503	5		
7260	5			7520	5		
		7270.35	20	7270.54	7		7
				7538	5		

<sup>a</sup>In our notation, 339.36 7  $\equiv$  339.36  $\pm$  0.07, 3187 5  $\equiv$  3187  $\pm$  5, etc.

the calculated direct capture were similar, implying that direct capture was the predominant component and that it could therefore be assumed that the lower value of the pair of compound-nuclear cross-section values was the correct one. In capture by the nickel isotopes, it appears that the direct

and compound-nuclear amplitudes are of similar magnitude and therefore we cannot select *a priori* the correct compound-nuclear cross section. We have therefore devised a statistical method to extract the magnitude of the average compound-nuclear capture cross section for each isotope. We compare these averages with theoretical models of the capture mechanism.

Briefly, in this method, we examine certain statistical properties of sequences of  $\sigma_{\text{CN},\gamma}$  values drawn from the pairs of values of all measured transitions and thus determine a range of mean  $\sigma_{\text{CN},\gamma}$  that is consistent with the Porter-Thomas [99] distribution for individual transitions. In principle, it is possible to do this for all possible sequences, but since there are  $2^{26}$  ( $\approx 67 \times 10^6$ ) sequences that can be formed, for example, from the 26 primary  $E1$  transitions measured in the  $^{58}\text{Ni}$  capture reaction, we believe that random sampling from the pairs of values should give a sufficiently accurate picture of the statistical properties of the sequences.

We first assume that the expectation value of the compound-nuclear cross section for a transition with energy  $\varepsilon_\gamma$  is given by

$$\langle \sigma_{\text{CN},\gamma} \rangle = a(\varepsilon_\gamma)^b. \quad (2)$$

The values of  $a$  and  $b$  are to be compared with the predictions of various theories. The value of  $b$  is expected to lie between 3 (the Weisskopf model [100] and variants) and 5 (Brink-Axel model [101,102]). We use the maximum likelihood method to determine the mean values of  $a$  and  $b$  for a given sequence ( $n$  in number) of  $\sigma_{\text{CN},\gamma}$  values (which are labeled  $y_i$  with transition energies  $\varepsilon_i$ ). For an assumed Porter-Thomas distribution of  $\sigma_{\text{CN},\gamma}/(\varepsilon_\gamma)^b$ , the estimates of  $a$  and  $b$  are given by the simultaneous equations

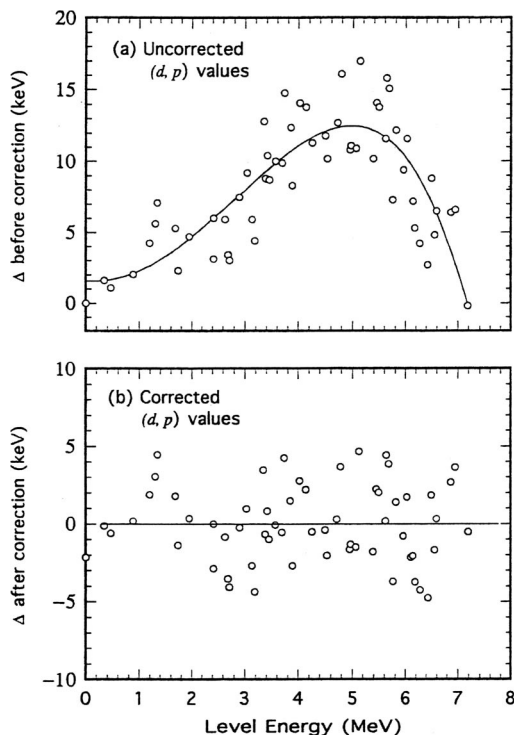


FIG. 3. Deviation  $\Delta$  of the  $^{59}\text{Ni}$  level energies measured in the  $(d, p)$  reaction [33] from the current  $(n, \gamma)$  values. Applying the correction given by the solid line in (a) removes the systematic differences as shown in (b). The corrected values are given in Table II.

TABLE III. Energies ( $E_\gamma$ ) and intensities ( $I_\gamma$ ) of  $\gamma$  rays from the  $^{58}\text{Ni}(n, \gamma)^{59}\text{Ni}$  reaction.

$E_\gamma$ (keV) <sup>a</sup>	$I_\gamma$ (mb) <sup>b</sup>	Placement <sup>c</sup>	$E_\gamma$ (keV) <sup>a</sup>	$I_\gamma$ (mb) <sup>b</sup>	Placement <sup>c</sup>	$E_\gamma$ (keV) <sup>a</sup>	$I_\gamma$ (mb) <sup>b</sup>	Placement <sup>c</sup>
310.78 4	3.02 7	1188 → 877	1256.49 18	0.55 7	unplaced	1725.33 <sup>g</sup> 21	4.0 8	4140 → 2414
339.37 3	221 5	339 → 0	1264.18 20	0.82 9	3686 → 2421	1728.71 7	3.78 13	C → 7270
412.96 9	0.64 6	877 → 464	1269.74 3	4.16 8	1734 → 464	1734.70 3	24.0 3	1734 → 0
423.46 3	13.7 14	1301 → 877	1274.5 7	0.28 9	unplaced	1778.92 20	0.81 8	4494 → 2715
450.0 3	0.28 5	3343 → 2893	1275.9 4	0.52 13	5808 → 4532	1782.97 10	1.95 10	unplaced
451.58 14	0.34 5	unplaced	1301.44 3	76.6 8	1301 → 0	1800.02 17	1.37 12	unplaced
454.77 10	0.40 4	unplaced	1337.87 5	1.68 12	1337 → 0	1802.0 3	0.95 13	2679 → 877
464.94 3	1126 28	464 → 0	1340.28 3	27.3 3	1679 → 339	1812.05 14	0.93 7	C → 7187
538.54 4	4.47 6	877 → 339	1379.40 19	0.50 5	5632 → 4252	1818.7 6	0.32 10	unplaced
545.87 3	4.47 7	1734 → 1188	1382.1 3	0.32 6	unplaced	1820.6 3	0.72 9	unplaced
609.2 3	0.16 4	unplaced	1386.8 3	0.31 6	6102 → 4715	1827.8 5	0.23 6	3562 → 1734
723.93 7	1.02 6	1188 → 464	1395.27 3	6.68 10	1734 → 339	1833.3 6	0.22 7	unplaced
731.85 20	0.31 5	unplaced	1405.7 <sup>d</sup> 8	0.17 7	4968 → 3562	1836.97 12	1.04 9	2715 → 877
735.2 4	0.15 5	2414 → 1679	1414.2 6	0.19 7	unplaced	1851.12 17	1.05 9	unplaced
759.3 3	0.23 5	1948 → 1188	1434.12 16	0.76 7	unplaced	1864.9 4	0.50 9	5754 → 3889
766.65 4	3.58 8	3181 → 2414	1438.58 10	2.03 8	3853 → 2414	1872.2 3	0.58 9	unplaced
797.03 6	0.97 5	4140 → 3343	1446.85 4	14.86 16	3181 → 1734	1880.12 5	5.61 13	3181 → 1301
801.78 15	0.34 4	1679 → 877	1449.0 4	0.48 9	unplaced	1889.13 17	1.88 16	6141 → 4252
816.3 3	0.29 5	5069 → 4252	1474.81 9	1.38 7	3889 → 2414	1891.0 7	0.40 14	unplaced
818.1 7	0.12 5	unplaced	1490.6 3	0.67 11	2679 → 1188	1901.9 3	0.75 14	5632 → 3730
822.6 3	0.21 5	unplaced	1492.3 4	0.48 11	5632 → 4140	1917.0 9	0.19 8	unplaced
827.9 5	0.16 5	3853 → 3025	1496.2 4	0.27 6	unplaced	1923.4 4	0.74 13	4949 → 3025
836.48 3	12.0 13	1301 → 464	1501.84 3	21.23 22	3181 → 1679	1937.7 3	0.93 13	4352 → 2414
840.6 3	0.35 6	4021 → 3181	1513.0 4	0.31 6	4140 → 2627	1943.3 4	0.73 13	4968 → 3025
849.36 4	3.4 8	1188 → 339	1536.90 3	27.3 4	2414 → 877	1948.3 4	1.3 2	1948 → 0
877.94 3	325 3	877 → 0	1539.5 3	0.58 8	unplaced	1949.92 3	67.6 14	2414 → 464
962.00 19	0.34 5	1301 → 339	1545.54 11	0.96 6	unplaced	1992.76 4	21.21 22	3181 → 1188
998.50 3	3.65 8	1337 → 339	1555.8 <sup>e</sup> 3	0.59 9	2893 → 1337	2001.93 10	2.34 12	unplaced
1006.3 4	0.22 5	3686 → 2679	1557.7 7	0.21 8	unplaced	2015.53 3	16.94 19	2893 → 877
1008.9 4	0.22 5	4352 → 3343	1567.5 6	0.18 6	unplaced	2042.0 <sup>h</sup> 7	1.0 3	5384 → 3343
1031.5 3	0.34 6	unplaced	1572.1 5	0.23 7	4949 → 3377	2050.78 15	1.35 11	C → 6948
1045.76 18	0.59 6	unplaced	1592.06 8	1.58 8	2893 → 1301	2075.37 6	3.44 12	4968 → 2893
1048.8 3	0.38 6	unplaced	1599.8 6	0.22 6	4021 → 2421	2094.05 16	1.21 9	unplaced
1051.0 6	0.18 6	3730 → 2679	1607.07 16	1.21 10	4021 → 2414	2112.0 3	0.74 9	3413 → 1301
1078.27 10	0.87 6	unplaced	1609.0 <sup>f</sup> 3	0.89 11	1948 → 339	2125.60 7	2.50 12	C → 6873
1103.2 4	0.22 5	3730 → 2627	1613.8 4	0.35 6	unplaced	2147.77 3	17.31 20	3025 → 877
1113.38 6	2.25 7	2414 → 1301	1617.0 5	0.29 7	5069 → 3452	2154.3 4	0.57 11	3343 → 1188
1147.98 10	0.64 5	3562 → 2414	1623.49 13	0.93 7	unplaced	2174.55 21	1.13 11	unplaced
1156.1 5	0.16 4	unplaced	1663.7 8	0.22 9	3343 → 1679	2177.3 9	0.26 9	6030 → 3853
1158.6 3	0.26 5	2893 → 1734	1665.8 3	0.55 9	unplaced	2242.9 5	0.32 8	unplaced
1163.5 3	0.38 8	unplaced	1679.73 14	4.3 4	1679 → 0	2248.2 <sup>i</sup> 3	0.51 8	3126 → 877
1188.77 3	76.9 8	1188 → 0	1688.00 14	1.08 9	3025 → 1337	2254.68 17	0.99 8	5632 → 3377
1210.5 4	0.37 8	3889 → 2679	1695.64 25	0.78 11	unplaced	2258.03 13	1.38 9	6279 → 4021
1213.81 9	2.95 18	2893 → 1679	1704.67 6	4.30 13	2893 → 1188	2261.44 15	2.42 15	3562 → 1301
1214.7 4	0.42 15	1679 → 464	1717.65 21	0.95 11	3452 → 1734	2263.35 <sup>j</sup> 25	1.14 17	3452 → 1188
1226.08 3	17.9 3	2414 → 1188	1724.17 12	7.43 9	3025 → 1301	2267.96 11	1.46 8	unplaced

$$a = \left[ \sum_i y_i / (\varepsilon_i)^b \right] / n$$

and

$$a \sum_i \ln \varepsilon_i - \sum_i y_i (\varepsilon_i)^{-b} \ln \varepsilon_i = 0.$$

- (3) In practice, we assume a value for  $b$ , calculate  $a$ , and the left-hand side of Eq. (4) which we call  $Mb$ . We also calculate the maximum likelihood estimator for the  $\chi$ -squared family of statistical distributions with characterizing parameter  $\nu$  (known as the “number of degrees of freedom”). The Porter-Thomas distribution is a member of this family with  $\nu=1$ . The expression for this maximum likelihood estimator is

TABLE III. (Continued.)

$E_\gamma$ (keV) <sup>a</sup>	$I_\gamma$ (mb) <sup>b</sup>	Placement <sup>c</sup>	$E_\gamma$ (keV) <sup>a</sup>	$I_\gamma$ (mb) <sup>b</sup>	Placement <sup>c</sup>	$E_\gamma$ (keV) <sup>a</sup>	$I_\gamma$ (mb) <sup>b</sup>	Placement <sup>c</sup>
2287.61	17 1.25	14 2627 → 339	2723.2	5 0.37	9 5617 → 2893	3184.56 <sup>s</sup>	25 1.64	13 6598 → 3413
2297.0	4 0.42	10 unplaced	2727.6	3 0.76	12 unplaced	3190.39	8 2.84	10 C → 5808
2303.53	5 5.94	14 3181 → 877	2739.0	4 0.61	9 5632 → 2893	3200.54	7 4.87	12 3540 → 339
2323.5	3 0.54	9 unplaced	2757.59	9 2.55	12 5384 → 2627	3214.7	4 0.55	11 4949 → 1734
2328.7	5 0.87	25 unplaced	2763.7	4 0.58	9 6106 → 3343	3221.04	5 21.5	3 3686 → 464
2330.8	4 1.55	20 unplaced	2771.07	24 0.82	9 unplaced	3234.2	4 0.59	11 4968 → 1734
2345.2	4 0.45	9 unplaced	2786.5	3 0.69	9 3126 → 339	3244.50	9 3.11	13 C → 5754
2380.4	5 0.44	8 unplaced	2808.09 <sup>m</sup>	5 12.25	20 3686 → 877	3250.0	4 0.70	10 6431 → 3181
2384.64	4 9.97	14 3686 → 1301	2815.52	14 2.14	12 C → 6183	3256.63	15 1.60	10 unplaced
2400.75	5 7.97	11 C → 6598	2823.1	4 0.74	11 unplaced	3262.01 <sup>t</sup>	18 1.59	16 4140 → 877
t 2414.86	4 18.0	3 2414 → 0	2833.18	11 2.74	13 4021 → 1188	3265.23	7 7.75	16 3730 → 464
2421.89 <sup>k</sup>	6 4.02	10 2421 → 0	2838.67	11 4.03	17 4140 → 1301	3268.8	4 0.89	12 4949 → 1679
2425.06	19 1.06	8 unplaced	2842.07	6 67.3	7 3181 → 339	3289.3	4 0.67	11 4968 → 1679
2428.53	4 9.7	12 2893 → 464	2852.2	4 0.76	12 3730 → 877	3295.57	20 2.35	25 unplaced
2437.06	6 3.54	9 C → 6562	2857.40	12 4.67	15 C → 6141	3297.0	3 4.9	6 C → 5702
2450.9	9 0.23	6 5632 → 3181	2878.22	18 1.53	18 3343 → 464	3303.20	16 1.66	11 unplaced
2460.2	4 0.44	4 4140 → 1679	2892.3	5 5.1	7 C → 6106	3317.58	23 1.09	11 unplaced
2465.5 <sup>l</sup>	4 0.39	8 5808 → 3343	2893.3	3 11.7	12 2893 → 0	3322.7	5 0.53	11 C → 5676
2483.16	12 1.41	8 unplaced	2897.50	9 4.72	17 C → 6101	3334.2	6 0.39	12 5069 → 1734
2491.3 <sup>m</sup>	4 0.50	8 5617 → 3126	2911.7 <sup>o</sup>	8 0.82	25 3377 → 464	3339.2	5 0.46	11 5754 → 2414
2497.33	6 8.35	15 3686 → 1188	2927.0	4 0.54	9 unplaced	3346.62	5 9.34	14 3686 → 339
2499.18	11 2.54	24 3377 → 877	2948.3	3 1.29	11 3413 → 464	3367.02	6 10.65	16 C → 5632
2500.6	3 1.23	15 C → 6498	2951.06	15 2.19	12 4252 → 1301	3374.9	7 0.60	17 4252 → 877
2505.1	5 0.36	9 5957 → 3452	2963.28	17 1.21	9 unplaced	3377.34	17 2.72	18 4715 → 1337
2535.3	4 0.76	12 3413 → 877	2968.5	7 12.6	3  C → 6030	3381.83	6 8.95	15 C → 5617
2541.30	22 1.19	12 3730 → 1188	2976.5	9 0.18	8 unplaced	3388.4	5 0.97	21 3853 → 464
2545.7	4 0.69	12 4494 → 1948	2980.2 <sup>p</sup>	4 0.60	10 6106 → 3126	3390.6	4 1.56	20 3730 → 339
2554.06	4 62.6	8 2893 → 339	2987.5 <sup>q</sup>	5 0.41	10 3452 → 464	3393.8	5 0.61	12 5808 → 2414
2567.89	9 3.20	14 C → 6431	3003.9	9 1.9	5 3343 → 339	3437.7	6 0.44	10 unplaced
2574.29	21 1.24	13 3452 → 877	3005.2	5 3.0	5 6030 → 3025	3452.08 <sup>u</sup>	17 1.33	13 3452 → 0
2616.2	3 0.97	13 unplaced	3025.63	5 17.65	20 3025 → 0	3496.9	6 0.52	12 6873 → 3377
2618.6	3 1.03	13 unplaced	3029.17	20 1.69	12 5443 → 2414	3504.94	12 3.28	20 C → 5494
2626.70	19 1.48	16 2627 → 0	3037.73	6 6.53	15 3377 → 339	3514.05	18 2.16	18 3853 → 339
2629.21	16 1.76	12 unplaced	3041.60	7 6.68	14 C → 5957	3525.8	8 0.38	12 4715 → 1188
2633.38	22 1.02	11 unplaced	3045.66	17 1.79	12 6498 → 3452	3545.2	3 1.38	17 unplaced
2636.61	22 1.00	11 unplaced	3051.5	3 0.83	16 4352 → 1301	3555.47	16 2.74	20 C → 5443
2645.94	19 1.51	10 unplaced	3063.85 <sup>r</sup>	11 2.86	13 4252 → 1188	3562.82	7 9.1	3 3562 → 0
2653.90	18 1.57	12 5069 → 2414	3072.2	4 0.64	12 5494 → 2421	3614.38	7 7.4	3 C → 5384
2662.0	3 0.40	13 3540 → 877	3111.0	3 1.06	12 unplaced	3635.2	5 0.69	15 unplaced
2664.80	19 1.19	11 3853 → 1188	3113.0	8 0.50	16 3452 → 339	3667.53	18 1.80	14 4968 → 1301
2679.6	3 0.90	12 2679 → 0	3125.6	6 0.52	12 3126 → 0	3675.23	4 39.4	5 4140 → 464
2684.97	5 16.0	3 3562 → 877	3136.6	3 0.99	13 6030 → 2893	3679.2	5 1.08	16 6101 → 2421
2689.0	4 0.86	12 6141 → 3452	3143.78	14 3.03	15 4021 → 877	3685.98	15 16.8	9 3686 → 0
2703.78	14 1.71	11 unplaced	3156.28	16 1.38	11 4494 → 1337	3705.3	5 0.55	12 5384 → 1679
2716.57	10 3.55	14 3181 → 464	3163.5	4 1.12	20 4352 → 1188	3712.07	18 2.44	20 unplaced
2719.38	7 4.89	15 C → 6279	3181.45	6 15.50	17 3181 → 0	3719.1	6 0.75	18 6141 → 2421

$$M\nu = \left[ \sum_i (\ln y_i - b \ln \varepsilon_i) \right] / (n - \ln a). \quad (5)$$

The expectation value of  $M\nu$  is  $-1.24$  for  $\nu=1$  with a standard deviation depending on  $n$ . For  $n=26$  ( $^{58}\text{Ni}$ ) the standard deviation is  $\pm 0.28$ , while that for  $Mb$  is  $\pm 1.25$ . For  $n=16$  ( $^{60}\text{Ni}$ ), it is  $\pm 0.34$  for  $M\nu$  and  $\pm 1.5$  for  $Mb$ . Sequences of  $\sigma_{\text{CN},\gamma}$  values that lie within these ranges of the maximum

likelihood estimators are considered statistically acceptable and thus give us an estimate of the mean value of  $a$  and its error range for a given value of  $b$ . More detail on the application of this method can be found in Secs. IV C and VI C.

### G. Shell-model calculations of energy levels

We have carried out large-scale shell-model calculations for the three nickel isotopes  $^{59,60,51}\text{Ni}$  using the shell-model

TABLE III. (*Continued.*)

$E_\gamma$ (keV) <sup>a</sup>	$I_\gamma$ (mb) <sup>b</sup>	Placement <sup>c</sup>	$E_\gamma$ (keV) <sup>a</sup>	$I_\gamma$ (mb) <sup>b</sup>	Placement <sup>c</sup>	$E_\gamma$ (keV) <sup>a</sup>	$I_\gamma$ (mb) <sup>b</sup>	Placement <sup>c</sup>
3730.11 <sup>v</sup> 5	2.0 <sup>w</sup> 3	3730 → 0	4507.9 5	0.80 25	7187 → 2679	5617.12 18	3.10 17	5617 → 0
3730.35 <sup>v</sup> 10	2.7 <sup>x</sup> 3	7270 → 3540	4604.1 7	0.44 13	5069 → 464	5621.6 14	5.29 20	C → 3377
3734.0 9	0.27 13	7187 → 3452	4609.3 4	0.66 14	4949 → 339	5632.4 9	0.47 15	5632 → 0
3767.3 5	0.80 16	5069 → 1301	4629.7 6	0.61 14	4968 → 339	5641.65 25	2.16 20	6106 → 464
3779.94 7	10.4 3	4968 → 1188	4646.69 9	5.67 25	C → 4352	5655.5 5	1.18 18	C → 3343
3787.5 4	1.12 18	4252 → 464	4715.16 6	12.0 4	4715 → 0	5682.5 7	0.67 16	unplaced
3800.69 15	3.05 24	4140 → 339	4729.8 5	0.83 15	5069 → 339	5701.5 4	1.38 17	5702 → 0
3838.1 5	0.71 16	unplaced	4746.19 10	5.84 25	C → 4252	5754.6 7	0.86 22	5754 → 0
3853.71 16	2.37 18	3853 → 0	4805.03 16	2.96 19	6106 → 1301	5817.35 5	151.9 20	C → 3181
3857.8 3	1.36 17	6279 → 2421	4824.1 5	1.10 18	5702 → 877	5843.7 7	1.05 25	6183 → 339
3867.15 20	2.06 19	C → 5131	4841.4 6	0.55 15	6030 → 1188	5887.1 6	0.94 17	unplaced
3879.8 6	0.58 15	5069 → 1188	4858.84 3	64.2 8	C → 4140	5901.6 6	0.90 18	unplaced
3889.47 15	3.06 19	3889 → 0	4912.1 9	0.41 15	6101 → 1188	5935.0 9	0.50 17	unplaced
3897.7 7	0.50 15	5632 → 1734	4919.8 3	1.32 21	5384 → 464	5956.9 3	2.5 3	5957 → 0
3905.8 7	0.51 15	unplaced	4949.02 10	11.7 5	4949 → 0	5973.14 5	36.8 8	C → 3025
3912.7 6	0.49 14	4252 → 339	4968.6 4	1.79 23	4968 → 0	5994.0 4	1.24 17	unplaced
3930.06 5	16.7 4	C → 5069	4977.27 8	10.6 4	C → 4021	6030.4 3	1.73 17	6030 → 0
3937.5 8	0.39 9	5617 → 1679	5029.6 9	0.38 18	5494 → 464	6105.38 6	98.0 14	C → 2893
3952.6 4	1.11 16	5632 → 1679	5044.9 4	1.06 17	5384 → 339	6111.6 4	1.48 23	unplaced
3972.64 21	1.51 17	unplaced	5068.97 13	4.47 22	5069 → 0	6141.42 23	2.37 19	6141 → 0
3989.9 4	0.72 14	unplaced	5078.9 5	0.94 16	5957 → 877	6160.0 7	0.74 16	unplaced
4021.69 21	1.73 16	4021 → 0	5109.37 12	4.36 21	C → 3889	6258.8 3	1.56 16	6598 → 339
4030.26 4	20.9 4	C → 4968	5113.8 9	0.49 16	unplaced	6279.0 9	0.38 16	6279 → 0
4049.99 5	14.1 3	C → 4949	5130.7 3	1.40 15	unplaced	6371.2 9	0.55 16	C → 2627
4056.1 6	0.56 14	unplaced	5140.3 6	0.79 15	unplaced	6391.9 5	1.10 17	7270 → 877
4067.4 6	0.64 15	4532 → 464	5145.34 10	5.91 23	C → 3853	6401.2 7	0.77 16	unplaced
4071.5 4	0.90 15	4949 → 877	5152.37 <sup>z</sup> 23	1.87 16	6030 → 877	6408.0 5	1.06 17	6873 → 464
4083.0 5	0.74 15	5384 → 1301	5169.2 9	0.35 14	unplaced	6499.0 8	0.65 15	unplaced
4090.6 5	0.67 14	4968 → 877	5224.0 4	0.95 15	6562 → 1337	6516.2 9	0.43 15	unplaced
4119.4 9	0.38 16	unplaced	5228.6 7	0.40 13	6106 → 877	6561.7 8	0.79 22	6562 → 0
4140.10 <sup>y</sup> 8	10.0 4	4140 → 0	5268.79 5	12.3 4	C → 3730	6576.8 6	1.47 23	C → 2421
4191.04 10	4.72 19	5069 → 877	5277.5 5	0.85 15	5617 → 339	6583.98 6	109.4 15	C → 2414
4216.08 20	1.87 20	C → 4782	5287.3 6	0.84 18	unplaced	6598.15 25	3.5 3	6598 → 0
4237.6 5	0.76 16	unplaced	5292.7 4	1.49 19	5632 → 339	6617.5 9	0.60 19	unplaced
4250.6 5	1.6 3	4715 → 464	5312.95 4	75.4 9	C → 3686	6644.2 9	0.44 18	unplaced
4253.6 4	2.20 5	5131 → 877	5362.5 3	1.93 21	5702 → 339	6752.6 8	0.58 16	unplaced
4283.77 5	18.5 5	C → 4715	5384.6 7	0.78 23	5384 → 0	6872.8 8	0.63 15	6873 → 0
4295.9 4	0.89 15	6030 → 1734	5409.4 6	0.88 18	6598 → 1188	6892.0 9	0.46 14	unplaced
4305.2 3	1.42 16	5494 → 1188	5436.00 4	26.3 5	C → 3562	6940.3 8	0.53 15	unplaced
4317.5 3	1.17 16	4782 → 464	5458.79 18	3.19 22	C → 3540	6947.6 4	1.33 16	6948 → 0
4352.4 3	2.22 19	4352 → 0	5469.4 6	0.68 16	5808 → 339	7050.1 9	0.43 16	C → 1948
4375.31 19	2.44 19	5676 → 1301	5492.1 6	0.68 14	5957 → 464	7264.18 6	9.3 3	C → 1734
4428.24 19	1.70 17	5617 → 1188	5546.8 14	2.87 17	C → 3452	7697.30 6	51.7 7	C → 1301
4452.3 9	0.30 12	6873 → 2421	5553.0 4	0.98 14	6431 → 877	8120.75 7	177 3	C → 877
4466.2 6	0.52 13	C → 4532	5566.4 8	0.61 16	unplaced	8533.71 7	996 15	C → 464
4504.7 3	2.33 18	C → 4494	5585.2 6	0.70 14	C → 3413	8998.63 7	2082 30	C → 0

code ANTOINE [103]. The full *pf* shell (orbits  $0f_{7/2}, 1p_{3/2}, 0f_{5/2}$ , and  $1p_{1/2}$ ) was used as valence space with the KB3G effective interaction [104]. Because the number of possible levels is very large, it is necessary to limit the total number of possible configurations using some truncation scheme. The configurations included in the calculations are of the type  $(f_{7/2})^{16-t}, (p_{3/2}, f_{5/2}, p_{1/2})^{n+t}$ , where  $n=3, 4$ , and 5 for  $^{59}\text{Ni}$ ,  $^{60}\text{Ni}$ , and  $^{61}\text{Ni}$ , respectively, and  $t$ , which is either 0,

1, 2, or 3, is the additional particles excited outside the  $f_{7/2}$  shell.

#### IV. REACTION $^{58}\text{Ni}(n, \gamma)$

##### A. Skeleton level scheme of $^{59}\text{Ni}$

Table I lists the variety of previous measurements that have been carried out concerning the energy levels in  $^{59}\text{Ni}$ .

TABLE III. (Continued.)

<sup>a</sup> In our notation, $310.78 \pm 0.04$ , etc.	<sup>n</sup> Can also be placed as a 6948 $\rightarrow$ 4140 transition.
<sup>b</sup> In our notation, $3.02 \pm 0.07$ , etc. Multiply by 0.0243 to obtain photons per 100 thermal neutron captures.	<sup>o</sup> Can also be placed as a 6598 $\rightarrow$ 3686 transition.
<sup>c</sup> C denotes the capturing state.	<sup>p</sup> Can also be placed as a 4715 $\rightarrow$ 1734 transition.
<sup>d</sup> Can also be placed as a 4782 $\rightarrow$ 3377 transition.	<sup>q</sup> Can also be placed as a 5702 $\rightarrow$ 2715 transition.
<sup>e</sup> Can also be placed as a 5808 $\rightarrow$ 4252 transition.	<sup>r</sup> Can also be placed as a 5957 $\rightarrow$ 2893 transition.
<sup>f</sup> Can also be placed as a 6141 $\rightarrow$ 4532 transition.	<sup>s</sup> Can also be placed as a 6562 $\rightarrow$ 3377 transition.
<sup>g</sup> Can also be placed as a 4352 $\rightarrow$ 2627 transition.	<sup>t</sup> Can also be placed as a 6948 $\rightarrow$ 3686 transition.
<sup>h</sup> Can also be placed as a 5494 $\rightarrow$ 3452 transition or as a 3343 $\rightarrow$ 1301 transition.	<sup>u</sup> Can also be placed as a 5131 $\rightarrow$ 1679 transition.
<sup>i</sup> Can also be placed as a 6101 $\rightarrow$ 3853 transition.	<sup>v</sup> Deduced for one member of a close doublet from level energies obtained by an overall least-squares fit excluding this transition.
<sup>j</sup> Can also be placed as a 5676 $\rightarrow$ 3413 transition.	<sup>w</sup> Inferred from the measured intensity of the 3730.11 + 3730.35 doublet.
<sup>k</sup> Can also be placed as a 6562 $\rightarrow$ 4140 transition.	<sup>x</sup> Inferred from the intensity balance requirement for the 7270 keV level.
<sup>l</sup> Can also be placed as a 3343 $\rightarrow$ 877 transition.	<sup>y</sup> Can also be placed as a 6562 $\rightarrow$ 2421 transition.
<sup>m</sup> Can also be placed as a 5384 $\rightarrow$ 2893 transition.	<sup>z</sup> Can also be placed as a 5617 $\rightarrow$ 464 transition.

Based on these measurements, we have assembled a list (see Table II) of  $\sim 217$  levels below 7.54 MeV. Eleven works [19–21,23,31,33,35–38,41] out of the 25 listed in Table I contain additional information leading to  $J^\pi$  values for  $\sim 90$  levels. We have critically evaluated this information and our adopted  $J^\pi$  values are also listed in Table II.

The  $^{58}\text{Ni}(d,p)^{59}\text{Ni}$  study by Cosman, Paris, Sperduto, and Enge [33] is the backbone of the skeleton level scheme. Herein lies a problem. These authors have listed 173 levels up to an excitation energy of 7.5 MeV. They estimate the uncertainties in the excitation energies as “ $\pm 5$  keV for the lowest states and  $\pm 10$  keV for the highest excited states.” Quite early in our attempts to construct an  $(n, \gamma)$  level scheme, we began to suspect that serious systematic uncertainties are present in the  $(d, p)$  excitation energies. This suspicion arose while trying to establish the expected one-to-one correspondence between energy levels populated strongly by primary  $\gamma$  rays in the  $(n, \gamma)$  reaction and levels with  $\ell_n=1$  angular distributions in the  $(d, p)$  reaction. The systematic differences that exist between the  $(d, p)$  and  $(n, \gamma)$  level energies are illustrated in Fig. 3(a). It is then straightforward to apply corrections to the  $(d, p)$  energies. These corrected values are used in Table II in constructing a cumulative list of  $\sim 217$  levels from a variety of experiments. About 30% of these are populated significantly in the current (thermal  $n, \gamma$ ) study.

### B. Thermal-neutron capture $\gamma$ -ray data

The  $^{58}\text{Ni}(n, \gamma)$  reaction with thermal neutrons has been studied previously with Ge detectors at the Pelindaba, McMaster, and Grenoble reactors by Hofmeyr [27], Ishaq *et al.* [28], and Harder *et al.* [30], respectively. The study by Harder *et al.* [30] at Grenoble is the most extensive of these three studies. The table of  $\gamma$  rays published in Ref. [30] is an abridged version of a more extensive table contained in the unpublished thesis of Harder [29]. (In the published paper, she chose to omit the unplaced  $\gamma$  rays and those that were very weak and therefore questionable.) The thesis [29] was made available to us and this report was of considerable help in our analysis of the  $\gamma$ -ray spectra.

The current (thermal  $n, \gamma$ ) measurements were made with a 120.5-mg, 99.93%-enriched  $^{58}\text{NiO}$  target. The results are given in Table III. In most measurements made at the Los Alamos Omega West reactor, the detection limit for a  $\gamma$  ray in the 0.1–10.0 MeV region is typically 2–4 photons per  $10^4$  thermal-neutron captures, which is a factor of 2–5 better than in measurements at other facilities also using Ge detectors. (The weakest  $\gamma$  ray that we have detected is the 7120-keV, primary transition from the neutron-capturing state to the 696-keV, first-excited state in  $^{144}\text{Nd}$  with an intensity of only  $\sim 3$  photons per  $10^5$  captures [105], but this was a case requiring special efforts.) The limitations on sensitivity arise as a result of the Compton tails of higher energy  $\gamma$  rays and room background. In the case of the  $^{58}\text{Ni}(n, \gamma)$  reaction, however, the sensitivity was much better than usual. We have detected nearly 50  $\gamma$  rays with intensities smaller than one photon per  $10^4$  captures, including ten  $\gamma$  rays below 2 MeV with intensities less than five photons per  $10^5$  captures. There is a reason for this apparent improvement in the sensitivity. In the  $^{58}\text{Ni}(\text{thermal } n, \gamma)$  reaction, the two highest-energy  $\gamma$  rays at 8534 and 8999 keV account for nearly 75% of the capture cross section of  $\sim 4$  b. The Compton backgrounds from these two  $\gamma$  rays are either eliminated by the pair-spectrometer requirement or reduced by Compton suppression. The ability to detect other  $\gamma$  rays remains largely unaffected except that when the sensitivity is expressed in units of photons per  $10^4$  neutron captures, there is now an apparent gain by a factor of  $\sim 4$ .

The level scheme resulting from this work is presented in Table IV. Nearly three-fourths of the observed  $\gamma$  rays, totaling 414 in number, have been incorporated into this scheme consisting of 65 bound levels. According to Harder *et al.* [30], 41 levels in  $^{59}\text{Ni}$  are populated significantly in the (thermal  $n, \gamma$ ) reaction. We confirm this conclusion for all except the levels at 3858.26 and 5994.17 keV. The 3858.26-keV level was introduced in Ref. [30] to accommodate a primary  $\gamma$  ray of energy 5140.76 keV and secondary  $\gamma$  rays of energies 2178.63, 2980.59, and 3858.04 keV. The strongest of the secondary  $\gamma$  rays at 2178.63 keV has a reported intensity of eight photons per  $10^4$  neutron captures. The relevant portion of the  $\gamma$ -ray spectrum from 2140 to 2190 keV is shown in Fig. 4. We do see a very weak shoulder at 2177.3 keV but the intensity of a peak at this energy is only  $\sim 6$  photons per

TABLE IV. Level scheme of  $^{59}\text{Ni}$  from this work in tabular form.

$E(\text{level})^a$ (keV)	$J^\pi$	Deexciting $\gamma$ rays <sup>b</sup>	$I_\gamma$ (in) <sup>a</sup> (mb)	$I_\gamma$ (out) <sup>a</sup> (mb)	$I_\gamma$ (in - out) <sup>a</sup> (mb)
0.0	$\frac{3}{2}^+$		4110 50		4110 50
339.399 16	$\frac{3}{2}^+$	339.37	219.7 17	221 5	-1 6
464.935 16	$\frac{1}{2}^-$	464.94	1179 16	1130 30	50 40
877.961 15	$\frac{3}{2}^-$	877.94, 538.54, 412.96	318 4	330 3	-12 5
1188.789 16	$\frac{3}{2}^-$	1188.77, 849.36, 723.93, 310.78	84.3 8	84.3 12	-0.1 14
1301.437 17	$\frac{1}{2}^-$	1301.44, 962.00, 836.48, 423.46	97.5 9	102.6 21	-5.1 23
1337.89 3	$\frac{3}{2}^-$	1337.87, 998.50	6.7 3	5.33 15	1.4 4
1679.700 24	$\frac{3}{2}^-$	1679.73, 1340.28, 1214.7, 801.78	28.6 4	32.4 6	-3.8 7
1734.687 17	$\frac{3}{2}^-$	1734.70, 1395.27, 1269.74, 545.87	28.5 5	39.3 4	-10.8 6
1948.32 17	$\frac{3}{2}^-$	1948.3, 1609.0, 759.3	1.12 20	2.42 24	-1.3 3
2414.892 17	$\frac{3}{2}^-$	2414.86, 1949.92, 1536.90, 1226.08, 1113.38, 735.2	127.5 18	133.2 16	-5.7 23
2421.95 6		2421.89	6.6 5	4.02 10	2.6 5
2627.05 8	$\frac{7}{2}^-$	2626.70, 2287.61	3.63 22	2.73 22	0.9 3
2679.57 14	$(\frac{5}{2}^-)$	2679.6, 1802.0, 1490.6	1.6 3	2.52 21	-1.0 4
2715.03 11		1836.97	0.81 8	1.04 9	-0.23 12
2893.521 20	$\frac{3}{2}^-$	2893.3, 2554.06, 2428.53, 2015.53, 1704.67, 1592.06, 1555.8, 1213.81, 1158.6	103.7 15	110.6 19	-6.9 24
3025.769 25	$(\frac{1}{2}^-, \frac{3}{2}^-)$	3025.63, 2147.77, 1724.17, 1688.00	41.4 10	43.5 4	-2.0 11
3126.10 17		3125.6, 2786.5, 2248.2	1.10 13	1.72 17	-0.62 22
3181.564 18	$\frac{3}{2}^-$	3181.45, 2842.07, 2716.57, 2303.53, 1992.76, 1880.12, 1501.84, 1446.85, 766.65	153.2 20	158.8 9	-5.6 22
3343.22 6		3003.9, 2878.22, 2154.3, 1663.7, 450.0	4.3 4	4.5 6	-0.2 7
3377.22 6		3037.73, 2911.7, 2499.18,	7.0 3	9.9 4	-2.9 5
3413.55 15	$\frac{1}{2}^+$	2948.3, 2535.3, 2112.0,	2.34 20	2.79 19	-0.5 3
3452.34 9	$\frac{3}{2}^-$	3452.08, 3113.0, 2987.5, 2574.29, 2263.35, 1717.65	6.4 3	5.6 4	0.9 5
3540.06 6		3200.54, 2662.0	5.9 4	5.27 18	0.6 5
3562.98 3	$\frac{1}{2}^-, \frac{3}{2}^-$	3562.82, 2684.97, 2261.44, 1827.8, 1147.98	26.5 5	28.4 5	-1.9 7
3686.110 22	$(\frac{3}{2}^+)$	3685.98, 3346.62, 3221.04, 2808.09, 2497.33, 2384.64, 1264.18, 1006.3	75.4 9	79.3 10	-3.8 14
3730.25 5	$(\frac{3}{2}^-)$	3730.20, 3390.6, 3265.23, 2852.2, 2541.30, 1103.2, 1051.0	13.1 5	13.7 5	0.6 6
3853.63 6	$\frac{3}{2}^-$	3853.71, 3514.05, 3388.4, 2664.80, 1438.58, 827.9	6.17 25	8.9 4	-2.7 5
3889.70 7		3889.47, 1474.81, 1210.5	4.86 23	4.81 22	0.1 4
4021.87 5	$\frac{1}{2}^-, \frac{3}{2}^-$	4021.69, 3143.78, 2833.18, 1607.07, 1599.8, 840.6	12.0 5	9.3 3	2.7 5
4140.242 25	$\frac{3}{2}^-$	4140.10, 3800.69, 3675.23, 3262.01, 2838.67, 2460.2, 1725.33, 1513.0, 797.03	64.7 8	63.8 11	0.9 14
4252.75 6	$(\frac{1}{2}^-, \frac{3}{2}^-)$	3912.7, 3787.5, 3374.9, 3063.85, 2951.06	8.5 3	7.3 4	1.3 5
4352.46 8		4352.4, 3163.5, 3051.5, 1937.7, 1008.9	5.67 25	5.3 4	0.4 5
4494.18 12	$\frac{5}{2}^+$	3156.28, 2545.7, 1778.92	2.33 18	2.88 19	-0.5 3
4532.8 3		4067.4	1.04 19	0.64 15	0.40 24
4715.34 4	$(\frac{3}{2}^-)$	4715.16, 4250.6, 3525.8, 3377.34	18.8 5	16.7 6	2.1 8
4782.91 17	$(\frac{3}{2}^+)$	4317.5	1.87 20	1.17 16	0.7 3
4949.17 5	$(\frac{1}{2}^-, \frac{3}{2}^-)$	4949.02, 4609.3, 4071.5, 3268.8, 3214.7, 1923.4, 1572.1	14.1 3	15.7 6	-1.6 7

TABLE IV. (Continued.)

$E(\text{level})^a$ (keV)	$J^\pi$	Deexciting $\gamma$ rays <sup>b</sup>	$I_\gamma$ (in) <sup>a</sup> (mb)	$I_\gamma$ (out) <sup>a</sup> (mb)	$I_\gamma$ (in - out) <sup>a</sup> (mb)
4968.89 4	$\frac{1}{2}^-, \frac{3}{2}^-$	4968.6, 4629.7, 4090.6, 3779.94, 3667.53, 3289.3, 3234.2, 2075.37, 1943.3, 1405.7	20.9 4	20.9 6	0.0 7
5069.10 5	$\frac{1}{2}^-, \frac{3}{2}^-$	5068.97, 4729.8, 4604.1, 4191.04, 3879.8, 3767.3, 3334.2, 2653.90, 1617.0, 816.3	16.7 4	14.4 5	2.3 6
5131.94 18	$\frac{1}{2}^+$	4253.6	2.06 19	2.20 5	-0.14 20
5384.76 7	$\frac{3}{2}^+$	5384.6, 5044.9, 4919.8, 4083.0, 3705.3, 2757.59, 2042.0	7.4 3	8.0 6	-0.6 6
5443.87 13	$\frac{3}{2}^+, \frac{5}{2}^+$	3029.17	2.74 20	1.69 12	1.05 24
5494.23 11		5029.6, 4305.2, 3072.2	3.28 20	2.4 3	0.8 4
5617.33 6	$\frac{1}{2}^-, \frac{3}{2}^-$	5617.12, 5277.5, 4428.24, 3937.5, 2723.2 2491.3	8.95 15	6.9 4	2.0 4
5632.17 6		5632.4, 5292.7, 3952.6, 3897.7, 2739.0, 2450.9, 2254.68, 1901.9, 1492.3, 1379.40	10.65 16	7.1 4	3.5 5
5676.87 18	$\frac{1}{2}^+$	4375.31	0.53 11	2.44 19	-1.91 22
5702.11 18		5701.5, 5362.5, 4824.1	4.9 6	4.4 4	0.5 7
5754.67 9	$\frac{1}{2}^-, \frac{3}{2}^-$	5754.6, 3339.2, 1864.9	3.11 13	1.8 3	1.3 3
5808.80 8		5469.4, 3393.8, 2465.5, 1275.9	2.84 10	2.2 3	0.6 3
5957.56 7		5956.9, 5492.1, 5078.9, 2505.1	6.68 14	4.5 4	2.2 4
6030.59 14	$(\frac{1}{2}^-, \frac{3}{2}^-)$	6030.4, 5152.37, 4841.4, 4295.9, 3136.6 3005.2, 2177.3	12.6 3	9.3 7	3.3 7
6101.72 9		4912.1, 3679.2, 1386.8	4.72 17	1.80 23	2.9 3
6106.74 12		5641.65, 5228.6, 4805.03, 2980.2, 2763.7	5.1 7	6.7 4	-1.6 8
6141.79 9	$\frac{1}{2}^-, \frac{3}{2}^-$	6141.42, 3719.1, 2689.0, 1889.13	4.67 15	5.9 4	-1.2 4
6183.68 14		5843.7	2.14 12	1.05 25	1.1 3
6279.86 7		6279.0, 3857.8, 2258.03	4.89 15	3.1 3	1.8 3
6431.34 9		5553.0, 3250.0	3.20 14	1.68 18	1.52 23
6498.21 17		3045.66	1.23 15	1.79 12	-0.56 20
6562.16 6		6561.7, 5224.0	3.54 9	1.7 3	1.8 3
6598.48 5		6598.15, 6258.8, 5409.4, 3184.56	7.97 11	7.6 4	0.4 5
6873.64 7		6872.8, 6408.0, 4452.3, 3496.9	2.50 12	2.5 3	0.0 3
6948.41 15	$\frac{1}{2}^+$	6947.6	1.35 11	1.33 16	0.02 20
7187.22 14		4507.9, 3734.0	0.93 7	1.1 3	-0.1 3
7270.54 7		6391.9, 3730.20	3.78 13	3.8 4	0.0 4
8999.28 <sup>c</sup> 3	$\frac{1}{2}^+$	8998.63, 8533.71, 8120.75, 7697.30, 7264.18, 7050.1, 6583.98, 6576.8, 6371.2, 6105.38, 5973.14, 5817.35, 5655.5, 5621.6, 5585.2, 5546.8, 5458.79, 5436.00, 5312.95, 5268.79, 5145.34, 5109.37, 4977.27, 4858.84, 4746.19, 4646.69, 4504.7, 4466.2, 4283.77, 4216.08, 4049.99, 4030.26, 3930.06, 3867.15, 3614.38, 3555.47, 3504.94, 3381.83, 3367.02, 3322.7, 3297.0, 3244.50, 3190.39, 3041.60, 2968.5, 2897.50, 2892.3, 2857.40, 2815.52, 2719.38, 2567.89, 2500.6, 2437.06, 2400.75, 2125.60, 2050.78, 1812.05, 1728.71		4130 40	-4130 40

<sup>a</sup>In our notation, 339.399 16  $\equiv$  339.399  $\pm$  0.016, 4110 50  $\equiv$  4110  $\pm$  50, etc.<sup>b</sup>See also Table III.<sup>c</sup>Capturing state.

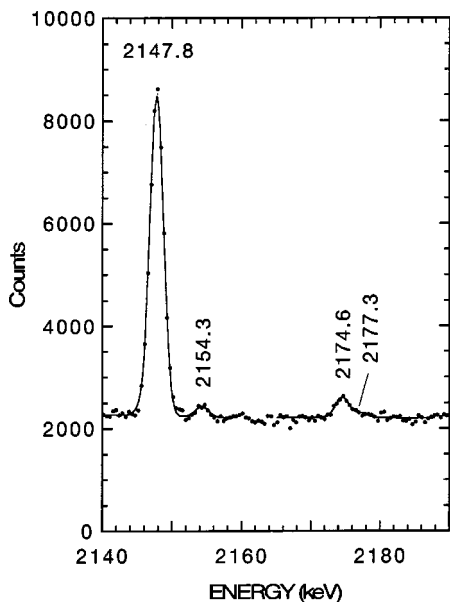


FIG. 4. Selected portion of the  $\gamma$ -ray spectrum from the  $^{58}\text{Ni}(n, \gamma)^{59}\text{Ni}$  reaction with thermal neutrons. See Sec. IV B for related discussion concerning a possible  $\gamma$  ray at 2178 keV.

$10^5$  captures. Therefore, the strongest argument in favor of a level at 3858.26 keV is invalid. The level at 5994.17 keV was introduced in Ref. [30] to accommodate eight  $\gamma$  rays. These  $\gamma$  rays are (i) not seen in the current more sensitive study, (ii) seen but remain unplaced, or (iii) are placed elsewhere in the level scheme.

In our level scheme (see Table IV), there is an  $(n, \gamma)$  level at  $4949.16 \pm 0.05$  keV corresponding to a  $(d, p), \ell_n = 1$  level (see Table II) at  $4948 \pm 5$  keV. This level is fed by a primary  $\gamma$  ray of energy  $4049.99 \pm 0.05$  keV and deexcites by emitting seven  $\gamma$  rays (see Table III). Out of the eight  $\gamma$  rays connected with this level, six were observed by Harder and listed in Table A3 of Ref. [29]. However, she carried only the strongest two out of these six to Table VI of the published paper [30]. Her primary  $\gamma$ -ray energy,  $4049.94 \pm 0.07$  keV, is in excellent agreement with our value, but her secondary  $\gamma$ -ray energy,  $4949.68 \pm 0.09$  keV, is drastically different

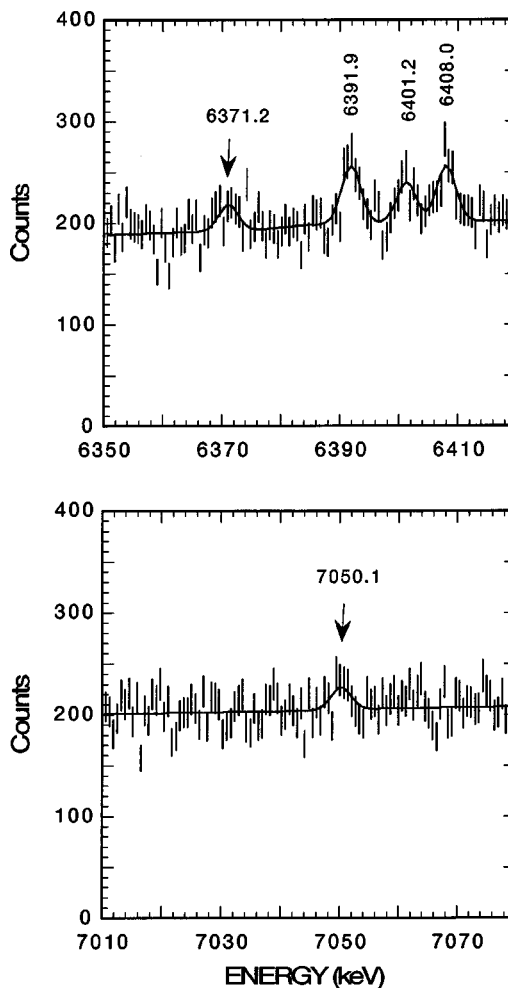


FIG. 5. Selected portions of the  $\gamma$ -ray spectrum from the  $^{58}\text{Ni}(n, \gamma)^{59}\text{Ni}$  reaction with thermal neutrons. See Sec. IV B for related discussion concerning the  $\gamma$  rays at 6371.2 and 7050.1 keV which are possible primary  $E3$  transitions.

from our value of  $4949.02 \pm 0.10$  keV. We have no explanation for this discrepancy.

In addition to the 39 levels common to this work and the earlier work by Harder *et al.* [30], 26 levels are populated

TABLE V. Increasing complexity in the study of the  $^{58}\text{Ni}(n, \gamma)^{59}\text{Ni}$  reaction.

Number of	Ishaq <i>et al.</i> [28]	Harder [29]	Harder <i>et al.</i> [30]	This work
	McMaster (1977)	unpublished Grenoble (1992)	Grenoble (1993)	LANL/ORNL
$\gamma$ rays	59 <sup>d</sup>	576	243	414
spurious $\gamma$ rays <sup>a</sup>	4	241	39	
placed $\gamma$ rays <sup>b</sup>	40	233	232	315
primary $\gamma$ rays	19	37	37	58
secondary $\gamma$ rays	21	196	195	257
unplaced $\gamma$ rays <sup>c</sup>	19	343	11	99
bound levels	20	41	41	65

<sup>a</sup>Gamma rays sought but not observed in this more sensitive work and, therefore, considered spurious.

<sup>b</sup>Some of the placed  $\gamma$  rays may be spurious.

<sup>c</sup>Some of the unplaced  $\gamma$  rays may be genuine.

<sup>d</sup>Measurements limited to  $E_\gamma > 1.9$  MeV using a Ge(Li)-NaI(Tl) pair spectrometer.

TABLE VI. Direct-capture cross sections for primary E1 transitions in the  $^{58}\text{Ni}(n, \gamma)^{59}\text{Ni}$  reaction. Columns 1, 2, and 3 give the energy,  $J^\pi$  value, and the  $l=1$  ( $d, p$ ), spectroscopic factor multiplied by  $(2J+1)$  for the final state, respectively. Column 4 is the primary transition energy. Column 5 is the average valency capture width and column 6 the potential-capture cross section, both calculated using a global optical potential (see Eqs. (4)–(7) of Ref. [3]). The entries in column 5 do not include the spin-coupling factor and the spectroscopic factor; those in column 6 do. Column 7 is the calculated cross section using the global plus valence ( $G+V$ ) procedure [11]. The measured cross sections are given in column 8. Column 9 gives the hypothesized compound-nuclear contributions deduced from the differences between column 7 and column 8 via Eq. (8) of Ref. [3]. In the table subheading  $a(X)$  refers to the experimental scattering length, while  $a(G)$  and  $\bar{\Gamma}_n^0/D$  refer to the scattering length and the neutron strength function, respectively, both calculated using the global optical potential.

$E_f$ (keV)	$J^\pi$	$(d, p)$ $(2J+1)S^a$	$E_\gamma$ (keV)	$\Gamma_{\gamma, \text{val}}/DE_\gamma^3$ ( $10^{-7} \text{ MeV}^{-3}$ )	$\sigma_{\text{pot}, \gamma}$ (mb)	$\sigma(G+V)$ (mb)	$\sigma_\gamma(X)^b$ (mb)	$\sigma_{\text{CN}, \gamma}$ (mb)
Reaction $^{58}\text{Ni}(n, \gamma)^{59}\text{Ni}$ ; $a(X) = 14.2 \text{ fm}$ ; $a(G) = 6.93 \text{ fm}$ ; $\bar{\Gamma}_n^0/D = 4.4 \times 10^{-4}$								
0	$\frac{3}{2}^-$	3.263	8999	0.64	0.30	4389	2082 30	420 or 12500
465	$\frac{1}{2}^-$	1.240	8534	0.21	0.053	1213	996 15	11 or 4410
878	$\frac{3}{2}^-$	0.286	8121	0.064	0.28	312	177 3	19 or 960
1301	$\frac{1}{2}^-$	0.572	7697	0.11	0.39	456	51.7 7	200 or 814
1735	$\frac{3}{2}^-$	0.034	7264	0.0089	0.090	29	9.3 3	5.6 or 72
2415	$\frac{3}{2}^-$	0.032	6584	0.0095	0.14	23	109 2	32 or 230
2894	if $\frac{1}{2}^-$	0.009	6105	0.0024	0.032	4.5	98.0 14	61 or 140
2894	if $\frac{3}{2}^-$	0.009	6105	0.0030	0.051	5.4	98.0 14	58 or 150
3026	if $\frac{1}{2}^-$	0.032	5973	0.0089	0.126	15	36.8 8	4.7 or 99
3026	if $\frac{3}{2}^-$	0.032	5973	0.011	0.19	18	36.8 8	3.2 or 107
3126	if $\frac{1}{2}^-$	0.006	5873	0.0017	0.025	2.8	< 3	0.006 or $12^c$
3126	if $\frac{3}{2}^-$	0.006	5873	0.0021	0.038	3.3	< 3	0.007 or $13^c$
3182	if $\frac{1}{2}^-$	0.032	5817	0.009	0.14	14	152 2	73 or 260
3182	if $\frac{3}{2}^-$	0.032	5817	0.011	0.21	17	152 2	67 or 270
3452	$\frac{3}{2}^-$	0.135	5547	0.050	0.99	65	2.9 2	41 or 96
3563	if $\frac{1}{2}^-$	0.093	5436	0.029	0.49	36	26.3 5	0.78 or 124
3563	if $\frac{3}{2}^-$	0.093	5436	0.035	0.71	62	26.3 5	7.6 or 169
3854	$\frac{3}{2}^-$	0.100	5145	0.041	0.85	41	5.9 3	16 or 78
4022	if $\frac{1}{2}^-$	0.048	4977	0.017	0.31	15	10.6 4	0.45 or 52
4022	if $\frac{3}{2}^-$	0.048	4977	0.020	0.43	18	10.6 4	1.0 or 56
4140	$\frac{3}{2}^-$	0.068	4859	0.030	0.63	24	64.2 8	9.5 or 168
4166	if $\frac{1}{2}^-$	0.012	4836	0.0044	0.082	3.6	< 3	0.03 or $13^c$
4166	if $\frac{3}{2}^-$	0.012	4836	0.0053	0.11	4.3	< 3	0.11 or $14^c$
4253	if $\frac{1}{2}^-$	0.110	4746	0.041	0.78	32	5.8 3	11 or 65
4253	if $\frac{3}{2}^-$	0.110	4746	0.050	1.06	37	5.8 3	14 or 73
4715	if $\frac{1}{2}^-$	0.090	4284	0.039	0.74	21	18.5 5	0.06 or 78
4715	if $\frac{3}{2}^-$	0.090	4284	0.046	0.98	24	18.5 5	0.37 or 85
4949	if $\frac{1}{2}^-$	0.054	4050	0.025	0.48	11	14.1 3	0.21 or 50
4949	if $\frac{3}{2}^-$	0.054	4050	0.030	0.62	13	14.1 3	0.04 or 53
4969	if $\frac{1}{2}^-$	0.050	4030	0.023	0.44	10	20.9 4	2.0 or 60
4969	if $\frac{3}{2}^-$	0.050	4030	0.027	0.57	12	20.9 4	1.4 or 64
5069	if $\frac{1}{2}^-$	0.033	3930	0.016	0.30	6.2	16.7 4	2.5 or 43
5069	if $\frac{3}{2}^-$	0.033	3930	0.019	0.39	7.2	16.7 4	2.0 or 46
5617	if $\frac{1}{2}^-$	0.033	3382	0.019	0.34	4.3	8.9 2	0.81 or 26
5617	if $\frac{3}{2}^-$	0.033	3382	0.022	0.42	5.0	8.9 2	0.58 or 27
5755	if $\frac{1}{2}^-$	0.058	3244	0.036	0.61	6.9	3.1 2	0.74 or 19
5755	if $\frac{3}{2}^-$	0.058	3244	0.041	0.75	7.8	3.1 2	1.1 or 21
5978	if $\frac{1}{2}^-$	0.024	3022	0.016	0.26	2.4	< 3	0.04 or $11^c$
5978	if $\frac{3}{2}^-$	0.024	3022	0.018	0.32	2.7	< 3	0.008 or $11^c$
6031	if $\frac{1}{2}^-$	0.047	2969	0.032	0.51	4.5	12.6 3	2.1 or 32
6031	if $\frac{3}{2}^-$	0.047	2969	0.037	0.62	5.0	12.6 3	1.7 or 34
6142	if $\frac{1}{2}^-$	0.084	2857	0.060	0.92	7.2	4.7 2	0.27 or 24
6142	if $\frac{3}{2}^-$	0.084	2857	0.068	1.1	8.1	4.7 2	0.47 or 25

<sup>a</sup>From Ref. [35].<sup>b</sup>From Table III.<sup>c</sup>Assuming the upper limit for  $\sigma_\gamma(X)$ .

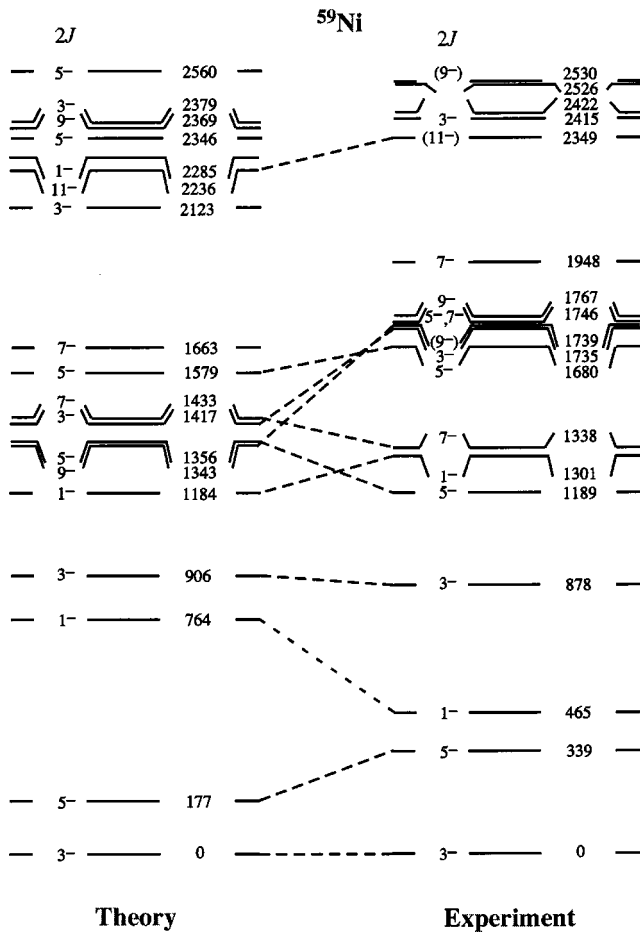


FIG. 6. Comparison between the shell-model predictions and the experimental level scheme of  $^{59}\text{Ni}$ . The levels are labeled by  $2J^\pi$  on the left and by level energies (in keV) on the right.

significantly in the  $^{58}\text{Ni}(\text{thermal } n, \gamma)$  reaction, bringing the total to 65 levels (see Table V). Of these, 60 levels correspond well with known levels in  $^{59}\text{Ni}$ . The remaining five levels (at 3540.05, 4352.45, 5702.11, 6101.73, and 7270.54 keV) are common to both this work and Ref. [30].

The  $J^\pi$  assignments for the levels populated in the  $^{58}\text{Ni}(\text{thermal } n, \gamma)$  reaction were initially assumed to be the same as the known assignments (see Table II). In Table IV, we have further narrowed the  $J^\pi$  choices for the levels at 3686, 3730, 4140, 4715, 4783, and 5385 keV by considering the decay properties of these levels. For common levels, our branching ratios are in reasonable agreement with those reported in the  $^{58}\text{Ni}(^3\text{He}, 2p\gamma)$  [23],  $^{59}\text{Co}(p, n\gamma)$  [25,26], and  $^{58}\text{Ni}(n, \gamma)$  [30] reactions. For the 1680-keV level, our branching ratios agree with  $(p, n\gamma)$  and not with  $(^3\text{He}, 2p\gamma)$ ; the reverse holds true for the 2627-keV level.

In the  $(n, \gamma)$  reaction, the observed primary  $\gamma$  rays (those originating from the capturing state) are predominantly  $E1$  or  $M1$ . Of these two, primary  $E1$  transitions are generally stronger than primary  $M1$  transitions. Primary  $E2$  transitions are extremely rare in the  $(n, \gamma)$  reaction [106–109]. In  $^{59}\text{Ni}$ , we observed a weak primary  $E2$  transition with an intensity of

$\sim 6$  photons per  $10^4$  captures to the known  $\frac{5}{2}^+$  state [36,37] at 4494 keV. (There are no other definite  $\frac{5}{2}^+$  states known in this nucleus.) Primary  $M2$  transitions are rarer than primary  $E2$  transitions and only one viable candidate (in  $^{20}\text{F}$ ) has been reported [14] till date. In this work, we sought but did not observe primary  $M2$  transitions to the known  $\frac{5}{2}^-$  levels at 339, 1189, and 1680 keV.

As shown in Fig. 5, we have detected very weak peaks at 6371.2 and 7050.1 keV with intensities of  $\sim 13$  and  $\sim 10$  photons per  $10^5$  captures, respectively. The energies of these  $\gamma$  rays and the purity of the  $^{58}\text{Ni}$  target virtually guarantee that these  $\gamma$  rays do not originate from an impurity [97]. The most logical placements for these  $\gamma$  rays are between the capturing state ( $J^\pi = \frac{1}{2}^+$ ) and the levels at 2627 and 1948 keV, respectively. These two levels have definite  $J^\pi = \frac{7}{2}^-$  assignments from (polarized  $p, d$ ) measurements [41]. If these placements and the  $J^\pi$  assignments are correct, these  $\gamma$  rays would represent the first examples of primary  $E3$  transitions in the  $(n, \gamma)$  reaction. According to the Weisskopf estimates, an  $E3$  transition of energy  $\sim 6.7$  MeV should be weaker than an  $E1$  transition of similar energy by a factor of  $\sim 10^7$ . However, it is known that the strengths of the (primary)  $E1$  transitions are themselves reduced by a factor of  $\sim 10^3$  as a result of the drawing away of the  $E1$  strength by the giant dipole resonance. The net result is that the weakness factor is only  $\sim 10^4$  instead of  $10^7$  and the current measurement is sensitive enough to detect such weak transitions.

The neutron separation energy determined in this work is  $S_n(^{60}\text{Ni}) = 8999.28 \pm 0.05$  keV, where the uncertainty includes the uncertainties in the primary calibration energies and in the nonlinearity curve. The value obtained by Harder *et al.* [30],  $S_n = 8999.15 \pm 0.23$  keV, is consistent with our value, but the value obtained by Ishaq *et al.* [28],  $S_n = 8999.91 \pm 0.20$  keV, is not. Harder *et al.* [30] have pointed out that the uncertainty in the latter value is probably underestimated.

### C. Capture cross sections of $^{58}\text{Ni}$

The measured values  $\Sigma I_\gamma(\text{primary}) = 4.110 \pm 0.050$  b,  $\Sigma E_\gamma I_\gamma / S_n = 4.145 \pm 0.020$  b, and  $\Sigma I_\gamma(\text{to ground state}) = 4.130 \pm 0.030$  b agree within their stated uncertainties. Our recommended cross-section value of  $4.13 \pm 0.05$  b for the  $^{58}\text{Ni}(n, \gamma)$  reaction is significantly more precise than the currently accepted value of  $4.6 \pm 0.4$  b [110].

Strictly speaking, the three measured values for  $\Sigma I_\gamma(\text{primary})$ ,  $\Sigma E_\gamma I_\gamma / S_n$ , and  $\Sigma I_\gamma(\text{to ground state})$  are lower limits because we cannot claim that we have either detected all possible  $\gamma$  rays from the  $^{58}\text{Ni}(n, \gamma)$  reaction or placed all  $\gamma$  rays correctly in the level scheme. The total intensity of the observed but unplaced  $\gamma$  rays is  $\sim 1.9\%$ . We estimate that any systematic uncertainty in our measured cross-section values is unlikely to exceed  $\sim 2\%$ . This uncertainty is not included in our recommended cross-section value.

The lowest  $s$ -wave resonance in the neutron cross section is at 15.35 keV neutron energy. From its resonance param-

TABLE VII. Partial list of references to previous measurements on  $^{60}\text{Ni}$  levels. See Ref. [93] for additional references.

Measurement	Author(s)	Year	Facility <sup>a</sup>	Reference
$^{46}\text{Ti}$ ( $^{16}\text{O}$ , $2p\gamma$ ) reaction	Kim <i>et al.</i>	1975	Saclay	[44]
$^{50}\text{Cr}$ ( $^{12}\text{C}$ , $2p\gamma$ ) reaction	Kim <i>et al.</i>	1975	Saclay	[44]
$^{51}\text{V}$ ( $^{12}\text{C}$ , $p2n\gamma$ ) reaction	Ivanov <i>et al.</i>	1975	Leningrad	[45]
$^{56}\text{Fe}$ ( $^7\text{Li}$ , $p2n\gamma$ ) reaction	Kearns <i>et al.</i>	1980	U. Liverpool	[46]
$^{56}\text{Fe}$ ( $^6\text{Li}$ , $d$ ) reaction	Stein, Sunier, and Woods	1977	Los Alamos	[47]
	Fulbright <i>et al.</i>	1977	U. Rochester	[48]
$^{58}\text{Ni}$ ( $^{14}\text{C}$ , $^{12}\text{C}$ ) reaction	Videbaek <i>et al.</i>	1985	Los Alamos	[49]
$^{58}\text{Ni}$ ( $\alpha$ , $2p\gamma$ ) reaction	Kim <i>et al.</i>	1975	Saclay	[44]
	Tsan Ung Chan <i>et al.</i>	1984	Grenoble	[50]
$^{58}\text{Ni}$ ( $t$ , $p$ ) reaction	Darcey, Chapman, and Hinds	1971	Aldermaston	[51]
$^{59}\text{Co}$ ( $^3\text{He}$ , $d\gamma$ ) reaction	Ronsin <i>et al.</i>	1973	Saclay	[52]
$^{59}\text{Co}$ ( $p$ , $\gamma$ ) reaction	Demeter <i>et al.</i>	1971	Budapest	[53]
	Erlandsson, Lyttkens, and Marcinkowski	1975	U. Lund	[54]
$^{59}\text{Co}$ ( $\alpha$ , $t$ ) reaction	Peterson <i>et al.</i>	1987	Indiana U.	[55]
$^{60}\text{Co}$ $\beta^-$ decay	Hansen and Spornol	1968	Geel	[56]
	Raman	1969	Oak Ridge	[57]
	Camp and Van Hise	1976	Livermore	[58]
$^{59}\text{Ni}$ (thermal $n$ , $\gamma$ ) reaction	Wilson, Thomas, and Jackson	1975	Argonne	[59]
	Raman and Journey	1979	Los Alamos	[60]
$^{60}\text{Ni}$ ( $\gamma$ , $\gamma'$ ) reaction	Metzger	1970	Bartol	[61]
$^{60}\text{Ni}$ ( $e$ , $e'$ ) reaction	Lindgren <i>et al.</i>	1981	MIT	[62]
$^{60}\text{Ni}$ ( $\pi$ , $\pi'$ ) reaction	Clausen <i>et al.</i>	1990	Los Alamos	[63]
$^{60}\text{Ni}$ ( $p$ , $p'$ ) reaction	Tee and Aspinall	1967	Aldermaston	[64]
$^{60}\text{Ni}$ ( $p$ , $p'\gamma$ ) reaction	Mohindra and Van Patter	1965	U. Pennsylvania	[65]
	Moazed <i>et al.</i>	1971	U. Pennsylvania	[66]
	Ronsin <i>et al.</i>	1973	Saclay	[52]
	Passoja <i>et al.</i>	1981	U. Jyväskylä	[67]
$^{60}\text{Cu}$ ( $\beta^+ + \epsilon$ ) decay	Van Patter and Rauch	1972	Bartol	[68]
$^{61}\text{Ni}$ ( $p$ , $d$ ) reaction	Koang, Chien, and Rossner	1976	Michigan State U.	[69]
$^{62}\text{Ni}$ ( $p$ , $t$ ) reaction	Kong-A-Siou <i>et al.</i>	1974	Grenoble	[70]

<sup>a</sup>Facility where the actual measurements were done. The symbol U stands for a university.

eters, we compute that its contribution to the thermal capture cross section is about 0.4 b. Resonances at higher neutron energy contribute less than 0.04 b. Most of the capture cross section ( $\approx 3.7$  b) can therefore be attributed to one or more bound levels. The large thermal-neutron scattering length  $a_{J=1/2} = 14.2$  fm indicates that the most important bound level either lies very close to the neutron separation energy or has a very large reduced neutron width. If we assume that only one level affects the scattering length, we can obtain an estimate for its ratio of reduced width to binding energy; it is about 2. From the capture cross section that we estimate as arising from the bound level ( $\approx 3.7$  b), we can then obtain the ratio of its radiation width to binding energy; this is about  $2.2 \times 10^{-4}$ . The measured radiation widths of the  $s$ -wave neutron resonances range from about 1 eV to 3 eV. We conclude therefore that the energy of the first bound level is about  $-10$  keV.

The cross sections for the individual primary  $E1$  transitions are given in Table VI along with their  $\gamma$ -ray energies and ( $d$ ,  $p$ ) spectroscopic factors of the final states. From these and the thermal-neutron scattering length, the direct-capture

cross sections are calculated. These are also presented in Table VI. In general, there are significant differences between the direct-capture cross section and the experimental value. These differences are attributed to the admixture of compound-nuclear capture resulting from the nearest resonance levels (bound and unbound). The two possible magnitudes of the compound-nuclear cross section, extracted using Eq. (1), for each transition are listed in the final column of Table VI.

The method for determining combinations of these compound-nuclear cross sections is described in Sec. III F. Before applying this method to the  $^{58}\text{Ni}$  data, we note that the higher value for the ground-state transition seems to be excessively large compared with nearly all other values. Quantitatively this conclusion is confirmed by our findings that this value, combined with the lower values for all other transitions, gives  $M\nu = -3.2$ ,  $Mb = 6.9$  for  $b = 3$  and  $M\nu = -2.2$ ,  $Mb = 5.6$  for  $b = 5$ . If the value for the ground-state transition is fixed at the higher of the two possible values and the values for the rest of the transitions are chosen randomly, we find that, for  $b = 3$ , none of the randomly chosen sequences have an acceptable value of  $M\nu$  (in the range  $-1.52$

TABLE VIII. Known energy levels in  $^{60}\text{Ni}$ .

Known		Previous	This work	Known		Previous	This work
$E(\text{level})^a$	$J^\pi$	$(n, \gamma)$	$(n, \gamma)$	$E(\text{level})^a$	$J^\pi$	$(n, \gamma)$	$(n, \gamma)$
(keV)		$E(\text{level})^a$	$E(\text{level})^a$	$E(\text{level})^a$		$E(\text{level})^a$	$E(\text{level})^a$
(keV)		(keV)	(keV)	(keV)		(keV)	(keV)
0.0	0 <sup>+</sup>	0.0	0.0	4319.0 5	1 <sup>+</sup> , 2 <sup>+</sup>	4318.3 11	4318.58 5
1332.51 3	2 <sup>+</sup>	1333.4 3	1332.536 16	4334.7 10		4335.1 11	4335.56 4
2158.61 4	2 <sup>+</sup>	2159.6 5	2158.671 18	4341 5	(0 <sup>+</sup> )		
2284.86 14	0 <sup>+</sup>	2284.9 5	2284.828 24	4355.7 5			4355.57 12
2505.71 3	4 <sup>+</sup>		2505.79 3	4407.40 14			
2625.99 8	3 <sup>+</sup>		2625.98 3	4493.43 25	2 <sup>+</sup>		4493.18 5
3119.66 9	4 <sup>+</sup>		3119.45 18	4535.7 10			4534.13 14
3123.98 13	2 <sup>+</sup>	3124.1 7	3123.750 21	4548.8 4	1 <sup>+</sup> , 2 <sup>+</sup>		4547.99 3
3185.99 8	3 <sup>+</sup>	3186.8 9	3186.23 4	4579.1 7	2 <sup>+</sup>		4577.46 6
3194.01 13	1 <sup>+</sup>	3194.6 7	3193.892 19	4613 7			
3269.34 16	2 <sup>+</sup>		3268.97 4	4760.5 7			4760.25 9
3316 7	0 <sup>+</sup>	3318.0 8	3317.85 3	4768 5			
3381 5				4781 7			4779.16 6
3393.4 3	2 <sup>+</sup>	3393.8 8	3393.16 3	4799.9 5			
3589 7	0 <sup>+</sup>	3587.9 9	3587.75 3	4844.2 13			4843.94 8
3619.45 13	(3) <sup>+</sup>		3619.47 4	4850.6 20			
		3622.9 10		4859 5			
3670.66 9	4 <sup>+</sup>			4891 7			
3730.64 6				4932 7			4929.00 14
3735.8 6	2 <sup>+</sup>	3735.2 9	3734.42 3	4958 5			4953.38 7
3872.1 9	1 <sup>+</sup> , 2 <sup>+</sup>	3870.8 9	3871.080 23	4970 5			
3887.8 4			3887.38 7	4985.69 9	(6 <sup>+</sup> )		
3895 5				5015.0 6			
3924.71 10	2 <sup>+</sup> , 3 <sup>+</sup>		3925.22 9	5048.3 7			
4007.9 7	1 <sup>+</sup> , 2 <sup>+</sup>		4006.46 3	5069 10	(1 <sup>-</sup> )		5065.03 6
4020.44 21	1 <sup>+</sup> , 2 <sup>+</sup>		4019.914 25	5106 5			
4035 5				5110 20	8 <sup>-</sup>		
4039.66 15	3 <sup>-</sup>		4039.92 6	5132 5			5127.18 17
4078.53 21	1 <sup>+</sup> , 2 <sup>+</sup>		4078.01 5	5148.6 6			
4111.7 4			4111.97 9	5174 5			
4165.35 10	5 <sup>+</sup>			5188 10			
4191 5				5205 5			
4265.05 10	6 <sup>+</sup>			5244 5	4 <sup>+</sup>		
4294.5 3				5264 10			

to  $-0.96$ ) and  $Mb$  (in the range  $-1.25$  to  $+1.25$ ). For  $b=4$  about 1% have acceptable  $M\nu$  and  $Mb$  values. For  $b=5$ , 29% have acceptable values of both  $M\nu$  and  $Mb$ . The value of  $a$  in this acceptable range is  $(3.5 \pm 1.4) \times 10^{-5}$  b MeV<sup>-5</sup>. This result is to be compared with the result from Lone's formula [111] from the Brink-Axel photonuclear model [101,102] for the neutron capture mechanism which would give for this bound level (and the observed average  $s$ -wave resonance spacing of  $\approx 20$  keV) a value of  $a=10^{-4}$  b MeV<sup>-5</sup>. Conversely, if we fix the compound-nuclear cross section of the ground-state transition at the lower of the two possible values, we find that 30% of sequences are statistically acceptable for  $b=3$  with  $a=(4.3 \pm 0.8) \times 10^{-4}$  b MeV<sup>-3</sup>; about 40% satisfy  $b=4$  with  $a=(1.1 \pm 0.3) \times 10^{-4}$  b MeV<sup>-4</sup>; and 22% are

acceptable for  $b=5$ , giving  $a=(2.0 \pm 0.5) \times 10^{-5}$  b MeV<sup>-5</sup>.

Brink's theory (unadapted by Axel) [101] for the radiation width gives  $b=4$ ,  $a=7 \times 10^{-5}$  b MeV<sup>-4</sup>. Cameron's semi-empirical estimate [112] for the radiation width gives  $b=3$ ,  $a=1.7 \times 10^{-4}$  b MeV<sup>-4</sup>. The Weisskopf model [100] gives  $b=3$ ,  $a=10^{-3}$  b MeV<sup>-4</sup> while a generalized valence model assessment [113] gives  $b=3$ ,  $a=6 \times 10^{-4}$  b MeV<sup>-4</sup>. All these theoretical estimates have at least a  $\pm 50\%$  uncertainty, because of the uncertainty in the energy of the bound state, placing all, except possibly the Brink-Axel-Lone [111] and Cameron models [112], into agreement with the data. It is clear that the differences between the calculated direct-capture cross sections and the experimental data may be fully attributed to the admixture of a compound-nuclear mecha-

TABLE VIII. (Continued.)

Known		Previous	This work	Known		Previous	This work
$E(\text{level})^a$	$J^\pi$	$(n, \gamma)$	$(n, \gamma)$	$E(\text{level})^a$	$J^\pi$	$(n, \gamma)$	$(n, \gamma)$
(keV)		$E(\text{level})^a$	$E(\text{level})^a$	$E(\text{level})^a$		$E(\text{level})^a$	$E(\text{level})^a$
		(keV)	(keV)	(keV)		(keV)	(keV)
5293 10			5288.57 14	6142 10			
5307 7				6181 10			
5318 5				6192 10			
5348.9 5	7 <sup>-</sup>			6239 10			6239.2 3
5379 5				6275 10			
5396 10	3 <sup>-</sup>			6292 10			
5428 10				6331 10			6327.23 15
5444.6 10	2 <sup>+</sup>			6362 10			6362.06 17
			5446.99 10	6380 10			6382.4 4
5474 10			5476.06 21	6403 10			
5531.6 10	(0 <sup>+</sup> )			6431 10			
5615 10			5612.44 4	6460.7 12			
5642 10				6468 10			6465.27 16
5662.7 6				6492 10			6489.17 23
5675 10			5672.39 7	6516 10			6516.73 23
5713 10			5710.82 4	6551 10			
5741 10				6568 10			6567.35 20
5780.4 5				6584 10			
5785.1 4	(7 <sup>+</sup> )			6610 10			
5799 5	2 <sup>+</sup>			6623 10			
5824 5				6652 10			6647.19 9
5848 10				6658 10			
5863 10			5860.0 5	6687 10			
			5878.08 8	6708 10			
5900 10			5902.45 7	6728 10			
5921 10			5918.56 21	6753 10			6756.3 3
5946 10				6765 10			
			5967.8 3	6791 10			
5973 10	(5 <sup>-</sup> )			6810.4 6			
5992 10				6832 10			6834.95 19
6028 10				6836.6 10			
6054 10				6859 10			
6071 10			6066.71 11	6892 10			
6121 10							6911.95 9

nism, but the present results cannot distinguish between a photonuclear giant resonance model and a Weisskopf-type model for that mechanism.

#### D. Shell-model calculations of $^{59}\text{Ni}$ levels

The calculated spectrum is compared with experiment in Fig. 6. There is good agreement between theory and experiment for the first ten states. It is pleasing that the two gaps at 465–878 keV and 1948–2349 keV, where no level is found experimentally, are reproduced by the theoretical spectrum.

However, the doublet of  $\frac{3}{2}^-$  states at 1739 and 1767 keV [19,21] is not reproduced by our calculations.

### V. REACTION $^{59}\text{Ni}(n, \gamma)$

#### A. Skeleton level scheme of $^{60}\text{Ni}$

In Table VII we have listed the previous measurements that have been carried out concerning the energy levels in  $^{60}\text{Ni}$ . From this list, we considered a subset of measurements and results given in Refs. [46,50,52,54,58,64,68,69] which led to the skeleton level scheme of 136 levels given under columns 1 and 5 in Table VIII. The backbone of this scheme

TABLE VIII. (*Continued.*)

Known		Previous	This work	Known		Previous	This work
$E(\text{level})^a$	$J^\pi$	$(n, \gamma)$	$(n, \gamma)$	$E(\text{level})^a$	$J^\pi$	$(n, \gamma)$	$(n, \gamma)$
(keV)		$E(\text{level})^a$	$E(\text{level})^a$	$E(\text{level})^a$		$E(\text{level})^a$	$E(\text{level})^a$
		(keV)	(keV)	(keV)		(keV)	(keV)
			6996.86 <i>20</i>				7950.95 <i>24</i>
			7056.29 <i>14</i>	8043.8 <i>9</i>			
			7207.7 <i>3</i>				8286.3 <i>3</i>
			7222.81 <i>11</i>				8504.7 <i>3</i>
			7316.15 <i>16</i>	8520.5 <i>10</i>			
			7339.71 <i>25</i>				8565.63 <i>18</i>
			7414.18 <i>23</i>				8638.57 <i>25</i>
			7473.50 <i>24</i>				8666.23 <i>22</i>
			7495.3 <i>4</i>				9045.23 <i>24</i>
			7552.0 <i>3</i>				9076.68 <i>17</i>
			7684.1 <i>4</i>	9132.1 <i>14</i>			
			7690.1 <i>3</i>				9346.84 <i>18</i>
			7761.7 <i>3</i>				9953.7 <i>3</i>
			7798.88 <i>25</i>	9989.4 <i>17</i>			
			7818.04 <i>13</i>				10029.04 <i>17</i>

<sup>a</sup>In our notation, 1332.51 *3*  $\equiv$   $1332.51 \pm 0.03$ , 4319.0 *5*  $\equiv$   $4319.0 \pm 0.5$ , etc.

is the Aldermaston spectrograph ( $p, p'$ ) measurements made by Tee and Aspinall [64]. These authors quote  $\pm 7$  keV for the energies of levels below 5 MeV and  $\pm 10$  keV above. More significantly, unlike in the  $^{59}\text{Ni}$  case, we found no systematic errors in the level energies quoted by Tee and Aspinall [64].

The  $J^\pi$  assignments for  $^{60}\text{Ni}$  levels arise from a variety of measurements. A convenient way to trace the evolution of these assignments is to follow the reasonings presented in Ref. [90].

### B. Thermal-neutron capture $\gamma$ -ray data

The enriched  $^{59}\text{Ni}$  material used in this work was prepared about three decades ago. Five grams of 99.9% enriched  $^{58}\text{Ni}$  were irradiated with neutrons for over 1 yr as part of the Savannah River High Flux Demonstration [114]. After return to Oak Ridge National Laboratory (ORNL), the target material, which had originally been loaded in 12 aluminum cans, was stored to allow short-lived activities to decay. Early in 1971, the nickel target material was reclaimed, and a chemical separation using anion-exchange techniques was made to remove the  $^{60}\text{Co}$  impurity. After further chemical treatment (hydroxide precipitation, electrolysis, etc.) to remove other minor radioactivities, the nickel sample was recovered as NiO and loaned to Knolls Atomic Power Laboratory (KAPL) for a preliminary cross-section measurement. The  $^{59}\text{Ni}$  content at this point was 4.3%. Upon return from KAPL, the 4.16-g nickel sample was again chemically processed, converted to low-fired oxide (600°C), and used as charge material by passing carbon tetrachloride over the oxide positioned directly in the ion source. The technique of introducing

$\text{NiCl}_2$  into the ionization region by chlorination with carbon tetrachloride was established on an experimental basis using normal nickel oxide. The isotopic separation, which was performed in a calutron outside the contained area, resulted in a recovery of 30 mg of nickel that was assayed to be 95.35%  $^{59}\text{Ni}$ . A portion of this material (7.0 mg) was available for our measurements. Subsequently, we diluted the sample with natural nickel such that the  $^{59}\text{Ni}$  enrichment dropped to  $(44.3 \pm 0.4)\%$ . We used 6.9 mg of the diluted material in a second set of measurements. Sample spectra obtained with the 7.0-mg metal sample of 95.35% enriched  $^{59}\text{Ni}$  are shown in Figs. 1 and 2.

The energies and intensities of 390  $\gamma$  rays assigned to  $^{60}\text{Ni}$  are given in Table IX. The 11 386.5-keV transition from the capturing state to the ground state is exceptionally strong ( $\sim 30\%$  of all captures). Since the early 1970s, the Negev group has been using this transition for photon scattering studies [115,116]. Because the ground state of  $^{59}\text{Ni}$  has  $J^\pi = \frac{3}{2}^-$ , thermal-neutron capture leads to a  $1^-$  or  $2^-$  capturing state. The strength of the 11 386.5-keV transition to the  $0^+$  ground state of  $^{60}\text{Ni}$  indicates that the capturing state is predominantly a  $1^-$  state. The nearest neutron resonance at 203 eV is known to be a  $1^-$  resonance [117] and thermal-neutron capture in  $^{59}\text{Ni}$  is believed to result primarily from the tail of this resonance. Even though there are no known  $2^-$  neutron resonances below 5 keV, there is some indication that the capturing state is partly  $2^-$  from the presence of a primary transition to the 3186.1-keV,  $3^+$  state, which is probably an  $E1$  and not an  $M2$  transition.

The level scheme resulting from this work is presented in Table X. Of the 132 known levels below 6.9 MeV, 59 levels are populated significantly in the  $(n, \gamma)$  reaction. The two

TABLE IX. Energies ( $E_\gamma$ ) and intensities ( $I_\gamma$ ) of  $\gamma$  rays from the  $^{59}\text{Ni}(n, \gamma)^{60}\text{Ni}$  reaction.

$E_\gamma$ (keV) <sup>a</sup>	$I_\gamma$ (b) <sup>b</sup>	Placement <sup>c</sup>	$E_\gamma$ (keV) <sup>a</sup>	$I_\gamma$ (b) <sup>b</sup>	Placement <sup>c</sup>	$E_\gamma$ (keV) <sup>a</sup>	$I_\gamma$ (b) <sup>b</sup>	Placement <sup>c</sup>
119.9 3	0.033 4	2625 → 2505	913.63 14	0.047 4	4953 → 4039	1568.0 5	0.014 3	6327 → 4760
123.65 20	0.011 2	unplaced	952.26 3	11.2 3	2284 → 1332	1575.84 13	0.071 5	5447 → 3871
139.11 17	0.013 3	unplaced	964.8 3	0.022 3	3123 → 2158	1585.33 13	0.067 5	4779 → 3193
158.34 12	0.016 2	unplaced	983.9 4	0.011 3	3268 → 2284	1592.53 4	0.440 11	5612 → 4019
215.16 18	0.015 3	unplaced	993.48 3	0.161 5	3619 → 2626	1606.10 14	0.059 5	4111 → 2505
216.95 25	0.014 3	unplaced	1005.83 10	0.054 4	unplaced	1621.2 5	0.017 5	6465 → 4843
229.62 10	0.027 3	unplaced	1027.56 4	0.228 5	3186 → 2158	1628.9 4	0.022 4	7339 → 5710
277.38 14	0.024 3	unplaced	1035.23 3	1.03 3	3193 → 2158	1632.99 18	0.053 5	5710 → 4078
305.7 3	0.016 3	3925 → 3619	1064.2 4	0.021 4	5612 → 4548	1636.42 13	0.082 5	4760 → 3123
355.67 11	0.026 4	unplaced	1091.42 9	0.067 3	5447 → 4355	1643.6 4	0.026 5	7316 → 5672
393.76 6	0.162 4	3587 → 3193	1110.31 9	0.081 6	3268 → 2158	1684.4 3	0.031 5	4953 → 3268
431.9 4	0.009 3	4019 → 3587	1113.9 3	0.053 6	3619 → 2505	1692.45 8	0.119 7	4318 → 2625
467.28 3	0.71 3	2625 → 2158	1154.82 12	0.046 4	4548 → 3393	1712.30 9	0.741 15	3871 → 2158
493.3 4	0.008 3	3119 → 2625	1159.09 13	0.043 4	3317 → 2158	1734.98 11	0.157 8	4019 → 2284
497.76 4	0.115 4	3123 → 2625	1173.24 3	0.47 4	2505 → 1332	1741.3 5	0.013 4	5612 → 3871
521.24 8	0.118 8	unplaced	1194.4 5	0.015 5	4929 → 3734	1766.5 3	0.029 4	3925 → 2158
541.0 3	0.014 3	unplaced	1234.51 7	0.072 4	3393 → 2158	1786.9 3	0.049 8	3119 → 1332
555.81 19	0.020 3	unplaced	1244.93 22	0.021 4	3871 → 2626	1791.19 3	3.07 3	3123 → 1332
569.5 4	0.009 3	3887 → 3317	1248.86 15	0.036 4	5288 → 4039	1813.5 5	0.066 7	4318 → 2505
604.62 23	0.014 3	unplaced	1293.2 9	0.37 5	2625 → 1332	1816.1 5	0.016 4	unplaced
642.96 5	0.088 3	3268 → 2625	1296.3 4	0.028 5	unplaced	1829.9 4	0.018 5	4335 → 2505
660.27 16	0.019 3	unplaced	1306.5 5	0.019 5	4493 → 3186	1853.67 7	0.173 6	3186 → 1332
667.4 5	0.007 3	4779 → 4111	1308.16 25	0.044 5	4577 → 3268	1861.33 3	1.34 3	3193 → 1332
672.90 6	0.073 3	unplaced	1332.54 3	44.6 9	1332 → 0	1878.0 4	0.022 5	5612 → 3734
677.17 5	0.137 3	3871 → 3193	1354.08 9	0.065 5	4548 → 3193	1881.15 12	0.074 5	4039 → 2158
680.42 4	0.144 3	3186 → 2505	1358.67 18	0.027 4	C → 10029	1888.4 3	0.031 4	5476 → 3587
693.57 11	0.037 3	3887 → 3193	1380.4 3	0.045 6	4006 → 2625	1919.28 7	0.132 6	4078 → 2158
702.11 14	0.025 3	4019 → 3317	1381.8 3	0.035 6	3887 → 2505	1936.41 6	0.186 5	3268 → 1332
727.07 18	0.020 3	unplaced	1385.97 14	0.035 5	4779 → 3393	1985.27 3	3.65 7	3317 → 1332
739.2 3	0.030 5	3925 → 3186	1392.3 5	0.009 3	5127 → 3734	2028.5 5	0.019 5	4534 → 2505
747.33 3	0.818 15	3871 → 3123	1399.4 4	0.010 3	7761 → 6362	2040.85 19	0.048 5	C → 9346
749.7 3	0.050 6	6362 → 5612	1404.4 3	0.017 4	unplaced	2060.58 3	0.571 13	3393 → 1332
751.9 4	0.026 5	3871 → 3119	1419.40 10	0.053 4	3925 → 2505	2152.6 3	0.035 5	6996 → 4843
758.5 4	0.020 6	4493 → 3734	1424.24 4	0.251 7	4548 → 3123	2158.63 3	0.98 3	2158 → 0
770.3 3	0.011 3	unplaced	1429.07 3	0.496 10	3587 → 2158	2176.84 4	0.285 8	4335 → 2158
805.6 4	0.011 3	3925 → 3119	1434.0 3	0.018 4	C → 9953	2198.1 4	0.027 5	6516 → 4318
813.48 7	0.068 3	4548 → 3734	1451.88 16	0.033 4	4078 → 2625	2245.40 15	0.063 5	unplaced
826.11 3	6.30 12	2158 → 1332	1472.6 6	0.021 6	7799 → 6327	2255.18 5	0.230 7	3587 → 1332
839.08 19	0.023 3	3123 → 2284	1474.6 3	0.049 6	5967 → 4493	2263.17 4	0.348 8	4548 → 2284
841.2 3	0.016 3	4953 → 4111	1485.94 19	0.039 4	4111 → 2625	2282.0 3	0.025 4	5476 → 3193
851.9 3	0.020 3	5612 → 4760	1491.5 3	0.030 5	4760 → 3268	2311.00 18	0.048 5	C → 9076
853.8 4	0.015 3	4039 → 3186	1497.91 25	0.033 5	unplaced	2317.65 20	0.048 6	5710 → 3393
868.06 20	0.022 3	unplaced	1510.83 21	0.028 4	unplaced	2320.7 4	0.025 4	6327 → 4006
883.1 3	0.016 3	4006 → 3123	1532.65 12	0.055 5	6066 → 4534	2334.4 3	0.031 5	4493 → 2158
896.23 6	0.119 5	4019 → 3123	1562.8 3	0.040 4	5918 → 4355	2341.9 4	0.023 4	C → 9045
909.05 4	0.601 14	3193 → 2284	1564.6 7	0.015 5	unplaced	2375.6 3	0.030 4	4534 → 2158

TABLE IX. (*Continued.*)

$E_\gamma$ (keV) <sup>a</sup>	$I_\gamma$ (b) <sup>b</sup>	Placement <sup>c</sup>	$E_\gamma$ (keV) <sup>a</sup>	$I_\gamma$ (b) <sup>b</sup>	Placement <sup>c</sup>	$E_\gamma$ (keV) <sup>a</sup>	$I_\gamma$ (b) <sup>b</sup>	Placement <sup>c</sup>
2389.25 5	0.300 8	4548 → 2158	3046.7 7	0.017 4	5672 → 2625	3703.4 8	0.039 11	C → 7684
2392.6 3	0.040 5	5710 → 3317	3058.0 7	0.016 4	6327 → 3268	3732.23 22	0.151 13	5065 → 1332
2401.83 3	0.778 15	3734 → 1332	3062.5 5	0.023 4	unplaced	3743.71 13	0.180 9	5902 → 2158
2418.65 20	0.042 5	4577 → 2158	3101.2 6	0.015 4	C → 8286	3794.8 4	0.049 6	5127 → 1332
2478.42 7	0.129 5	5672 → 3193	3123.70 5	0.34 2	3123 → 0	3817.7 5	0.040 7	unplaced
2488.73 10	0.088 4	5612 → 3123	3129.6 3	0.033 4	7207 → 4078	3836.1 <sup>h</sup> 5	0.033 6	C → 7552
2493.8 3	0.032 3	4779 → 2284	3160.60 6	0.260 8	4493 → 1332	3870.94 7	0.356 12	3871 → 0
2496.9 3	0.019 3	6516 → 4019	3167.7 4	0.045 5	6362 → 3193	3892.4 <sup>i</sup> 5	0.043 7	C → 7494
2517.00 9	0.246 8	5710 → 3193	3193.77 4	0.602 11	3193 → 0	3895.4 5	0.045 7	unplaced
2525.4 3	0.033 6	5918 → 3393	3215.27 8	0.122 6	4548 → 1332	3913.7 3	0.042 6	C → 7473
2538.53 4	0.451 10	3871 → 1332	3233.0 3	0.030 5	unplaced	3939.5 4	0.042 6	unplaced
2547.35 21	0.043 5	6567 → 4019	3244.90 9	0.151 5	4577 → 1332	3955.2 <sup>j</sup> 6	0.025 6	5288 → 1332
2554.69 10	0.124 5	3887 → 1332	3264.0 5	0.019 4	unplaced	3973.4 5	0.042 7	C → 7414
2572.2 4	0.017 4	8638 → 6066	3268.78 12	0.074 5	3268 → 0	3983.6 4	0.050 6	6489 → 2505
2578.2 5	0.014 4	6465 → 3887	3276.32 20	0.044 5	5902 → 2625	4006.30 4	1.20 3	4006 → 0
2586.98 12	0.071 5	5710 → 3123	3288.5 3	0.019 5	5447 → 2158	4019.74 5	1.68 4	4019 → 0
2593.3 4	0.015 4	6911 → 4318	3296.3 3	0.038 5	7316 → 4019	4021.4 5	0.075 8	6647 → 2625
2601.5 4	0.025 5	4760 → 2158	3302.11 24	0.035 4	7414 → 4111	4048.2 4	0.048 6	C → 7339
2607.10 22	0.041 5	6647 → 4039	3352.8 4	0.025 6	unplaced	4066.3 3	0.062 8	unplaced
2613.9 3	0.026 4	8286 → 5672	3354.5 4	0.048 5	7690 → 4335	4071.49 22	0.073 8	C → 7316
2620.40 8	0.125 5	4779 → 2158	3359.5 4	0.027 5	unplaced	4077.6 9	0.022 5	4078 → 0
2627.4 3	0.029 4	6647 → 4019	3369.4 4	0.023 4	6489 → 3119	4080.0 7	0.027 6	7950 → 3871
2633.3 3	0.032 5	5902 → 3268	3393.05 20	0.042 4	3393 → 0	4111.6 8	0.041 7	4111 → 0
2673.86 4	1.60 3	4006 → 1332	3426.3 5	0.094 24	5710 → 2284	4114.4 6	0.070 8	5447 → 1332
2684.19 12	0.166 8	5878 → 3193	3428.0 4	0.096 25	4760 → 1332	4164.75 11	0.193 8	C → 7222
2687.33 4	0.712 16	4019 → 1332	3436.9 3	0.076 6	C → 7950	4168.32 19	0.099 8	6327 → 2158
2707.44 8	0.145 5	4039 → 1332	3440.37 17	0.092 8	6066 → 2625	4180.5 <sup>k</sup> 7	0.018 4	C → 7207
2721.59 25	0.038 5	C → 8666	3446.77 17	0.081 7	4779 → 1332	4204.0 <sup>l</sup> 7	0.021 6	6489 → 2284
2745.47 6	0.240 7	4078 → 1332	3453.67 11	0.131 5	5612 → 2158	4255.6 6	0.026 4	unplaced
2749.5 4	0.026 5	C → 8638	3487.1 <sup>d</sup> 4	0.023 5	6756 → 3268	4279.8 <sup>m</sup> 4	0.034 6	5612 → 1332
2770.5 3	0.039 5	4929 → 2158	3495.12 16	0.108 5	unplaced	4305.2 6	0.019 5	unplaced
2779.42 14	0.084 5	4111 → 1332	3511.07 <sup>e</sup> 18	0.174 8	4843 → 1332	4318.52 11	0.130 7	4318 → 0
2785.73 14	0.085 5	unplaced	3513.6 3	0.072 7	5672 → 2158	4331.24 <sup>n</sup> 15	0.113 6	C → 7056
2797.7 5	0.021 5	6066 → 3268	3517.3 3	0.042 5	6834 → 3317	4335.37 23	0.087 8	4335 → 0
2822.3 3	0.040 5	C → 8565	3551.94 14	0.130 6	5710 → 2158	4338.3 3	0.064 7	unplaced
2831.3 6	0.018 5	6756 → 3925	3569.53 <sup>f</sup> 13	0.088 5	C → 7818	4348.2 4	0.031 5	unplaced
2846.9 5	0.026 5	7339 → 4493	3589.0 3	0.051 8	C → 7799	4356.6 3	0.046 6	unplaced
2874.42 19	0.068 6	unplaced	3596.4 4	0.040 6	4929 → 1332	4370.7 <sup>o</sup> 5	0.025 4	6996 → 2625
2883.0 4	0.037 5	C → 8504	3603.4 <sup>g</sup> 7	0.020 5	7222 → 3619	4377.65 13	0.120 6	unplaced
2907.5 3	0.033 5	unplaced	3620.64 14	0.117 8	4953 → 1332	4390.4 3	0.042 5	C → 6996
2938.6 4	0.024 5	7473 → 4534	3625.6 4	0.034 6	C → 7761	4430.3 4	0.040 5	7056 → 2625
2985.97 7	0.320 9	4318 → 1332	3632.4 6	0.024 6	7950 → 4318	4475.58 10	0.150 7	C → 6911
3002.5 4	0.025 5	4335 → 1332	3641.1 4	0.045 6	6834 → 3193	4487.56 25	0.055 5	8565 → 4078
3022.90 20	0.064 5	4355 → 1332	3658.9 3	0.050 6	unplaced	4492.3 6	0.022 4	7761 → 3268
3027.86 16	0.075 6	6647 → 3619	3697.7 6	0.032 7	C → 7690	4507.04 18	0.163 10	unplaced
3040.5 4	0.030 5	6911 → 3871	3700.9 9	0.031 8	5860 → 2158	4545.9 <sup>p</sup> 5	0.074 15	5878 → 1332

TABLE IX. (Continued.)

$E_\gamma$ (keV) <sup>a</sup>	$I_\gamma$ (b) <sup>b</sup>	Placement <sup>c</sup>	$E_\gamma$ (keV) <sup>a</sup>	$I_\gamma$ (b) <sup>b</sup>	Placement <sup>c</sup>	$E_\gamma$ (keV) <sup>a</sup>	$I_\gamma$ (b) <sup>b</sup>	Placement <sup>c</sup>
4548.2 3	0.163 16	4548 → 0	5306.7 4	0.040 5	9346 → 4039	6382.3 5	0.033 5	6382 → 0
4553.0 3	0.071 6	C → 6834	5320.69 <sup>r</sup> 18	0.094 6	C → 6066	6434.01 10	0.223 7	C → 4953
4577.37 14	0.144 8	4577 → 0	5393.3 3	0.062 5	7552 → 2158	6458.42 18	0.098 6	C → 4929
4617.2 4	0.048 6	8504 → 3887	5407.76 13	0.155 6	unplaced	6464.9 3	0.090 5	6465 → 0
4631.2 5	0.036 6	C → 6756	5419.5 <sup>s</sup> 6	0.025 5	C → 5967	6543.44 18	0.586 24	C → 4843
4639.1 6	0.030 6	unplaced	5452.1 5	0.028 5	8638 → 3186	6608.29 15	0.293 13	C → 4779
4678.3 5	0.050 5	8565 → 3887	5468.5 6	0.028 5	C → 5918	6627.12 19	0.128 8	C → 4760
4683.0 5	0.043 6	unplaced	5472.8 5	0.036 5	8666 → 3193	6809.91 9	0.333 13	C → 4577
4693.6 5	0.042 6	7818 → 3123	5485.02 8	0.377 9	C → 5902	6839.38 12	1.21 7	C → 4548
4740.48 12	0.227 10	C → 6647	5509.46 11	0.223 8	C → 5878	6894.23 11	0.275 10	C → 4493
4744.7 5	0.047 7	unplaced	5527.4 5	0.035 5	C → 5860	6911.7 3	0.098 6	6911 → 0
4760.1 4	0.054 6	4760 → 0	5578.7 6	0.022 5	6911 → 1332	7032.9 7	0.026 5	unplaced
4819.9 6	0.032 6	C → 6567	5611.8 <sup>t</sup> 4	0.036 5	5612 → 0	7051.67 12	0.220 9	C → 4335
4843.76 9	0.389 15	4843 → 0	5640.4 7	0.020 5	7799 → 5152	7068.67 8	0.415 12	C → 4318
4871.7 8	0.024 6	C → 6516	5659.9 8	0.015 4	8286 → 2625	7275.9 9	0.019 5	C → 4111
4898.4 4	0.064 6	C → 6489	5676.64 4	0.935 18	C → 5710	7309.22 14	0.214 10	C → 4078
4906.1 5	0.043 6	6239 → 1332	5710.52 10	0.362 12	5710 → 0	7367.31 5	1.95 5	C → 4019
4922.34 25	0.155 11	C → 6465	5714.96 18	0.159 9	C → 5672	7380.77 4	2.43 7	C → 4006
4950.1 5	0.101 15	unplaced	5723.0 5	0.035 5	7056 → 1332	7473.0 8	0.030 6	7473 → 0
5005.5 <sup>q</sup> 7	0.031 7	C → 6382	5759.1 <sup>u</sup> 7	0.024 5	9076 → 3317	7499.4 4	0.076 7	C → 3887
5025.43 25	0.092 8	C → 6362	5775.08 6	0.713 15	C → 5612	7516.17 4	2.04 5	C → 3871
5046.4 7	0.032 6	8666 → 3619	5875.2 7	0.017 4	7207 → 1332	7652.88 8	0.430 10	C → 3734
5059.8 6	0.040 7	C → 6327	5886.3 7	0.023 5	unplaced	7689.5 5	0.043 6	7690 → 0
5064.79 7	0.509 15	5065 → 0	5889.9 5	0.033 5	7222 → 1332	7761.6 8	0.027 6	7761 → 0
5097.8 6	0.031 6	unplaced	5911.3 8	0.016 5	C → 5476	7799.40 6	0.689 14	C → 3587
5132.6 5	0.028 6	6465 → 1332	5933.3 7	0.018 5	9953 → 4019	7915.1 9	0.022 6	unplaced
5148.1 3	0.062 5	C → 6239	5940.5 3	0.074 6	C → 5447	7951.4 8	0.025 6	7950 → 0
5152.61 25	0.070 5	unplaced	5944.3 5	0.039 5	unplaced	7993.95 10	0.310 11	C → 3393
5157.9 9	0.015 5	unplaced	5952.4 5	0.024 5	9076 → 3123	8069.26 4	3.18 6	C → 3317
5173.6 3	0.049 5	9045 → 3871	5967.5 8	0.014 5	5967 → 0	8117.6 9	0.044 13	C → 3268
5184.9 5	0.029 5	10029 → 4843	5983.4 5	0.024 5	7316 → 1332	8193.24 4	1.90 5	C → 3193
5193.4 3	0.056 5	unplaced	6003.9 7	0.017 5	unplaced	8200.88 17	0.207 9	C → 3186
5234.82 10	0.230 7	unplaced	6067.2 8	0.014 5	6066 → 0	8263.35 5	1.59 5	C → 3123
5245.5 5	0.030 5	unplaced	6099.4 3	0.062 6	C → 5288	8504.2 9	0.020 4	8504 → 0
5254.46 14	0.146 6	unplaced	6162.5 6	0.032 5	7494 → 1332	9102.10 4	8.83 16	C → 2284
5287.8 7	0.022 5	5288 → 0	6260.19 20	0.070 6	C → 5127	9228.19 9	1.14 4	C → 2158
5292.3 9	0.016 5	7793 → 2505	6322.29 11	0.557 14	C → 5065	10054.14 7	8.22 15	C → 1332
5299.1 5	0.074 16	unplaced	6351.2 4	0.032 5	7684 → 1332	11386.50 9	21.5 8	C → 0

<sup>a</sup>In our notation, 119.9 3 ≡ 119.9 ± 0.3, etc.

<sup>b</sup>In our notation, 3.02 7 ≡ 3.02 ± 0.07, etc. Multiply by 1.357 to obtain photons per 100 thermal neutron captures.

<sup>c</sup>C denotes the capturing state.

<sup>d</sup>Can also be placed as a 9346 → 5860 transition.

<sup>e</sup>Can also be placed as a 8638 → 5127 transition.

<sup>f</sup>Can also be placed as a 7495 → 3925 transition.

<sup>g</sup>Can also be placed as a 6996 → 3393 transition.

<sup>h</sup>Can also be placed as a 7761 → 3925 transition.

<sup>i</sup>Can also be placed as a 7818 → 3925 transition.

<sup>j</sup>Can also be placed as a 7690 → 3734 transition.

<sup>k</sup>Can also be placed as a 6465 → 2285 transition.

<sup>l</sup>Can also be placed as a 7473 → 3269 transition.

<sup>m</sup>Can also be placed as a 8286 → 4006 transition.

<sup>n</sup>Can also be placed as a 7950 → 3619 transition.

<sup>o</sup>Can also be placed as a 7495 → 3123 transition.

<sup>p</sup>Can also be placed as a 8565 → 4019 transition.

<sup>q</sup>Can also be placed as a 9045 → 4039 transition.

<sup>r</sup>Can also be placed as a 8638 → 3317 transition.

<sup>s</sup>Can also be placed as a 9953 → 4534 transition.

<sup>t</sup>Can also be placed as a 9347 → 3734 transition.

<sup>u</sup>Can also be placed as a 9347 → 3588 transition.

TABLE X. Level scheme of  $^{60}\text{Ni}$  from this work in tabular form.

$E(\text{level})^a$ (keV)	$J^\pi$	Deexciting $\gamma$ rays <sup>b</sup>	$I_\gamma$ (in) <sup>a</sup> (b)	$I_\gamma$ (out) <sup>a</sup> (b)	$I_\gamma$ (in - out) <sup>a</sup> (b)
0.0	0 <sup>+</sup>		73.7 12		73.7 12
1332.536 16	2 <sup>+</sup>	1332.543	42.1 4	44.6 9	-2.5 10
2158.671 18	2 <sup>+</sup>	2158.63, 826.11	6.42 7	7.28 13	-0.86 14
2284.828 24	0 <sup>+</sup>	952.26	10.12 17	11.2 3	-1.1 4
2505.79 3	4 <sup>+</sup>	1173.24	0.546 18	0.47 4	0.08 5
2625.98 3	3 <sup>+</sup>	1293.2, 467.28, 119.9	0.937 21	1.11 6	-0.18 7
3119.45 18	4 <sup>+</sup>	1786.9, 493.3	0.060 7	0.057 9	0.003 11
3123.750 21	2 <sup>+</sup>	3123.70, 1791.19, 964.8, 839.08, 497.76	3.10 6	3.57 5	-0.47 7
3186.23 4	3 <sup>+</sup>	1853.67, 1027.56, 680.42	0.299 13	0.545 9	-0.246 16
3193.892 19	1 <sup>+</sup>	3193.77, 1861.33, 1035.23, 909.05	3.06 6	3.57 5	-0.51 7
3268.97 4	2 <sup>+</sup>	3268.78, 1936.41, 1110.31, 983.9, 642.96	0.263 19	0.440 11	-0.177 12
3317.85 3	0 <sup>+</sup>	1985.27, 1159.09	3.32 6	3.69 7	-0.37 10
3393.16 3	2 <sup>+</sup>	3393.05, 2060.58, 1234.51	0.472 16	0.685 15	-0.213 21
3587.75 3	0 <sup>+</sup>	2255.18, 1429.07, 393.76	0.729 15	0.888 13	-0.159 20
3619.47 4	(3) <sup>+</sup>	1113.9, 993.48,	0.143 11	0.214 8	-0.071 13
3734.42 3	2 <sup>+</sup>	2401.83	0.564 15	0.778 15	-0.214 21
3871.080 23	1 <sup>+</sup> , 2 <sup>+</sup>	3870.94, 2538.53, 1712.30, 1244.93, 751.9, 747.33, 677.17	2.23 6	2.55 3	-0.32 6
3887.38 7		2554.69, 1381.8, 693.57, 569.5	0.188 12	0.205 9	-0.017 15
3925.22 9	2 <sup>+</sup> , 3 <sup>+</sup>	1766.5, 1419.40, 805.6, 739.2, 305.7	0.018 5	0.139 9	-0.121 10
4006.46 3	1 <sup>+</sup> , 2 <sup>+</sup>	4006.30, 2673.86, 1380.4, 883.1	2.45 7	2.86 5	-0.41 9
4019.914 25	1 <sup>+</sup> , 2 <sup>+</sup>	4019.74, 2687.33, 1734.98, 896.23, 702.11, 431.9	2.54 6	2.70 5	-0.17 7
4039.92 6	3 <sup>-</sup>	2707.44, 1881.15, 853.8	0.164 9	0.234 8	-0.070 12
4078.01 5	1 <sup>+</sup> , 2 <sup>+</sup>	4077.6, 2745.47, 1919.28, 1451.88	0.355 13	0.427 12	-0.072 17
4111.97 9		4111.6, 2779.42, 1606.10, 1485.94	0.077 8	0.223 11	-0.146 14
4318.58 5	1 <sup>+</sup> , 2 <sup>+</sup>	4318.52, 2985.97, 1813.5, 1692.45	0.481 15	0.635 15	-0.154 22
4335.56 4		4335.37, 3002.5, 2176.84, 1829.9	0.268 11	0.415 14	-0.147 17
4355.57 12		3022.90	0.107 5	0.064 5	0.043 7
4493.18 6	2 <sup>+</sup>	3160.60, 2334.4, 1306.5, 758.5	0.350 13	0.330 13	0.020 18
4534.13 14		2375.6, 2028.5,	0.079 7	0.049 7	0.030 10
4547.99 3	1 <sup>+</sup> , 2 <sup>+</sup>	4548.2, 3215.27, 2389.25, 2263.17, 1424.24, 1354.08, 1154.82, 813.48	1.23 7	1.363 23	-0.13 3
4577.46 6	2 <sup>+</sup>	4577.37, 3244.90, 2418.65, 1308.16	0.333 13	0.381 12	-0.048 18
4760.25 9		4760.1, 3428.0, 2601.5, 1636.42, 1491.5	0.162 9	0.29 3	-0.13 3
4779.16 6		3446.77, 2620.40, 2493.8, 1585.33, 1385.97, 667.4	0.293 13	0.347 12	-0.054 18
4843.94 8		4843.76, 3511.07	0.67 3	0.563 17	0.10 3
4929.00 14		3596.4, 2770.5, 1194.4	0.098 6	0.094 10	0.004 11
4953.38 7		3620.64, 1684.4, 913.63, 841.2	0.223 7	0.211 11	0.012 13
5065.03 6	(1 <sup>-</sup> )	5064.79, 3732.23	0.557 14	0.660 20	-0.103 25
5127.18 17		3794.8, 1392.3	0.070 6	0.058 7	0.012 9
5288.57 14		5287.8, 3955.2, 1248.86	0.062 6	0.083 9	-0.021 11
5446.99 10		3288.5, 1575.84, 1091.42	0.074 6	0.227 11	-0.153 13
5476.06 21		2282.0, 1888.4	0.016 5	0.056 6	-0.040 8

levels at 5446.99 and 5967.8 keV and the 27 levels above 6.9 MeV (see Table X) should be viewed with caution, based as they are only on energy fits and not on coincidence data or corroboration in another reaction experiment. The  $\gamma$ -ray branching ratios determined in this work are reasonably consistent with those adopted in Ref. [93].

The neutron separation energy determined in this work is  $S_n(^{60}\text{Ni}) = 11\,387.73 \pm 0.05$  keV. The value obtained by Wilson *et al.* [59],  $S_n = 11\,387.5 \pm 0.7$  keV, is consistent with our more accurate value.

The improved sensitivity of the current measurement has resulted in a significant increase (see Table XI) in both the

TABLE X. (Continued.)

$E(\text{level})^a$ (keV)	$J^\pi$	Deexciting $\gamma$ rays <sup>b</sup>	$I_\gamma$ (in) <sup>a</sup> (b)	$I_\gamma$ (out) <sup>a</sup> (b)	$I_\gamma$ (in - out) <sup>a</sup> (b)
5612.44	4	5611.8, 4279.8, 3453.67, 2488.73, 1878.0, 1741.3, 1592.53, 1064.2, 851.9	0.763 17	0.805 17	-0.042 24
5672.39	7	3513.6, 3046.7, 2478.42	0.211 11	0.218 10	-0.007 15
5710.82	4	5710.52, 3551.94, 3426.3, 2586.98, 2517.00, 2392.6, 2317.65, 1632.99	0.957 19	1.04 3	-0.09 4
5860.0	5	3700.9	0.035 5	0.031 8	0.004 10
5878.08	9	4545.9, 2684.19	0.223 8	0.240 17	-0.017 19
5902.45	7	3743.71, 3276.32, 2633.3	0.377 9	0.256 12	0.121 15
5918.56	21	2525.4, 1562.8	0.028 5	0.073 8	-0.045 9
5967.8	3	5967.5, 1474.6	0.025 5	0.063 8	-0.038 10
6066.71	11	3440.37, 2797.7, 1532.65	0.111 8	0.182 12	-0.071 14
6239.2	3	4906.1	0.062 5	0.043 6	0.019 8
6327.23	15	3058.0, 2320.7, 1568.0	0.061 10	0.154 11	-0.093 14
6362.06	17	3167.7, 749.7	0.102 9	0.095 8	0.007 12
6382.4	4	6382.3	0.031 7	0.033 5	-0.002 9
6465.27	16	6464.9, 5132.6, 2578.2, 1621.2	0.155 11	0.149 10	0.006 15
6489.17	23	4204.0, 3369.4	0.064 6	0.094 10	-0.030 12
6516.73	23	2496.9, 2198.1	0.024 6	0.046 6	-0.022 9
6567.35	20	2547.35	0.032 6	0.043 5	-0.011 8
6647.19	9	4021.4, 3027.86, 2627.4, 2607.10	0.227 10	0.220 12	0.007 16
6756.3	3	3487.1, 2831.3	0.036 6	0.041 7	-0.005 10
6834.95	19	3641.1, 3517.3	0.071 6	0.087 8	-0.016 10
6911.95	9	6911.7, 5578.7, 3040.5, 2593.3	0.150 7	0.165 10	-0.015 13
6996.86	20	4370.7, 2152.6	0.042 5	0.060 7	-0.018 9
7056.29	14	5723.0, 4430.3	0.113 6	0.075 7	0.038 10
7207.7	3	5875.2, 3129.6	0.018 4	0.050 6	-0.032 7
7222.81	11	5889.9, 3603.4	0.193 8	0.053 7	0.140 11
7316.15	16	5983.4, 3296.3, 1643.6	0.073 8	0.088 9	-0.015 12
7339.71	25	2846.9, 1628.9	0.048 6	0.048 7	0.000 9
7414.18	23	3302.11	0.042 7	0.035 4	0.007 8
7473.50	24	7473.0, 2938.6,	0.042 6	0.054 8	-0.012 10
7495.3	4	6162.5, 1005.83,	0.043 7	0.032 5	0.011 9
7552.0	3	5393.3	0.033 6	0.062 5	-0.029 8
7684.1	4	6351.2	0.039 11	0.032 5	0.007 12
7690.1	3	7689.5, 3354.5	0.032 7	0.091 8	-0.059 11
7761.7	3	7761.6, 4492.3, 1399.4	0.034 6	0.059 8	-0.025 10
7798.88	25	5640.4, 1472.6	0.051 8	0.057 10	-0.006 13
7818.04	13	4693.6	0.088 5	0.042 6	0.046 8
7950.95	24	7951.4, 3632.4	0.076 6	0.076 11	0.000 12
8286.3	3	5659.9, 2613.9	0.015 4	0.041 6	-0.026 7
8504.7	3	8504.2, 4617.2	0.037 5	0.068 8	-0.031 9
8565.63	19	4678.3, 4487.56	0.040 5	0.105 7	-0.065 9
8638.57	25	5452.1, 2572.2	0.026 5	0.045 7	-0.019 9

number of detected  $\gamma$  rays and the number of bound states found to be populated in the ( $n, \gamma$ ) reaction.

### C. Thermal-neutron cross sections for $^{59}\text{Ni}$

In 1970, Weitman, D averh og, and Farvolden [118] reported an anomalously large production of helium gas in

nickel samples irradiated with neutrons. Nickel is a constituent of reactor construction materials such as stainless steel. Excessive helium production can cause swelling and embrittlement which, in turn, can limit the useful lifetimes of structures. In a reactor, neutrons are captured by  $^{58}\text{Ni}$  to produce  $^{59}\text{Ni}$ . It is now well established that the  $^{59}\text{Ni}(n, \alpha)$  reaction is a major factor in the helium production. Because of

TABLE X. (*Continued.*)

$E(\text{level})^a$ (keV)	$J^\pi$	Deexciting $\gamma$ rays <sup>b</sup>	$I_\gamma$ (in) <sup>a</sup> (b)	$I_\gamma$ (out) <sup>a</sup> (b)	$I_\gamma$ (in - out) <sup>a</sup> (b)
8666.23	22	5472.8, 5046.4	0.038 5	0.068 8	-0.030 10
9045.23	24	5173.6	0.023 4	0.049 5	-0.026 7
9076.68	17	5952.4, 5759.1	0.048 5	0.048 7	0.000 9
9346.84	18	5306.7	0.048 5	0.040 5	0.008 5
9953.7	3	5933.3	0.018 4	0.018 5	0.000 7
10029.04	17	5184.9	0.027 4	0.029 5	-0.002 7
11387.727 <sup>c</sup>	19	11386.50, 10054.14, 9228.19, 9102.10, 8263.35, 8200.88, 8193.24, 8117.6, 8069.26, 7993.95, 7799.40, 7652.88, 7516.17, 7499.4, 7380.77, 7367.31, 7309.22, 7275.9, 7068.67, 7051.67, 6894.23, 6839.38, 6809.91, 6627.12, 6608.29, 6543.44, 6458.42, 6434.01, 6322.29, 6260.19, 6099.4, 5940.5, 5911.3, 5775.08, 5714.96, 5676.64, 5527.4, 5509.46, 5485.02, 5468.5, 5419.5, 5320.69, 5148.1, 5059.8, 5025.43, 5005.5, 4922.34, 4898.4, 4871.7, 4819.9, 4740.48, 4631.2, 4553.0, 4475.58, 4390.4, 4331.24, 4180.5, 4164.75, 4071.49, 4048.2, 3973.4, 3913.7, 3892.4, 3836.1, 3703.4, 3697.7, 3625.6, 3589.0, 3569.53, 3436.9, 3101.2, 2883.0, 2822.3, 2749.5, 2721.59, 2341.9, 2311.00, 2040.85, 1434.0, 1358.67	64.2 9	-64.2 9	

<sup>a</sup>In our notation, 1332.536 16  $\equiv$  1332.536  $\pm$  0.016, 73.7 12  $\equiv$  73.7  $\pm$  1.2, etc.

<sup>b</sup>See also Table IX.

<sup>c</sup>Capturing state.

TABLE XI. Increasing complexity in the study of the  $^{59}\text{Ni}(n, \gamma)^{60}\text{Ni}$ .

Number of	Wilson, Thomas, and Jackson [59]	Raman and Jurney [60] unpublished	This work
	ANL (1975)	LANL/ORNL (1979)	LANL/ORNL
$\gamma$ rays	17	250	390
spurious $\gamma$ rays <sup>a</sup>	1	33	
placed $\gamma$ rays <sup>b</sup>	17	210	326
primary $\gamma$ rays	17	40	80
secondary $\gamma$ rays	0	170	246
unplaced $\gamma$ rays <sup>c</sup>	0	40	64
bound levels	17	73	88

<sup>a</sup>Gamma rays sought but not observed in this more sensitive work and, therefore, considered spurious.

<sup>b</sup>Some of the placed  $\gamma$  rays may be spurious.

<sup>c</sup>Some of the unplaced  $\gamma$  rays may be genuine.

TABLE XII. Thermal-neutron cross sections (in *b*) for  $^{59}\text{Ni}$ . In our notation, 70 5 $\equiv$ 70 $\pm$ 5, 73.7 18 $\equiv$ 73.7 $\pm$ 1.8, etc.

Reaction	Cross		Cross		Cross		Cross	
	section	Reference	section	Reference	section	Reference	section	Reference
$^{59}\text{Ni}(n, \gamma)$	70 5	[120, 123]						
	73.7 18	This work						
$^{59}\text{Ni}(n, p)$			2.0 5	[123]				
			4 1	[124]				
			1.34 18	[125]				
$^{59}\text{Ni}(n, \alpha)$					13.7 12	[119]		
					18.0 16	[121]		
					12 1	[123]		
					22.3 16	[124]		
$^{59}\text{Ni}(n, \text{abs})^a$					13.3 12	[125]		
							87 6	[120, 123]
							92 4	[122]

<sup>a</sup>Absorption (abs) denotes sum of all interactions except scattering.

their relevance to power reactors, the thermal-neutron cross sections for  $^{59}\text{Ni}$  have been measured at several laboratories [119–125]. The results are summarized in Table XII. There is general agreement concerning the magnitudes of the  $(n, p)$ ,  $(n, \alpha)$ , and absorption cross sections for  $^{59}\text{Ni}$  (see Table XII) but definitive values are not known at this time and require additional experiments.

The  $(n, \gamma)$  cross-section value of  $70 \pm 5$  b reported in Ref. [123] was based on  $\gamma$ -ray spectrum measurements using a NaI detector and a 7.0-mg nickel-metal target enriched to 95.35% in  $^{59}\text{Ni}$  [120,123]. The cross section in this case was normalized to the value of  $\sigma_\gamma(2200 \text{ m/s}) = 332.6 \pm 0.7$  mb [87] for  $^1\text{H}$  present in a 97-mg,  $\text{CH}_2$  standard. The current cross-section value of  $73.7 \pm 1.8$  b is based on  $\gamma$ -ray spectrum measurements using a Ge detector and a 6.9-mg nickel-metal target enriched to  $(44.3 \pm 0.4)\%$  in  $^{59}\text{Ni}$ . The current value agrees with the previous value, but is more accurate. The normalization in the current case was provided by the known value of  $(37.9 \pm 0.4)\%$  for the  $^{58}\text{Ni}$  content in the sample and the value of  $\sigma_\gamma(2200 \text{ m/s}) = 4.13 \pm 0.05$  b for the  $^{58}\text{Ni}(n, \gamma)$  reaction as determined in this work earlier. The  $^{60}\text{Ni}$  content  $[(14.5 \pm 0.3)\%$  of the sample] and  $\sigma_\gamma(2200 \text{ m/s}) = 2.34 \pm 0.05$  b for the  $^{60}\text{Ni}(n, \gamma)$  reaction (also determined in this work) provided a cross check of the normalization. The quoted uncertainty of 1.8 b in the  $^{59}\text{Ni}$  cross section includes contributions from all sources including the normalization.

The measured values  $\Sigma I_\gamma(\text{primary}) = 64.2 \pm 0.9$  b,  $\Sigma E_\gamma I_\gamma / S_n = 69.9 \pm 9.9$  b, and  $\Sigma I_\gamma(\text{to ground state}) = 73.7 \pm 1.2$  b do not agree mainly because we have not detected all primary  $\gamma$  rays. In such cases, it is customary to adopt  $\Sigma I_\gamma(\text{to ground state})$  as the recommended cross-section value. The 1332.54-keV transition from the first-excited state to the ground state and the 11 386.50-keV transition from the capturing state to the ground state together account for  $\sim 90\%$  of this cross section. Holden [110] does not explicitly recommend a value for the capture cross section, but the absorption,  $(n, \alpha)$ , and  $(n, \gamma)$  cross sections listed by him imply a capture cross section of  $76 \pm 5$  b.

Within the direct-capture theory, the two crucial quantities entering the calculation of a partial cross section for a particular  $\gamma$  ray are the final-state  $(d, p)$  spectroscopic strength and the (normally spin-dependent) neutron scattering length. Because these quantities are unknown for a  $^{59}\text{Ni}$  target, we have not calculated the partial cross sections given by theory.

**D. Shell-model calculations of  $^{60}\text{Ni}$  levels**

The calculated spectrum is compared with experiment in Fig. 7. There is a one-to-one correspondence between experiment and theory for the first ten excited states. The theoretical spectrum is compressed in energy compared to the experimental spectrum.

**VI. REACTION  $^{60}\text{Ni}(n, \gamma)$**

**A. Skeleton level scheme of  $^{61}\text{Ni}$**

In Table XIII, we have listed the previous measurements that have been carried out concerning the energy levels in

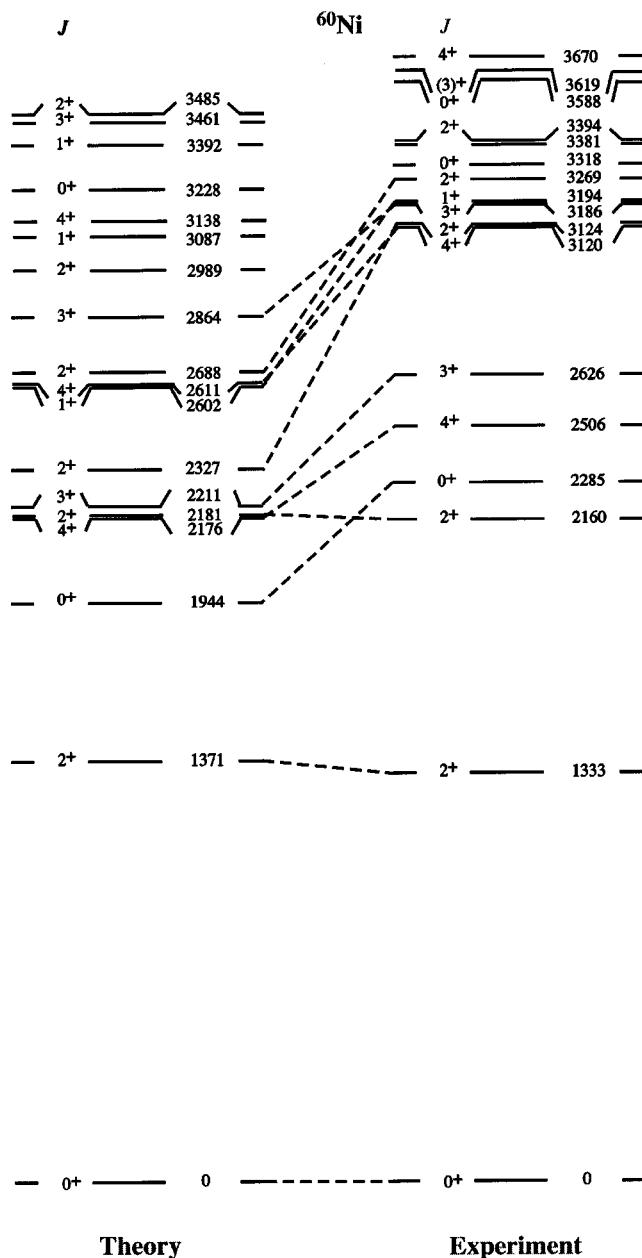


FIG. 7. Comparison between the shell-model predictions and the experimental level scheme of  $^{60}\text{Ni}$ . The levels are labeled by  $J^\pi$  on the left and by level energies (in keV) on the right.

$^{61}\text{Ni}$ . Based on these measurements, we have assembled a list (see Table XIV) of  $\sim 168$  levels below 5.5 MeV. The backbone of this level scheme is the  $^{60}\text{Ni}(d, p)^{61}\text{Ni}$  study by Cosman *et al.* [78]. Just as in the  $^{59}\text{Ni}$  case, it was necessary to apply a substantial correction (as large as  $-12$  keV in the 3.2–4.0 keV region and smaller corrections elsewhere) to the level energies reported by Cosman *et al.* [78].

Nine works [69,72–74,76–79,83] out of the 20 listed in Table XIII contain information leading to the  $J^\pi$  assignments given in Table XIV for about half of all known levels below 5.5 MeV.

TABLE XIII. Partial list of references to previous measurements on  $^{61}\text{Ni}$  levels. See Ref. [96] for additional references.

Measurement	Author(s)	Year	Facility <sup>a</sup>	Reference
$^{48}\text{Ca}(^{18}\text{O}, 5n)$ reaction	Warburton <i>et al.</i>	1978	Brookhaven	[71]
$^{53}\text{Cr}(^{11}\text{B}, p2n\gamma)$ reaction	Wadsworth <i>et al.</i>	1977	U. Liverpool	[72]
$^{58}\text{Fe}(\alpha, n\gamma)$ reaction	Wadsworth <i>et al.</i>	1977	U. Liverpool	[73]
$^{58}\text{Ni}(\text{polarized } d, t)$ reaction	Huttlin <i>et al.</i>	1976	U. Notre Dame	[74]
$^{59}\text{Co}(^3\text{He}, p)$ reaction	Cosman, Schramm, and Enge	1968	MIT	[75]
$^{59}\text{Ni}(t, p)$ reaction	Nann <i>et al.</i>	1978	Los Alamos	[76]
$^{60}\text{Ni}(\text{thermal } n, \gamma)$ reaction	Ishaq <i>et al.</i>	1977	McMaster U.	[28]
	Harder <i>et al.</i>	1993	Grenoble	[30]
$^{60}\text{Ni}(\text{polarized } n, \gamma)$ reaction	Stecher-Rasmussen <i>et al.</i>	1972	Petten	[31]
	Kopecky <i>et al.</i>	1972	Petten	[77]
$^{60}\text{Ni}(d, p)$ reaction	Fulmer <i>et al.</i>	1964	U. Pittsburgh	[32]
	Cosman <i>et al.</i>	1967	MIT	[78]
$^{60}\text{Ni}(\text{polarized } d, p)$ reaction	Aymar <i>et al.</i>	1973	U. Notre Dame	[79]
$^{61}\text{Ni}(n, n'\gamma)$ reaction	Kosyak, Kaipov, and Chekushina	1989	Alma-Ata	[80]
$^{61}\text{Ni}(p, p')$ reaction	Cosman <i>et al.</i>	1967	MIT	[78]
	Tee and Aspinall	1967	Aldermaston	[64]
$^{61}\text{Ni}(d, d')$ reaction	Cosman <i>et al.</i>	1967	MIT	[78]
	Meyer <i>et al.</i>	1978	Livermore	[81]
$^{61}\text{Cu}(\beta^+ + \varepsilon)$ decay	Satyanarayana <i>et al.</i>	1988	Calcutta	[82]
	Sherr <i>et al.</i>	1965	U. Colorado	[40]
$^{62}\text{Ni}(p, d)$ reaction	Koang, Chien, and Rossner	1976	Michigan State U.	[69]
	Matoba <i>et al.</i>	1996	Osaka U.	[83]

<sup>a</sup>Facility where the actual measurements were done. The symbol U stands for a university.

### B. Thermal-neutron capture $\gamma$ -ray data

The  $^{60}\text{Ni}(n, \gamma)$  reaction with thermal neutrons has been studied previously with Ge detectors at the McMaster and Grenoble reactors by Ishaq *et al.* [28] and Harder *et al.* [30], respectively. The study by Harder *et al.* [30] at Grenoble is the more extensive of these two studies. These authors claim to have observed 312  $\gamma$  rays from the  $^{60}\text{Ni}(n, \gamma)$  reaction, but the published paper lists only 143  $\gamma$  rays. The unavailability of the complete list has hampered our efforts to fully resolve the differences between our data and the Grenoble data.

The current (thermal  $n, \gamma$ ) measurements were made with a 200.1-mg, 99.83%-enriched  $^{60}\text{NiO}$  target. The results are given in Table XV. The level scheme resulting from this work is presented in Table XVI. Nearly three-fourths of the observed  $\gamma$  rays, totaling 240 in number, have been incorporated into this scheme consisting of 40 bound levels.

Gamma rays of energies 3089.7, 3898.5, 6429.5, and 6752.0 keV, reported by Ishaq *et al.* [28], were not observed either by Harder *et al.* [30] or by us. Similarly, the levels at 3590.63, 3968.49, 4290.92, and 4405.16 keV, proposed by Ishaq *et al.* [28], remain unconfirmed by both latter studies.

According to Harder *et al.* [30], 31 levels in  $^{61}\text{Ni}$  are populated significantly in the (thermal  $n, \gamma$ ) reaction. We confirm this conclusion for all levels except those at 4713, 4886, 4963, and 5112 keV. Harder *et al.* [30] list 20  $\gamma$  rays associated with these four levels. We have observed only seven of these  $\gamma$  rays. We have placed four of the observed  $\gamma$  rays elsewhere in the level scheme and kept the remaining three as unplaced. In addition, we conclude that the pub-

lished data of Harder *et al.* [30] contain a larger fraction of spurious  $\gamma$  rays in  $^{61}\text{Ni}$  (~23%) than in  $^{59}\text{Ni}$  (~16%).

In addition to the 27 levels common to this work and the earlier work by Harder *et al.* [30], we propose that 13 more levels are populated significantly in the  $^{60}\text{Ni}(n, \gamma)$  reaction, bringing the total to 40 levels (see Table XVII). Of these, all levels except those at 3144.98, 4793.12, and 5036.24 keV correspond well with the known levels in  $^{61}\text{Ni}$ .

The neutron separation energy determined in this work is  $S_n(^{61}\text{Ni}) = 7820.11 \pm 0.05$  keV. The values  $7820.14 \pm 0.20$  and  $7820.07 \pm 0.20$  obtained by Ishaq *et al.* [28] and Harder *et al.* [30], respectively, are consistent with our more accurate value.

### C. Capture cross sections for $^{60}\text{Ni}$

The measured values  $\Sigma I_\gamma$  (primary) =  $2.308 \pm 0.018$  b,  $\Sigma E_\gamma I_\gamma / S_n = 2.330 \pm 0.020$  b, and  $\Sigma I_\gamma$  (to ground state) =  $2.390 \pm 0.030$  b agree reasonably well. Our recommended cross-section value of  $2.34 \pm 0.05$  b for the  $^{60}\text{Ni}(n, \gamma)$  reaction is significantly more precise than the currently accepted value of  $2.9 \pm 0.3$  b [110]. The total intensity of the observed but unplaced transitions is  $\sim 0.03$  b. The 2.1% uncertainty quoted for the recommended cross-section value does not include a systematic uncertainty of similar magnitude caused by unplaced and missing transitions.

Unlike  $^{58}\text{Ni}$ , the thermal-neutron capture cross section of  $^{60}\text{Ni}$  is mostly due to the first resonance in the cross section at 12.5 keV. From its resonance parameters, we compute that

TABLE XIV. Known energy levels in  $^{61}\text{Ni}$ .

Known $E(\text{level})^a$ (keV)	$J^\pi$	Previous ( $n, \gamma$ ) $E(\text{level})^a$ (keV)	This work ( $n, \gamma$ ) $E(\text{level})^a$ (keV)	Known $E(\text{level})^a$ (keV)	$J^\pi$	Previous ( $n, \gamma$ ) $E(\text{level})^a$ (keV)	This work ( $n, \gamma$ ) $E(\text{level})^a$ (keV)
0.0	$\frac{3}{2}^-$	0.0	0.0	2902 10	$\frac{7}{2}^-$		
67.412 3	$\frac{5}{2}^-$	67.418 24	67.41 3	3040 5	$(\frac{1}{2}^-, \frac{3}{2}^-)$		
282.957 2	$\frac{1}{2}^-$	282.887 22	282.973 21	3062 5	$\frac{1}{2}^+$	3062.29 8	3062.16 5
656.012 3	$\frac{1}{2}^-$	656.050 22	656.039 22	3105 5	$\frac{5}{2}^-, \frac{7}{2}^-$		
908.620 11	$\frac{5}{2}^-$	908.64 5	908.59 3	3130 5	$\frac{7}{2}^-$		
1015.12 17	$\frac{7}{2}^-$		1015.32 9			3145.03 8	3144.98 3
1099.622 10	$\frac{3}{2}^-$	1099.67 3	1099.684 22	3153 5	$(\frac{1}{2}^-, \frac{3}{2}^-)$		
1132.332 17	$\frac{5}{2}^-$	1132.40 3	1132.41 3	3188 7			
1185.236 11	$\frac{3}{2}^-$	1185.37 3	1185.301 22	3229 5	$\frac{1}{2}^-, \frac{3}{2}^-$	3231.81 8	3231.67 4
1454.5 3	$\frac{7}{2}^-$		1454.84 11	3256 5	$(\frac{1}{2}^-, \frac{3}{2}^-)$		
1609.639 21	$\frac{5}{2}^-$	1609.88 5	1609.80 5	3259.1 5	$\frac{7}{2}^-, \frac{11}{2}^-$		
1729.471 10	$\frac{3}{2}^-$	1729.72 5	1729.63 3	3268 7			
1807.5 5	$\frac{9}{2}^-$			3286	$(\frac{1}{2}^-, \frac{3}{2}^-)$		
1987.6 3	$\frac{9}{2}^-$			3295 10	$\frac{7}{2}^-$		
1997.5 3	$\frac{5}{2}^-$		1998.12 7	3298.7 8	$\frac{11}{2}^+$		
2018.0 5	$\frac{7}{2}^-$			3306 10	$\frac{7}{2}^-$		
2121.67 25	$\frac{9}{2}^+$			3358 5	$\frac{1}{2}^-, \frac{3}{2}^-$		
2124.0 7	$\frac{1}{2}^-$	2124.05 4	2123.949 19	3397 7			
2129.22 25	$\frac{11}{2}^-$			3415 5	$\frac{1}{2}^-, \frac{3}{2}^-$	3415.18 9	3415.14 4
2408 5	$(\frac{3}{2}^-)$			3426.2 4	$\frac{13}{2}^-$		
2409.7 3	$\frac{9}{2}^-$			3436 5	$\frac{3}{2}^+, \frac{5}{2}^+$		
2465 5	$\frac{7}{2}^-$			3436.5 6	$\frac{13}{2}^+$		
2527 5	$\frac{5}{2}^-, \frac{7}{2}^-$			3461 5			
2593 5	$\frac{7}{2}^-$			3480 5	$\frac{9}{2}^+$		
2638 5	$\frac{1}{2}^-, \frac{3}{2}^-$	2639.74 4	2639.51 5	3495 5	$\frac{3}{2}^+, \frac{5}{2}^+$		
2697 5	$\frac{5}{2}^+$			3525 5		3525.57 11	3525.60 8
2716 7			2707.63 9	3561 5			
2734 10	$(\frac{7}{2}^-)$			3570 7			
2763 5	$\frac{3}{2}^-$	2765.11 8	2765.03 9	3596 5			
2794 5	$\frac{5}{2}^-, \frac{7}{2}^-$			3616 5			
2807 7				3635 5	$\frac{3}{2}^+, \frac{5}{2}^+$		
2860 10	$\frac{5}{2}^-, \frac{7}{2}^-$			3644.6 8			
2863 5	$\frac{1}{2}^-, \frac{3}{2}^-$	2863.58 8	2862.94 9	3665.4 9	$\frac{7}{2}^-$		
2899 5				3671 5	$\frac{1}{2}^-, \frac{3}{2}^-$	3669.01 10	3668.99 4

TABLE XIV. (*Continued.*)

Known $E(\text{level})^a$ (keV)	$J^\pi$	Previous ( $n, \gamma$ ) $E(\text{level})^a$ (keV)	This work ( $n, \gamma$ ) $E(\text{level})^a$ (keV)	Known $E(\text{level})^a$ (keV)	$J^\pi$	Previous ( $n, \gamma$ ) $E(\text{level})^a$ (keV)	This work ( $n, \gamma$ ) $E(\text{level})^a$ (keV)
3696 5				4326 5			
3713 5	$\frac{1}{2}^-, \frac{3}{2}^-$	3711.38 11	3711.49 6	4350 5			
3741 5	$(\frac{1}{2}^+)$	3738.44 11	3738.34 18	4364 5			
3769 10	$\frac{7}{2}^-$			4376 5	$\frac{7}{2}^-$		
3779 5	$(\frac{1}{2}^-, \frac{3}{2}^-)$	3776.57 11	3776.80 9	4393 5			
3793 7				4415 5			
3807 5	$(\frac{1}{2}^-, \frac{3}{2}^-)$			4438 5			4439.88 13
3848 5				4457 7			
3867 5		3869.92 11	3869.99 7	4467 5			
3883 7				4487 10	$\frac{7}{2}^-$		
3930 5	$\frac{7}{2}^-$			4492 5			
3942 5				4513 5			4514.69 13
3972 5				4542 5			
3980 7				4560 5			
4007 5				4580 5	$\frac{3}{2}^+, \frac{5}{2}^+$		
4019.2 6	$\frac{15}{2}^+$			4586 10	$\frac{7}{2}^-$		
4024 7	$\frac{7}{2}^-$			4596 5			
4033 5	$(\frac{1}{2}^-, \frac{3}{2}^-)$			4615 5			
4063 7				4627 5			
4071 5				4642 5			
4082 5				4655 10	$\frac{7}{2}^-$		
4120 5	$(\frac{1}{2}^+)$			4657 5			
4143 7	$\frac{7}{2}^-$			4686 5			
4152 5	$\frac{3}{2}^+, \frac{5}{2}^+$			4708 5			
4178 5		4178.67 14	4178.90 14			4713.12 14	
4189 5				4728 5			
4204 5			4204.3 4	4729 10	$\frac{7}{2}^-$		
4215 5				4755 5	$\frac{3}{2}^+, \frac{5}{2}^+$		
4241 5		4239.73 11	4239.76 5	4788 5			
4258 10	$\frac{7}{2}^-$			4791 10	$\frac{7}{2}^-$		
4272 7							4793.12 16
4277 5				4811 5			
4285 5				4818.6 8	$(\frac{17}{2}^+)$		
4304 5				4830 5			

TABLE XIV. (Continued.)

Known $E(\text{level})^a$ (keV)	$J^\pi$	Previous ( $n, \gamma$ ) $E(\text{level})^a$ (keV)	This work ( $n, \gamma$ ) $E(\text{level})^a$ (keV)	Known $E(\text{level})^a$ (keV)	$J^\pi$	Previous ( $n, \gamma$ ) $E(\text{level})^a$ (keV)	This work ( $n, \gamma$ ) $E(\text{level})^a$ (keV)
4850 5				5116 5	$\frac{1}{2}^-, \frac{3}{2}^-$		5116.61 17
4865 5				5163 5			
4876 5				5182 5	$\frac{1}{2}^+$		
4880 10	$\frac{7}{2}^-$			5212 5	$\frac{3}{2}^+, \frac{5}{2}^+$		
		4886.09 13		5232 10	$\frac{7}{2}^-$		
4910 5				5237 5			
4948 5				5259 5			
4956 10	$\frac{7}{2}^-$			5276 5			
4962 5		4963.19 16		5291 5			
4974 5				5305 5	$\frac{1}{2}^+$		
4999 5				5316.2 12			
5014 5				5332 5			
5028 5				5352 5			
5031 10	$\left(\frac{7}{2}^-\right)$			5362 5			
		5036.12 14	5036.24 9	5391 5			5390.85 14
5059 5	$\frac{1}{2}^+$			5402 5			
5079 10	$\frac{7}{2}^-$			5437 5			
5092 5	$\frac{1}{2}^-, \frac{3}{2}^-$			5463 5			
		5112.31 15		5484 <sup>b</sup> 5			

<sup>a</sup>In our notation, 67.412 3  $\equiv 67.412 \pm 0.003$ , 2902 10  $\equiv 2902 \pm 10$ , etc.

<sup>b</sup>For levels above this energy, see Ref. [96].

TABLE XV. Energies ( $E_\gamma$ ) and intensities ( $I_\gamma$ ) of  $\gamma$  rays from the  $^{60}\text{Ni}(n, \gamma)^{61}\text{Ni}$  reaction.

$E_\gamma$ (keV) <sup>a</sup>	$I_\gamma$ (mb) <sup>b</sup>	Placement <sup>c</sup>	$E_\gamma$ (keV) <sup>a</sup>	$I_\gamma$ (mb) <sup>b</sup>	Placement <sup>c</sup>	$E_\gamma$ (keV) <sup>a</sup>	$I_\gamma$ (mb) <sup>b</sup>	Placement <sup>c</sup>
67.42 20	32.9 6	67 → 0	1116.46 25	0.42 6	4178 → 3062	1877.1 4	0.39 8	3062 → 1185
159.46 20	0.18 3	unplaced	1118.39 99	0.69 7	1185 → 67	1931.2 7	0.23 6	1998 → 67
191.16 8	0.64 5	1099 → 908	1132.40 4	5.89 9	1132 → 0	1943.0 5	0.23 7	unplaced
215.51 9	0.38 3	282 → 67	1146.69 16	0.69 7	3144 → 1998	1959.71 7	1.77 8	3144 → 1185
277.0 5	0.37 6	1185 → 908	1154.9 3	0.41 6	2765 → 1609	1998.10 11	1.44 10	1998 → 0
282.99 5	812 27	282 → 0	1185.29 4	52.6 6	1185 → 0	2012.47 22	0.81 12	3144 → 1132
355.85 14	0.29 3	unplaced	1188.18 12	0.47 7	unplaced	2045.32 5	4.76 13	3144 → 1099
373.07 5	4.27 5	656 → 282	1195.3 4	0.24 6	unplaced	2085.7 <sup>e</sup> 3	0.62 9	4793 → 2707
394.33 5	1.77 6	2123 → 1729	1204.2 3	0.28 5	C → 6615	2088.26 25	0.79 10	unplaced
477.6 5	0.34 7	1609 → 1132	1215.35 5	2.00 6	2123 → 908	2093.10 21	0.81 9	unplaced
514.33 14	0.69 8	2123 → 1609	1233.4 3	0.42 7	3231 → 1998	2099.27 7	3.34 10	3231 → 1132
529.27 3	5.37 6	1185 → 656	1244.39 18	0.67 7	C → 6575	2108.99 18	1.12 10	2765 → 656
546.3 3	0.14 4	1454 → 908	1253.23 20	0.57 7	2862 → 1609	2111.6 4	0.47 10	unplaced
588.59 5	2.33 5	656 → 67	1315.2 4	0.20 5	unplaced	2115.2 3	0.49 11	4239 → 2123
625.60 17	0.30 5	908 → 282	1342.3 4	0.26 6	1998 → 656	2123.90 3	145.6 15	2123 → 0
629.86 25	0.20 4	1729 → 1099	1377.3 <sup>d</sup> 4	0.23 5	4439 → 3062	2126.9 3	1.19 16	unplaced
650.1 4	0.20 6	3415 → 2765	1387.6 4	0.21 5	1454 → 67	2207.0 3	0.86 14	2862 → 656
651.14 25	0.50 11	unplaced	1415.43 10	0.90 7	3144 → 1729	2229.84 20	0.96 22	3415 → 1185
656.02 4	20.39 22	656 → 0	1434.20 23	0.41 5	unplaced	2282.66 14	0.70 6	3415 → 1132
701.22 11	0.61 5	1609 → 908	1446.71 6	2.08 7	1729 → 282	2301.3 4	0.28 6	unplaced
780.4 3	0.21 4	unplaced	1454.80 12	0.87 6	1454 → 0	2306.3 5	0.24 6	unplaced
806.0 3	0.19 6	3668 → 2862	1488.0 3	0.34 6	unplaced	2315.35 16	0.82 7	3415 → 1099
816.70 4	38.7 4	1099 → 282	1502.01 10	0.77 6	3231 → 1729	2340.56 22	0.46 6	3525 → 1185
820.90 10	0.87 6	1729 → 908	1535.60 99	0.61 8	3144 → 1609	2347.5 4	0.28 6	unplaced
841.2 1	1.46 7	908 → 67	1542.42 7	2.50 9	1609 → 67	2351.3 4	0.30 6	5116 → 2765
848.54 13	0.58 5	3711 → 2862	1580.03 20	0.46 6	2765 → 1185	2356.6 3	0.37 6	2639 → 282
888.0 3	0.23 5	unplaced	1587.77 23	0.48 6	3711 → 2123	2387.21 14	0.94 7	unplaced
900.2 3	0.26 5	unplaced	1601.9 4	0.23 8	unplaced	2406.05 6	3.24 9	3062 → 656
902.27 7	1.27 5	1185 → 282	1610.04 99	2.04 9	1609 → 0	2429.15 14	1.11 8	C → 5390
908.59 4	7.66 9	908 → 0	1621.86 8	2.02 9	3231 → 1609	2432.2 4	0.39 7	unplaced
938.62 4	16.28 17	2123 → 1185	1633.08 20	0.70 9	2765 → 1132	2436.14 13	1.34 8	unplaced
947.90 9	0.82 6	1015 → 67	1645.0 3	0.35 6	unplaced	2455.5 6	0.21 6	unplaced
977.12 18	0.30 5	unplaced	1662.17 99	2.13 7	1729 → 67	2460.7 4	0.46 7	unplaced
980.81 25	0.24 5	unplaced	1665.18 99	0.92 6	2765 → 1099	2463.1 7	0.25 7	unplaced
982.6 4	0.14 5	1998 → 1015	1685.54 10	1.13 7	3415 → 1729	2482.07 18	1.10 15	2765 → 282
998.0 4	0.14 5	unplaced	1716.46 25	0.63 8	unplaced	2483.6 7	0.32 14	3668 → 1185
1015.28 24	0.29 6	1015 → 0	1721.5 5	0.26 7	5390 → 3668	2488.84 12	1.16 7	3144 → 656
1021.06 8	0.95 6	3144 → 2123	1729.74 8	2.03 9	1729 → 0	2510.0 <sup>f</sup> 3	0.53 7	4239 → 1729
1024.27 7	1.22 6	2123 → 1099	1750.9 6	0.21 6	5955 → 4204	2575.63 14	0.89 7	3231 → 656
1032.25 4	6.06 9	1099 → 67	1760.2 4	0.35 6	unplaced	2579.84 15	0.91 7	2862 → 282
1039.8 3	0.26 5	unplaced	1778.83 12	1.09 7	3776 → 1998	2611.73 16	1.01 8	3711 → 1099
1065.01 5	3.29 6	1132 → 67	1795.61 24	0.50 7	3525 → 1729	2620.7 5	0.35 8	unplaced
1073.52 6	1.85 6	1729 → 656	1819.7 6	0.25 7	unplaced	2634.0 4	0.38 7	unplaced
1089.65 22	0.37 6	1998 → 908	1840.94 5	4.78 12	2123 → 282	2639.44 6	3.90 9	2639 → 0
1099.67 4	27.6 3	1099 → 0	1843.87 17	1.15 9	unplaced	2644.23 22	0.61 7	3776 → 1132
1107.71 9	0.68 6	3231 → 2123	1864.55 18	0.80 8	C → 5955	2676.5 5	0.30 8	3776 → 1099

TABLE XV. (Continued.)

$E_\gamma$ (keV) <sup>a</sup>	$I_\gamma$ (mb) <sup>b</sup>	Placement <sup>c</sup>	$E_\gamma$ (keV) <sup>a</sup>	$I_\gamma$ (mb) <sup>b</sup>	Placement <sup>c</sup>	$E_\gamma$ (keV) <sup>a</sup>	$I_\gamma$ (mb) <sup>b</sup>	Placement <sup>c</sup>	
2684.58	25	0.51 8	3869 → 1185	3213.9 3	0.64 9	3869 → 656	4150.92 6	11.8 4	C → 3668
2698.22	22	0.94 9	unplaced	3231.47 9	2.38 9	3231 → 0	4171.7 6	0.45 12	4239 → 67
2703.38	19	1.25 9	C → 5116	3242.59 11	1.87 9	3525 → 282	4225.9 8	0.59 18	5955 → 1729
2707.58	9	2.60 11	2707 → 0	3254.8 6	0.28 8	4439 → 1185	4228.6 7	0.75 18	unplaced
2759.38	19	1.37 8	3415 → 656	3305.30 14	1.62 9	C → 4514	4239.66 9	5.43 24	4239 → 0
2764.69	16	1.60 9	2765 → 0	3328.6 6	0.35 8	4514 → 1185	4284.0 6	0.25 9	unplaced
2771.4	7	0.25 8	unplaced	3347.7 4	0.64 9	3415 → 67	4294.44 15	1.99 13	C → 3525
2778.9	4	0.44 8	3062 → 282	3359.5 3	0.38 9	unplaced	4404.82 5	16.2 4	C → 3415
2783.80	9	2.41 10	C → 5036	3369.1 4	0.53 8	unplaced	4439.2 4	0.83 12	4439 → 0
2795.3 <sup>g</sup>	4	0.47 8	2862 → 67	3380.29 21	2.38 23	C → 4439	4514.6 4	0.83 12	4514 → 0
2802.7	4	0.40 8	3711 → 908	3382.3 7	0.80 21	4514 → 1132	4588.26 6	11.7 3	C → 3231
2816.95	14	1.45 8	unplaced	3385.92 5	9.23 13	3668 → 282	4675.05 5	20.3 3	C → 3144
2823.07	16	1.18 9	unplaced	3391.6 3	0.70 9	unplaced	4714.2 7	0.49 13	unplaced
2856.48	13	1.33 7	unplaced	3398.6 3	1.16 15	unplaced	4753.0 6	0.72 15	5036 → 282
2861.95	4	6.59 11	3144 → 282	3415.04 <sup>h</sup> 6	5.05 11	3415 → 0	4757.86 10	4.98 25	C → 3062
2903.0	7	0.27 11	unplaced	3525.1 9	0.20 7	3525 → 0	4793.2 7	0.51 13	4793 → 0
2914.5	7	0.25 8	unplaced	3531.51 20	2.00 18	4439 → 908	4818.8 4	0.89 14	unplaced
2933.80	12	2.96 12	unplaced	3580.18 7	9.8 3	C → 4239	4833.2 9	0.34 13	5116 → 282
2947.5	7	0.25 7	unplaced	3583.47 14	3.10 19	4239 → 656	4957.1 4	2.2 3	C → 2862
2977.79	25	0.69 7	unplaced	3601.8 4	0.64 12	3668 → 67	5055.02 12	4.22 20	C → 2765
3000.2	5	0.36 8	unplaced	3615.9 4	0.56 11	C → 4204	5112.1 5	0.84 13	C → 2707
3012.66	11	2.89 10	3668 → 656	3640.99 18	1.95 16	C → 4178	5180.36 9	3.93 14	C → 2639
3027.02	18	1.06 8	C → 4793	3644.0 4	0.90 15	3711 → 67	5322.2 7	0.73 12	5390 → 67
3054.36	18	0.92 7	4239 → 1185	3687.24 21	3.00 25	unplaced	5515.4 7	0.45 12	6615 → 1099
3062.16	10	1.75 8	3062 → 0	3709.3 5	1.2 3	3776 → 67	5695.86 4	157 3	C → 2123
3077.5	3	0.60 7	3144 → 67	3711.42 11	6.8 3	3711 → 0	5955.3 8	0.41 12	5955 → 0
3082.21	21	0.78 8	3738 → 656	3850.7 <sup>i</sup> 6	0.53 14	5036 → 1185	6090.5 5	0.72 12	C → 1729
3104.6	8	0.47 15	4204 → 1099	3869.83 12	3.81 22	3869 → 0	6105.8 4	0.33 13	unplaced
3106.8	4	1.30 16	4239 → 1132	3949.97 9	5.61 23	C → 3869	6292.3 7	0.53 13	6575 → 282
3129.1	6	0.43 10	unplaced	3974.37 22	1.39 13	unplaced	6634.40 5	29.5 4	C → 1185
3132.05	8	5.10 13	3415 → 282	4043.33 14	2.66 18	C → 3776	6719.97 5	55.8 7	C → 1099
3144.7	7	4.09 13	3144 → 0	4081.6 3	1.64 15	C → 3738	7163.9 5	1.3 3	C → 656
3164.49	24	0.84 10	3231 → 67	4108.52 8	10.5 3	C → 3711	7536.62 6	705 9	C → 282
3180.8	4	0.50 11	unplaced	4111.5 4	1.05 19	4178 → 67	7819.56 6	1236 15	C → 0

<sup>a</sup>In our notation, 67.42 20  $\equiv$  67.42  $\pm$  0.20, etc.<sup>b</sup>In our notation, 32.9 6  $\equiv$  32.9  $\pm$  0.6, etc. Multiply by 0.0427 to obtain photons per 100 thermal neutron captures.<sup>c</sup>C denotes the capturing state.<sup>d</sup>Can also be placed as a 4240 → 2863 transition.<sup>e</sup>Can also be placed as a 5956 → 3870 transition.<sup>f</sup>Can also be placed as a 3526 → 1015 transition.<sup>g</sup>Can also be placed as a 4793 → 1998 transition.<sup>h</sup>Can also be placed as a 4515 → 1100 transition.<sup>i</sup>Can also be placed as a 6616 → 2765 transition.

TABLE XVI. Level scheme of  $^{61}\text{Ni}$  from this work in tabular form.

$E(\text{level})^a$ (keV)	$J^\pi$	Deexciting $\gamma$ rays <sup>b</sup>	$I_\gamma$ (in) <sup>a</sup> (mb)	$I_\gamma$ (out) <sup>a</sup> (mb)	$I_\gamma$ (in - out) <sup>a</sup> (mb)
0.0	$\frac{3}{2}^-$		2390 30		2390 30
67.41 3	$\frac{1}{2}^-$	67.42	27.6 6	32.9 6	-5.3 8
282.973 21	$\frac{1}{2}^-$	282.99, 215.51	784 9	812 28	-28 30
656.039 22	$\frac{1}{2}^-$	656.02, 588.59, 373.07	24.8 5	27.0 3	-2.2 6
908.59 3	$\frac{1}{2}^-$	908.59, 841.2, 625.60	7.40 25	9.42 13	-2.0 3
1015.32 9	$\frac{1}{2}^-$	1015.28, 947.90	0.14 5	1.11 9	-0.97 10
1099.684 22	$\frac{1}{2}^-$	1099.67, 1032.25, 816.70, 191.16	65.9 8	73.0 6	-7.1 10
1132.41 3	$\frac{1}{2}^-$	1132.40, 1065.01	8.6 4	9.18 11	-0.6 4
1185.301 22	$\frac{1}{2}^-$	1185.29, 1118.39, 902.27, 529.27, 277.0	52.7 6	60.3 7	-7.6 9
1454.84 11	$\frac{1}{2}^-$	1454.80, 1387.6, 546.3		1.22 9	-1.22 9
1609.80 5	$\frac{1}{2}^-$	1610.04, 1542.42, 701.22, 477.6,	4.30 18	5.49 16	-1.19 23
1729.63 3	$\frac{1}{2}^-$	1729.74, 1662.17, 1446.71, 1073.52, 820.90, 629.86	6.9 3	9.16 17	-2.2 4
1998.12 7	$\frac{1}{2}^-$	1998.10, 1931.2, 1342.3, 1089.65, 982.6,	2.20 13	2.44 16	-0.24 20
2123.949 19	$\frac{1}{2}^-$	2123.90, 1840.94, 1215.35, 1024.27, 938.62, 514.33, 394.33	160 3	173 3	-13 4
2639.51 5	$\frac{1}{2}^-, \frac{3}{2}^-$	2639.44, 2356.6	3.93 14	4.27 11	-0.34 18
2707.63 9	$\frac{1}{2}^-$	2707.58	1.46 16	2.60 11	-1.14 20
2765.03 7	$\frac{3}{2}^-$	2764.69, 2482.07, 2108.99, 1665.18, 1633.08, 1580.03, 1154.9	4.72 22	6.31 25	-1.6 4
2862.94 9	$\frac{1}{2}^-, \frac{3}{2}^-$	2795.3, 2579.84, 2207.0, 1253.23	3.0 4	2.81 19	0.2 4
3062.16 5	$\frac{1}{2}^+$	3062.16, 2778.9, 2406.05, 1877.1	5.6 3	5.82 17	-0.2 3
3144.98 3	$\frac{1}{2}^-$	3144.7, 3077.5, 2861.95, 2488.84, 2045.32, 2012.47, 1959.71, 1535.60, 1415.43, 1146.69, 1021.06	20.3 3	22.9 4	-2.6 5
3231.67 4	$\frac{1}{2}^-, \frac{3}{2}^-$	3231.47, 3164.49, 2575.63, 2099.27, 1621.86, 1502.01, 1233.4, 1107.71	11.7 3	11.34 23	0.4 4
3415.14 4	$\frac{1}{2}^-, \frac{3}{2}^-$	3415.04, 3347.7, 3132.05, 2759.38, 2315.35, 2282.66, 2229.84, 1685.54, 650.1	16.2 4	16.0 4	0.2 6
3525.60 8	$\frac{1}{2}^-$	3525.1, 3242.59, 2340.56, 1795.61,	1.99 13	3.03 15	-1.04 20
3668.99 4	$\frac{1}{2}^-, \frac{3}{2}^-$	3601.8, 3385.92, 3012.66, 2483.6, 806.0,	12.1 4	13.3 3	-1.2 5
3711.49 6	$\frac{1}{2}^-, \frac{3}{2}^-$	3711.42, 3644.0, 2802.7, 2611.73, 1587.77, 848.54	10.5 3	10.2 4	0.3 5
3738.34 18	$\left(\frac{1}{2}^+\right)$	3082.21	1.64 15	0.78 8	0.86 17
3776.80 9	$\left(\frac{1}{2}^-, \frac{3}{2}^-\right)$	3709.3, 2676.5, 2644.23, 1778.83,	2.66 8	3.2 4	-0.5 4
3869.99 7	$\frac{1}{2}^-$	3869.83, 3213.9, 2684.58	5.61 23	5.0 3	0.6 4
4178.90 14	$\frac{1}{2}^-$	4111.5, 1116.46	1.95 16	1.47 20	0.5 3
4204.3 4	$\frac{1}{2}^-$	3104.6	0.77 13	0.47 15	0.30 20
4239.76 5	$\frac{1}{2}^-$	4239.66, 4171.7, 3583.47, 3106.8, 3054.36, 2510.0, 2115.2	9.8 3	12.2 4	-2.4 5
4439.88 13	$\frac{1}{2}^-$	4439.2, 3531.51, 3254.8, 1377.3	2.38 23	3.34 24	-1.0 4

its contribution to the thermal-neutron capture cross section is about 2.1 b. Resonances at higher neutron energy contribute less than 0.05 b, leaving a bound level contribution of perhaps 0.25 b. The small thermal-neutron scattering length  $a_{J=1/2}=2.8$  fm is consistent with the dominance of the first resonance.

The cross sections for the individual primary  $E1$  transitions are given in Table XVIII along with their  $\gamma$  ray energies and  $(d,p)$  spectroscopic factors of the final states. From these and the thermal-neutron scattering length, the direct-capture cross sections are calculated. These are also presented in Table XVIII. As with  $^{58}\text{Ni}$  capture, there are significant dif-

ferences between the direct-capture cross section and the experimental value. Again, these differences are attributed to the admixture of compound-nuclear capture resulting from the nearest resonance levels. The two possible magnitudes of the compound-nuclear cross section, extracted using Eq. (1), for each transition are listed in the final column of Table XVIII.

The statistical method of Sec. III F is applied to these results. The results are summarized in Table XIX and compared with the model estimates, which are more precise than in the  $^{58}\text{Ni}$  case because the energy of the resonance level is known. Again, it is clear that the differences between the

TABLE XVI. (Continued.)

$E(\text{level})^a$ (keV)	$J^\pi$	Deexciting $\gamma$ rays <sup>b</sup>	$I_\gamma$ (in) <sup>a</sup> (mb)	$I_\gamma$ (out) <sup>a</sup> (mb)	$I_\gamma$ (in - out) <sup>a</sup> (mb)
4514.69 13		4514.6, 3382.3, 3328.6	1.62 9	2.0 3	-0.4 3
4793.12 16		4793.2, 2085.7	1.06 8	1.13 16	-0.07 18
5036.24 9		4753.0, 3850.7	2.41 10	1.25 21	1.16 23
5116.61 17	$\frac{1}{2}^-, \frac{3}{2}^-$	4833.2, 2351.3	1.25 9	0.64 15	0.61 17
5390.85 14		5322.2, 1721.5	1.11 8	0.99 14	0.12 16
5955.52 17		5955.3, 4225.9, 1750.9	0.80 8	1.21 23	-0.41 24
6575.70 18		6292.3	0.67 7	0.53 13	0.14 15
6615.8 3		5515.4	0.28 5	0.45 12	-0.17 13
7020.113 <sup>c</sup> 21	$\frac{1}{2}^+$	7819.56, 7536.62, 7163.9, 6719.97, 6634.40, 6090.5, 5695.86, 5180.36, 5112.1, 5055.02, 4957.1, 4757.86, 4675.05, 4588.26, 4404.82, 4294.44, 4150.92, 4108.52, 4081.6, 4043.33, 3949.97, 3640.99, 3615.9, 3580.18, 3380.29, 3305.30, 3027.02, 2783.80, 2703.38, 2429.15, 1864.55, 1244.39, 1204.2		2308 18	-2308 18

<sup>a</sup>In our notation, 67.41 3  $\equiv$  67.41  $\pm$  0.03, 2390 30  $\equiv$  2390  $\pm$  30, etc.

<sup>b</sup>See also Table XV.

<sup>c</sup>Capturing state.

theoretical direct-capture cross sections and the experimental values are consistent with one or more of the standard models of the compound-nuclear mechanism.

#### D. Capture cross section of natural nickel

Combining the capture cross sections for  $^{58}\text{Ni}$  and  $^{60}\text{Ni}$  measured in this work with literature values [110], we obtain the following set (isotope, natural abundance in at. %, capture cross section):  $^{58}\text{Ni}$ , 68.077 $\pm$ 0.009, 4.13 $\pm$ 0.05 b,  $^{60}\text{Ni}$ , 26.223 $\pm$ 0.008, 2.34 $\pm$ 0.05 b,  $^{61}\text{Ni}$ , 1.140 $\pm$ 0.001, 2.5 $\pm$ 0.5 b,  $^{62}\text{Ni}$ , 3.634 $\pm$ 0.002, 15 $\pm$ 1 b, and  $^{64}\text{Ni}$ , 0.926 $\pm$ 0.001, 1.6 $\pm$ 0.1 b. The resulting capture cross section for natural nickel, 4.01 $\pm$ 0.06 b, is lower and more precise than the value 4.6 $\pm$ 0.4 b calculated by Holden [110] from previous literature values.

#### E. Shell-model calculations of $^{61}\text{Ni}$ levels

The calculated spectrum is compared with experiment in Fig. 8. There is a one-to-one correspondence between experi-

ment and theory for the first 18 states. The doublet of  $\frac{9}{2}^-$  states at 1807 and 1988 keV [73,76] is nicely reproduced (at 1847 and 1961 keV) by our calculations.

## VII. SUMMARY

We have studied the energy levels of  $^{59}\text{Ni}$ ,  $^{60}\text{Ni}$ , and  $^{61}\text{Ni}$  via the  $(n, \gamma)$  reaction with thermal neutrons. Approximately a third of the known number of levels in these nuclei below the respective neutron separation energies are populated measurably in this reaction. For these levels, we have determined accurate level energies and, whenever possible, good branching ratios. We have applied the direct-capture theory and current models of compound-nuclear capture to satisfactorily reproduce the partial cross sections of the strong primary  $E1$  transitions. The low-lying portions of the level schemes have been compared with shell-model predictions. The overall agreement is good.

TABLE XVII. Increasing complexity in the study of the  $^{60}\text{Ni}(n, \gamma)^{61}\text{Ni}$  reaction.

Number of	Ishaq <i>et al.</i> [28] McMaster (1977)	Harder <i>et al.</i> [30] Grenoble (1993)	This work LANL/ORNL
$\gamma$ rays	49 <sup>d</sup>	143 <sup>e</sup>	240
spurious $\gamma$ rays <sup>a</sup>	4	33	
placed $\gamma$ rays <sup>b</sup>	42	136	179
primary $\gamma$ rays	22	25	33
secondary $\gamma$ rays	20	111	146
unplaced $\gamma$ rays <sup>c</sup>	7	7	61
bound levels	23	31	40

<sup>a</sup>Gamma rays sought but not observed in this more sensitive work and, therefore, considered spurious.

<sup>b</sup>Some of the placed  $\gamma$  rays may be spurious.

<sup>c</sup>Some of the unplaced  $\gamma$  rays may be genuine.

<sup>d</sup>Measurements limited to  $E_\gamma > 2.1$  MeV using a Ge(Li)-NaI(Tl) pair spectrometer.

<sup>e</sup>This number represents placed  $\gamma$  rays as well as the strongest unplaced  $\gamma$  rays. A more complete list of 312  $\gamma$  rays was created in the course of the Grenoble study, but this list is not available from the authors.

TABLE XVIII. Direct-capture cross sections for primary  $E1$  transitions in the  $^{60}\text{Ni}(n, \gamma)^{61}\text{Ni}$  reaction. Columns 1, 2, and 3 give the energy,  $J^\pi$  value, and the  $l=1(d, p)$  spectroscopic factor multiplied by  $(2J+1)$  for the final state, respectively. Column 4 is the primary transition energy. Column 5 is the average valency capture width and column 6 the potential-capture cross section, both calculated using a global optical properties (see Eqs. (4)–(7) of Ref. [3]). The entries in column 5 do not include the spin-coupling factor and the spectroscopic factor; those in column 6 do. Column 7 is the calculated cross section using the global plus valence ( $G+V$ ) procedure. The measured cross sections are given in column 8. Column 9 gives the hypothesized compound-nuclear contributions deduced from the differences between column 7 and column 8 via Eq. (8) of Ref. [3]. In the table subheading,  $a(X)$  refers to the experimental scattering length, while  $a(G)$  and  $\bar{\Gamma}_n^0/D$  refer to the scattering length and the neutron strength function, respectively, both calculated using the global optical potential.

$E_f$ (keV)	$J^\pi$	$(d, p)$ $(2J+1)S^a$	$E_\gamma$ (keV)	$\Gamma_{\gamma, \text{val}}/DE_\gamma^3$ ( $10^{-7} \text{ MeV}^{-3}$ )	$\sigma_{\text{pot}, \gamma}$ (mb)	$\sigma(G+V)$ (mb)	$\sigma_\gamma(X)^b$ (mb)	$\sigma_{\text{CN}, \gamma}$ (mb)
Reaction $^{60}\text{Ni}(n, \gamma)^{61}\text{Ni}$ ; $a(X) = 2.8 \text{ fm}$ ; $a(G) = 7.03 \text{ fm}$ ; $\bar{\Gamma}_n^0/D = 3.8 \times 10^{-4}$								
0	$\frac{3}{2}^-$	1.49	7820	0.30	1.1	579	1236 $15$	123 or 3510
283	$\frac{1}{2}^-$	1.23	7537	0.21	0.46	355	706 $9$	60 or 2060
656	$\frac{3}{2}^-$	0.053	7164	0.0097	0.040	15	1.3 $3$	7.2 or 25
1100	$\frac{3}{2}^-$	0.108	6720	0.027	0.30	36	55.8 $7$	2.1 or 180
1185	$\frac{3}{2}^-$	0.255	6634	0.24	0.73	84	29.5 $4$	14 or 210
1730	$\frac{3}{2}^-$	0.044	6091	0.012	0.18	13	0.72 $12$	7.8 or 20
2124	$\frac{1}{2}^-$	0.392	5696	0.30	1.37	88	157 $3$	10 or 480
2640	if $\frac{1}{2}^-$	0.087	5180	0.025	0.41	18	3.9 $2$	5.0 or 38
2640	if $\frac{3}{2}^-$	0.087	5180	0.030	0.60	22	3.9 $2$	7.4 or 35
2765	$\frac{3}{2}^-$	0.054	5055	0.018	0.39	13	4.2 $3$	2.6 or 32
2863	if $\frac{1}{2}^-$	0.032	4957	0.010	0.17	6.3	2.2 $3$	1.0 or 16
2863	if $\frac{3}{2}^-$	0.032	4957	0.012	0.24	7.7	2.2 $3$	1.7 or 18
3232	if $\frac{1}{2}^-$	0.011	4588	0.0037	0.069	2.0	11.7 $3$	4.0 or 2.3
3232	if $\frac{3}{2}^-$	0.011	4588	0.0044	0.093	2.4	11.7 $3$	3.5 or 2.5
3358	if $\frac{1}{2}^-$	0.022	4462	0.0076	0.144	3.9	< 3	0.05 or 14 <sup>c</sup>
3358	if $\frac{3}{2}^-$	0.022	4462	0.0090	0.194	4.7	< 3	0.2 or 15 <sup>c</sup>
3415	if $\frac{1}{2}^-$	0.045	4405	0.016	0.30	7.8	16.2 $4$	1.5 or 47
3415	if $\frac{3}{2}^-$	0.045	4405	0.019	0.40	9.5	16.2 $4$	0.90 or 50
3669	if $\frac{1}{2}^-$	0.054	4151	0.020	0.40	8.8	11.8 $4$	0.22 or 41
3669	if $\frac{3}{2}^-$	0.054	4151	0.024	0.52	11	11.8 $4$	0.03 or 45
3711	if $\frac{1}{2}^-$	0.033	4109	0.013	0.24	5.3	1.64 $5$	1.1 or 13
3711	if $\frac{3}{2}^-$	0.033	4109	0.015	0.32	6.4	1.64 $5$	1.6 or 15
5116	if $\frac{1}{2}^-$	0.108	2703	0.069	1.1	11	1.25 $9$	4.7 or 19
5116	if $\frac{3}{2}^-$	0.108	2703	0.078	1.3	12	1.25 $9$	5.9 or 22

<sup>a</sup>From Ref. [78].

<sup>b</sup>From Table XV.

<sup>c</sup>Assuming the upper limit for  $\sigma_\gamma(X)$ .

TABLE XIX. Average compound-nuclear cross sections for  $E1$  transitions in the  $^{60}\text{Ni}(n, \gamma)^{61}\text{Ni}$  reaction and comparison with model predictions. See discussion in Sec. III F. The quantity  $a$  is in units of  $b \cdot \text{MeV}^{-b}$ . Model 1 is Cameron's semi-empirical result [112]. Model 2 is the Weisskopf single-particle model [100]. Model 3 is the generalized valence model [113]. Model 4 is Brink's version of the photonuclear giant-dipole resonance model [101]. Model 5 is Brink-Axel-Lone model [111].

	Experiment	Model 1	Model 2	Model 3	Model 4	Model 5
$b$	$a$	$a$	$a$	$a$	$a$	$a$
3	$(4 \pm 2) \times 10^{-4}$	$6 \times 10^{-5}$	$3.5 \times 10^{-4}$	$2 \times 10^{-4}$		
4	$(1.0 \pm 0.3) \times 10^{-4}$				$2.3 \times 10^{-5}$	
5	$(2.0 \pm 0.7) \times 10^{-5}$					$3.5 \times 10^{-5}$

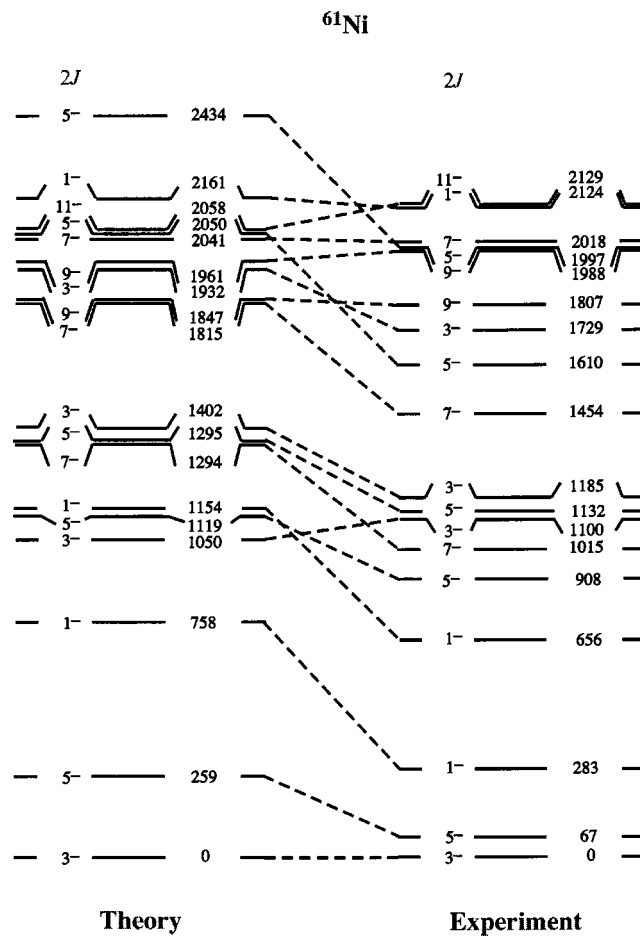


FIG. 8. Comparison between the shell-model predictions and the experimental level scheme of  $^{61}\text{Ni}$ . The levels are labeled by  $2J^\pi$  on the left and by level energies (in keV) on the right.

#### ACKNOWLEDGMENTS

The current work was sponsored by the U.S. Department of Energy, under Contract No. DE-AC05-00OR22725 with UT-Battelle, LLC (Oak Ridge) and Contract No. W-7405-ENG-36 with the University of California (Los Alamos).

Two of the authors (X.O. and M.A.I.) were sponsored by the Joint Institute of Heavy-Ion Research. This Institute has as member institutions: The University of Tennessee, Vanderbilt University, and Oak Ridge National Laboratory; it is supported by the members and by the U.S. Department of Energy.

- 
- [1] S. Raman, R. F. Carlton, J. C. Wells, E. T. Jurney, and J. E. Lynn, Phys. Rev. C **32**, 18 (1985).
- [2] J. E. Lynn, S. Kahane, and S. Raman, Phys. Rev. C **35**, 26 (1987).
- [3] S. Kahane, J. E. Lynn, and S. Raman, Phys. Rev. C **36**, 533 (1987).
- [4] S. Raman, S. Kahane, and J. E. Lynn, in *Proceedings of the International Conference on Nuclear Data for Science and Technology, Mito, 1988*, edited by S. Igarasi (Saikon, Tokyo, 1988), p. 645.
- [5] S. Raman, S. Kahane, R. M. Moon, J. A. Fernandez-Baca, J. L. Zarestky, J. E. Lynn, and J. W. Richardson, Phys. Rev. C **39**, 1297 (1989).
- [6] S. Raman, M. Igashira, Y. Dozono, H. Kitakawa, M. Mizumoto, and J. E. Lynn, Phys. Rev. C **41**, 458 (1990).
- [7] S. Raman, J. A. Fernandez-Baca, R. M. Moon, and J. E. Lynn, Phys. Rev. C **44**, 518 (1991).
- [8] J. E. Lynn, E. T. Jurney, and S. Raman, Phys. Rev. C **44**, 764 (1991).
- [9] J. E. Lynn and S. Raman, in *Capture Gamma-Ray Spectroscopy*, edited by R. W. Hoff, AIP Conf. Proc. No. 238 (AIP, New York, 1991), p. 555.
- [10] T. A. Walkiewicz, S. Raman, E. T. Jurney, J. W. Starner, and J. E. Lynn, Phys. Rev. C **45**, 1597 (1992).
- [11] S. Raman, E. T. Jurney, J. W. Starner, and J. E. Lynn, Phys. Rev. C **46**, 972 (1992).
- [12] S. Raman and J. E. Lynn, in *Beijing International Symposium on Fast Neutron Physics, Beijing, 1991*, edited by Sun Zuxun,

- Tang Hongqing, Xu Jincheng, and Zhang Jingshang (World Scientific, Singapore, 1992), p. 107.
- [13] M. C. Moxon, J. A. Harvey, S. Raman, J. E. Lynn, and W. Ratynski, *Phys. Rev. C* **48**, 553 (1993).
- [14] S. Raman, E. K. Warburton, J. W. Starner, E. T. Journey, J. E. Lynn, P. Tikkanen, and J. Keinonen, *Phys. Rev. C* **53**, 616 (1996).
- [15] E. T. Journey, J. W. Starner, J. E. Lynn, and S. Raman, *Phys. Rev. C* **56**, 118 (1997).
- [16] S. Raman, E. T. Journey, J. W. Starner, and J. E. Lynn, *Phys. Rev. C* **61**, 067303 (2000).
- [17] A. M. Lane and J. E. Lynn, *Nucl. Phys.* **17**, 563 (1960).
- [18] A. M. Lane and J. E. Lynn, *Nucl. Phys.* **17**, 586 (1960).
- [19] M. Pichevar, J. Delaunay, B. Delaunay, H. J. Kim, Y. El Masri, and J. Vervier, *Nucl. Phys.* **A264**, 132 (1976).
- [20] J. D. Hutton, N. R. Roberson, C. R. Gould, and D. R. Tilley, *Nucl. Phys.* **A206**, 403 (1973).
- [21] Ph. Monseu, K. Forssten, and Z. P. Sawa, *Phys. Scr.* **9**, 26 (1974).
- [22] P. Roussel, G. Bruge, A. Bussiere, H. Faraggi, and J. E. Testoni, *Nucl. Phys.* **A155**, 306 (1970).
- [23] S. Juutinen, J. Hattula, M. Jaaskelainen, A. Virtanen, and T. Lonroth, *Nucl. Phys.* **A504**, 205 (1989).
- [24] P. H. Stelson (private communication), quoted in *Nucl. Data Sheets* **69**, 851 (1993).
- [25] P. H. Stelson, J. K. Dickens, and F. G. Perey (private communication), quoted in *Nucl. Data Sheets* **69**, 851 (1993).
- [26] V. K. Mittal, D. K. Avasthi, and I. M. Govil, *J. Phys. G* **9**, 91 (1983).
- [27] C. Hofmeyr, in *Neutron Capture Gamma-Ray Spectroscopy*, edited by K. Abrahams (Reactor Centrum Nederland, Petten, 1975), p. 537.
- [28] A. F. M. Ishaq, A. Robertson, W. V. Prestwich, and T. J. Kennett, *Z. Phys. A* **281**, 365 (1977).
- [29] A. Harder, Diplomarbeit, II. Physikalisches Institut der Georg-August-Universität zu Göttingen, 1992.
- [30] A. Harder, S. Michaelsen, K. P. Lieb, and A. P. Williams, *Z. Phys. A* **345**, 143 (1993).
- [31] F. Stecher-Rasmussen, J. Kopecký, K. Abrahams, and W. Ratyński, *Nucl. Phys.* **A181**, 250 (1972).
- [32] R. H. Fulmer, A. L. McCarthy, B. L. Cohen, and R. Middleton, *Phys. Rev.* **133**, B955 (1964).
- [33] E. R. Cosman, C. H. Paris, A. Sperduto, and H. A. Enge, *Phys. Rev.* **142**, 673 (1963).
- [34] V. F. Litvin, Yu. A. Nemilov, L. V. Krasnov, K. A. Gridnev, K. I. Zherebtzova, Yu. A. Lakomkin, T. V. Orlova, V. P. Bochinn, and V. S. Romanov, *Nucl. Phys.* **A184**, 105 (1972).
- [35] M. S. Chowdhury and H. M. Sen Gupta, *Nucl. Phys.* **A205**, 454 (1973).
- [36] J. A. Aymar, H. R. Hiddleston, S. E. Darden, and A. A. Rollefson, *Nucl. Phys.* **A207**, 596 (1973).
- [37] T. Taylor and J. A. Cameron, *Nucl. Phys.* **A337**, 389 (1980).
- [38] D. M. Van Patter, F. Rauch, and B. Seim, *Nucl. Phys.* **A204**, 172 (1973).
- [39] P. Sen, C. Sen, and D. Basu, *Z. Phys. A* **280**, 211 (1977).
- [40] R. Sherr, B. F. Bayman, E. Rost, M. E. Rickey, and C. G. Hoot, *Phys. Rev.* **139**, B1272 (1965).
- [41] H. Nann, D. W. Miller, W. W. Jacobs, D. W. Devins, W. P. Jones, and A. G. M. van Hees, *Phys. Rev. C* **28**, 642 (1983).
- [42] W. R. Zimmerman, J. J. Kraushaar, M. J. Schneider, and H. Rudolph, *Nucl. Phys.* **A297**, 263 (1978).
- [43] H. M. Sen Gupta, J. B. A. England, E. M. E. Rawas, F. Khazaie, and G. T. A. Squier, *J. Phys. G* **16**, 1039 (1990).
- [44] H. J. Kim, R. Ballini, B. Delaunay, J. Delaunay, J. P. Fouan, and M. Pichevar, *Nucl. Phys.* **A250**, 211 (1975).
- [45] M. A. Ivanov, I. Kh. Lemberg, A. S. Mishin, L. K. Peker, and I. N. Chugunov, *Izv. Akad. Nauk SSSR, Ser. Fiz.* **39**, 1695 (1975); [*Bull. Acad. Sci. USSR, Phys. Ser. (Engl. Transl.)* **39**, 108 (1975)].
- [46] F. Kearns, L. P. Ekström, G. D. Jones, T. P. Morrison, O. M. Mustaffa, H. G. Price, D. N. Simister, P. J. Twin, R. Wadsworth, and N. J. Ward, *J. Phys. G* **6**, 1131 (1980).
- [47] N. Stein, J. W. Sunier, and C. W. Woods, *Phys. Rev. Lett.* **38**, 587 (1977).
- [48] H. W. Fulbright, C. L. Bennett, R. A. Lindgren, R. G. Markham, S. C. McGuire, G. C. Morrison, U. Strohhusch, and J. Töke, *Nucl. Phys.* **A284**, 329 (1977).
- [49] F. Videbæk, Ole Hansen, B. S. Nilsson, E. R. Flynn, and J. C. Peng, *Nucl. Phys.* **A433**, 441 (1985).
- [50] Tsan Ung Chan, C. Morand, F. Azgui, M. Agard, J. F. Bruandet, B. Chambon, A. Dauchy, D. Drain, A. Giorni, and F. Glasser, *Phys. Rev. C* **29**, 441 (1984).
- [51] W. Darcey, R. Chapman, and S. Hinds, *Nucl. Phys.* **A170**, 253 (1971).
- [52] H. Ronsin, P. Beuzit, J. Delaunay, R. Ballini, I. Fodor, and J. P. Fouan, *Nucl. Phys.* **A207**, 577 (1973).
- [53] I. Demeter, Ilona Fodor, L. Keszthelyi, I. Szentpétery, Judit Szüics, Z. Szókefalvi-Nagy, L. Varga, and J. Zimányi, *Acta Physiol. Acad. Sci. Hung.* **30**, 1 (1971).
- [54] B. Erlandsson, J. Lyttkens, and A. Marcinkowski, *Z. Phys. A* **272**, 67 (1975).
- [55] R. J. Peterson, B. L. Clausen, J. J. Kraushaar, R. A. Lindgren, M. A. Plum, W. W. Jacobs, and H. Nann, *Phys. Rev. C* **35**, 495 (1987).
- [56] H. H. Hansen and A. Spornol, *Z. Phys.* **209**, 111 (1968).
- [57] S. Raman, *Z. Phys.* **228**, 387 (1969).
- [58] D. C. Camp and J. R. Van Hise, *Phys. Rev. C* **14**, 261 (1976).
- [59] W. M. Wilson, G. E. Thomas, and H. E. Jackson, *Phys. Rev. C* **11**, 1477 (1975).
- [60] S. Raman and E. T. Journey, in *Neutron Capture Gamma-Ray Spectroscopy*, edited by R. E. Chrien (Plenum, New York, 1979), p. 728.
- [61] F. R. Metzger, *Nucl. Phys.* **A158**, 88 (1970).
- [62] R. A. Lindgren, M. A. Plum, W. J. Gerace, R. S. Hicks, B. Parker, G. A. Peterson, R. Singhal, C. F. Williamson, X. K. Maruyama, and F. Petrovich, *Phys. Rev. Lett.* **47**, 1266 (1981).
- [63] B. L. Clausen, J. T. Brack, M. R. Braunstein, J. J. Kraushaar, R. A. Loveman, R. J. Peterson, R. A. Ristinen, R. A. Lindgren, and M. A. Plum, *Phys. Rev. C* **41**, 2246 (1990).
- [64] R. G. Tee and A. Aspinall, *Nucl. Phys.* **A98**, 417 (1967).
- [65] R. K. Mohindra and D. M. Van Patter, *Phys. Rev.* **139**, B274 (1965).
- [66] C. Moazed, T. Becker, P. A. Assimakopoulos, and D. M. Van Patter, *Nucl. Phys.* **A169**, 651 (1971).
- [67] A. Passoja, R. Julin, J. Kantele, and M. Luontama, *Nucl. Phys.* **A363**, 399 (1981).
- [68] D. M. Van Patter and F. Rauch, *Nucl. Phys.* **A191**, 245 (1972).
- [69] D. H. Koang, W. S. Chien, and H. Rossner, *Phys. Rev. C* **13**, 1470 (1976).
- [70] D. H. Kong-A-Siou, A. J. Cole, A. Giorni, and J. P. Longe-

- queue, Nucl. Phys. **A221**, 45 (1974).
- [71] E. K. Warburton, J. W. Olness, A. M. Nathan, and A. R. Poletti, Phys. Rev. C **18**, 1637 (1978).
- [72] R. Wadsworth, G. D. Jones, A. Kogan, P. R. G. Lornie, T. Morrison, O. Mustaffa, H. G. Price, D. Simister, and P. J. Twin, J. Phys. G **3**, 833 (1977).
- [73] R. Wadsworth, A. Kogan, P. R. G. Lornie, M. R. Nixon, H. G. Price, and P. J. Twin, J. Phys. G **3**, 35 (1977).
- [74] G. A. Huttlin, J. A. Aymar, J. A. Bieszk, S. Sen, and A. A. Rollefson, Nucl. Phys. **A263**, 445 (1976).
- [75] E. R. Cosman, D. N. Schramm, and H. A. Enge, Nucl. Phys. **A109**, 305 (1968).
- [76] H. Nann, E. R. Flynn, D. L. Hanson, and S. Raman, Phys. Rev. C **18**, 2511 (1978).
- [77] J. Kopecký, K. Abrahams, and F. Stecher-Rasmussen, Nucl. Phys. **A188**, 535 (1972).
- [78] E. R. Cosman, D. N. Schramm, H. A. Enge, A. Sperduto, and C. H. Paris, Phys. Rev. **163**, 1134 (1967).
- [79] J. A. Aymar, H. R. Hiddleston, E. D. Berners, and A. A. Rollefson, Nucl. Phys. **A213**, 125 (1973).
- [80] Yu. G. Kosyak, D. K. Kaipov, and L. V. Chekushina, Izv. Akad. Nauk SSSR, Ser. Fiz. **53**, 2130 (1989); [Bull. Acad. Sci. USSR, Phys. Ser. (Engl. Transl.) **53**, 68 (1989)].
- [81] R. A. Meyer, A. L. Prindle, W. A. Myers, P. K. Hopke, D. Dieterly, and J. E. Koops, Phys. Rev. C **17**, 1822 (1978).
- [82] G. Satyanarayana, N. Venkateswara Rao, G. S. Sri Krishna, M. V. S. Chandrasekhar Rao, S. Bhuloka Reddy, D. L. Sastry, S. N. Chinthalapudi, and V. V. Rao, Nuovo. Cim. **99**, 309 (1988).
- [83] M. Matoba, K. Kurohmaru, O. Iwamoto, A. Nohtomi, Y. Uozumi, T. Sakae, N. Koori, H. Ohgaki, H. Ijiri, T. Maki, M. Nakano, and H. M. Sen Gupta, Phys. Rev. C **53**, 1792 (1996).
- [84] A. H. Wapstra, Nucl. Instrum. Methods Phys. Res. A **292**, 671 (1990).
- [85] G. Audi and A. H. Wapstra, Nucl. Phys. **A565**, 1 (1993).
- [86] S. Raman, C. Yonezawa, H. Matsue, H. Iimura, and N. Shinohara, Nucl. Instrum. Methods Phys. Res. A **454**, 389 (2000).
- [87] D. Cokinos and E. Melkonian, Phys. Rev. C **15**, 1636 (1977).
- [88] P. Andersson, L. P. Ekstrom, and J. Lyttkens, Nucl. Data Sheets **39**, 641 (1983), A=59.
- [89] C. M. Baglin, Nucl. Data Sheets **69**, 733 (1993), A=59.
- [90] S. Raman, Nucl. Data, Sect. B **2**, 41 (1968), A=60.
- [91] R. L. Auble, Nucl. Data Sheets **28**, 103 (1979), A=60.
- [92] P. Andersson, L. P. Ekström, and J. Lyttkens, Nucl. Data Sheets **48**, 251 (1986), A=60.
- [93] M. M. King, Nucl. Data Sheets **69**, 1 (1993), A=60.
- [94] L. P. Ekström and J. Lyttkens, Nucl. Data Sheets **38**, 463 (1983), A=61.
- [95] Zhou Chunmei, Nucl. Data Sheets **67**, 271 (1992), A=61.
- [96] M. R. Bhat, Nucl. Data Sheets **88**, 417 (1999), A=61.
- [97] M. A. Lone, R. A. Levitt, and D. A. Harrison, At. Data Nucl. Data Tables **26**, 511 (1981).
- [98] R. C. Reedy and S. C. Frankle, At. Data Nucl. Data Tables **80**, 1 (2002).
- [99] C. E. Porter and R. G. Thomas, Phys. Rev. **104**, 483 (1956).
- [100] J. M. Blatt and V. F. Weisskopf, *Theoretical Nuclear Physics* (Wiley, New York, 1952).
- [101] D. M. Brink, Ph.D. thesis, Oxford University 1955.
- [102] P. Axel, Phys. Rev. **126**, 671 (1962).
- [103] E. Caurier, Computer code ANTOINE (unpublished).
- [104] A. Poves, J. Sánchez-Solano, E. Caurier, and F. Nowacki, Nucl. Phys. **694**, 157 (2001).
- [105] S. Raman, E. T. Journey, G. G. Slaughter, J. A. Harvey, J. C. Wells, Jr., J. Lin, and D. A. McClure, Bull. Am. Phys. Soc. **17**, 898 (1972).
- [106] S. Raman, M. Mizumoto, G. G. Slaughter, and R. L. Macklin, Phys. Rev. Lett. **40**, 1306 (1978).
- [107] S. Raman, in *Proceedings of the Fourth International Symposium on Neutron-Capture Gamma-Ray Spectroscopy and Related Topics, Grenoble, 1981*, edited by T. von Egidy, F. Gönnerwein, and B. Maier (Institute of Physics, Bristol, 1982), p. 357.
- [108] J. Kopecky, Netherlands Energy Research Foundation Report No. ECN-99, 1981.
- [109] W. V. Prestwich, M. A. Islam, and T. J. Kennett, Can. J. Phys. **69**, 855 (1991).
- [110] N. E. Holden, in *CRC Handbook of Chemistry and Physics*, edited by D. R. Lide (CRC Press, Boca Raton, 1999), p. 159.
- [111] M. A. Lone, in *Proceedings of the Third International Symposium on Neutron Capture Gamma-Ray Spectroscopy and Related Topics, Brookhaven, 1978*, edited by R. E. Chrien and W. R. Kane (Plenum, New York, 1979), p. 161.
- [112] A. G. W. Cameron, Can. J. Phys. **37**, 322 (1959).
- [113] I. E. Lynn, *Theory of Neutron Resonance Reactions* (Clarendon, Oxford, 1968).
- [114] J. A. Smith, E. J. Henelly, C. H. Ice, and H. F. Allen, in *The Savannah River High Flux Demonstration*, edited by J. L. Crandall, E. I. Du Pont de Nemours and Co. Report No. D-999, 1965.
- [115] R. Moreh and T. Bar-Noy, Nucl. Instrum. Methods **105**, 557 (1972).
- [116] S. Kahane and R. Moreh, Phys. Rev. C **50**, 2000 (1994).
- [117] J. A. Harvey, in *Proceedings of the International Conference on the Interactions of Neutrons with Nuclei, Lowell, Massachusetts, 1976*, edited by E. Sheldon, ERDA Report CONF-760715-P1.
- [118] J. Weitman, N. Däverhög, and S. Farvolden, Trans. Am. Nucl. Soc. **13**, 557 (1970).
- [119] H. M. Eiland and G. J. Kirouac, Nucl. Sci. Eng. **53**, 1 (1974).
- [120] S. Raman, E. T. Journey, J. A. Harvey, and N. W. Hill, Oak Ridge National Laboratory, Physics Division Annual Progress Report ORNL-5025, 1974, p. 110.
- [121] R. D. Werner and D. C. Santry, Nucl. Sci. Eng. **56**, 98 (1975).
- [122] G. J. Kirouac and H. M. Eiland, Bull. Am. Phys. Soc. **20**, 149 (1975).
- [123] J. A. Harvey, J. Halperin, N. W. Hill, S. Raman, and R. L. Macklin, Oak Ridge National Laboratory, Physics Division Annual Progress Report ORNL-5137, 1975, p. 2.
- [124] J. McDonald and N. G. Sjöstrand, Atomkernenergie **27**, 112 (1976).
- [125] M. Asghar, A. Emsallem, and N. G. Sjöstrand, Z. Phys. A **282**, 375 (1977).